Improvement of the Stress Corrosion Resistance of Alloy 718 in the PWR Environment

WARNING:
Please read the Export Control Agreement on the back cover.

Technical Report

Improvement Of The Stress Corrosion Resistance Of Alloy 718 In The PWR Environment

TR-105808
3154-03

Final Report, August 1996

Prepared by:
THE BABCOCK & WILCOX CO.
Research and Development Division
Alliance Research Center
1562 Beeson Street
Alliance, Ohio 44601

Principal Investigator:
M.T. Miglin

Prepared for
Electric Power Research Institute
3412 Hillview Avenue
Palo Alto, California 94304

EPRI Project Manager
J.L. Nelson

ORGANIZATION(S) THAT PREPARED THIS REPORT

THE BABCOCK & WILCOX CO.

REPORT SUMMARY

The costs associated with replacement of high-strength, nickel-base in-core components has led to efforts to improve corrosion resistance by various thermal, chemical and mechanical means. This report describes efforts designed to optimize the SCC resistance of alloy 718 in the PWR environment.

Background
High-strength, nickel-base alloys have been used extensively in pressurized water reactors (PWRs) and in boiling water reactors (BWRs) where combinations of high strength and excellent corrosion resistance are required. Although in-core experience has generally been quite good, failures in several components have been observed. Most failures of these components have occurred by stress corrosion cracking or fatigue. The most common of these high-strength alloys, alloys 718 and X-750, were originally developed for jet engine service. The melting, composition and thermomechanical processing were optimized for resistance to jet engine operating conditions. When applied to light water reactor service, the chemistry and processing variables have been found to be less than optimal, with components failing generally due to stress corrosion cracking and with some failures observed as the result of fatigue.

Objectives
- To determine the effect of heat treatment on the SCC resistance of alloy 718 in PWR primary water environments.
- To determine the effect of melt practice, thermomechanical processing, and alloy composition on the SCC resistance of alloy 718 in these environments.

Approach
Constant displacement-rate fracture mechanics tests were performed on alloy 718 in various conditions in a continuously refreshed simulated PWR primary side water environment at 360°C. Various heats of materials representing differences in composition, melt practice and heat treatment were used in the test program. Other age-hardenable, nickel-base alloys were also included in the test program. These included alloy X-750, the experimental alloys Hicoroy and Ticolloy and three experimental compositions similar to Ticolloy. Most heat treatments included an annealing treatment at 1093°C followed by various single or multiple-step aging heat treatments. These heat treatment conditions were compared to each other and to the

conventional heat treatment condition developed for aerospace use and now commonly found in light water reactors. The comparison evaluations were made by means of mechanical tests including hardness and tensile tests and by the fracture mechanics crack growth SCC tests.

Results

The stress corrosion cracking tests performed on alloys 718, X-750 and the other alternative alloys revealed that heat treatment had a profound effect on SCC resistance in PWR primary water environments. Specifically, long-term aging at low temperatures is beneficial to alloy 718. Material which had been annealed and given a two-step age (718°C/50h + 663°C/50h) or given a single lengthy age (663°C/100h) produced no SCC under the test conditions used. When tested in the aerospace heat treatment condition, alloy 718 exhibited SCC in this environment. The addition of 0.1% yttrium also improved the SCC resistance of alloy 718 for a given heat treatment. In addition, triple melted alloy 718 had better resistance to SCC than material remelted by the electroslag remelt or the electron beam remelt practices. It was also noteworthy that alloy 718, in the most SCC resistant heat treatment condition, was the best choice of the alloys examined, having greater resistance to SCC than alloy X-750 in the HTH condition or Hicoroy in the recommended LWR heat treatment condition.

EPRI Perspective

This study has identified the heat treatments, composition and melting practice, which can produce superior SCC resistance in PWR primary water applicationsfor alloy 718. The results of this effort clearly demonstrate that alloy 718 is the best choice among those materials evaluated in this program and is superior to the currently used HTH alloy X-750 for in-core component applications. Other SCC studies have been performed on these materials in EPRI sponsored programs and are described in EPRI Report Numbers TR-103290, TR-103970 and TR-103971.

TR-105808

Interest Category

Nuclear Plant Corrosion Control

Key Words

PWR
Reactor Components
Nickel Alloys
Stress Corrosion Cracking
Heat Treatment
Irradiation

ABSTRACT

Stress corrosion cracking (SCC) tests were conducted in 360 °C pressurized-water-reactor (PWR) primary water using alloy 718 in various heat treatment conditions. Alloy X-750 in the HTH condition and an experimental heat of an alloy 718 variation, Hicoroy, were also tested for comparison. Fatigue-precracked, 12.5-mm-thick compact fracture specimens were subjected to a constant extension rate of 1.3 x 10^{-9} m/s. Crack growth rate was measured during testing using a reversing DC potential drop technique. Results in the form of SCC crack growth rate versus applied stress intensity demonstrate that the SCC resistance of alloy 718 in the PWR primary-side environment can be improved by changes in heat treatment.

ACKNOWLEDGMENTS

The author would like to acknowledge E.A. DeStephen for conducting the experiments, J. V. Monter and C. S. Wade for technical assistance, and W. A. Van Der Sluys for helpful discussions. Teledyne-Allvac, Special Metals, Nippon Mining Company, and Hitachi Metals generously donated test materials, and Wyman-Gordon performed the forging operations.

CONTENTS

LIST OF TABLES

LIST OF FIGURES

EXECUTIVE SUMMARY

The high-strength, age-hardenable, nickel-base alloy 718 is used in pressurized-water reactors (PWRs) and boiling-water reactors (BWRs) for bolts, springs, and beams—components that require high strength, relaxation resistance, and corrosion resistance. Although the performance of alloy 718 is generally good, premature failure of some components—such as fuel-assembly hold-down springs—has caused unnecessary expense. One of the failure mechanisms is intergranular stress corrosion cracking (IGSCC). EPRI is sponsoring research to investigate IGSCC susceptibility as part of a larger program to optimize alloy 718 for use in light water reactor internal components. The objective of this research is to investigate variations in heat treatment and melt practice to produce optimal SCC resistance.

Constant-displacement rate K_{ISCC} tests are used to evaluate the effects of heat treatment of alloy 718 on SCC resistance in the PWR primary-side environment. The influence of melt practice, thermomechanical processing, and alloy chemistry are also investigated. For comparison, alloy X-750 is tested in the HTH condition, and additional experimental alloys are included.

Alloy 718 given a high-temperature anneal (1093 °C) followed by two-step aging (718 °C/8h + 621 °C/8h/AC) has a yield strength of 1145 MPa, compared with 741 MPa for alloy X-750, and superior SCC resistance. Combining the same anneal with long-term aging (718 °C/50h + 663 °C/50h) makes alloy 718 immune to SCC under the test conditions.

1

INTRODUCTION

Usage and Failure History

The high-strength, age-hardenable, nickel-base alloy 718 is used in pressurized-water reactors (PWRs) and boiling-water reactors (BWRs) for bolts, springs, and beams — components that require high strength, relaxation resistance, and corrosion resistance. It is also used in some lower stress applications such as the seal ring under the top head of the reactor. The overall performance of alloy 718 has been good, although there have been some failures, most commonly of fuel-assembly hold-down springs. Spring failures have occurred by stress corrosion cracking and by fatigue. These springs are replaced periodically along with the fuel assembly, and spring failure is not a safety problem. However, premature spring failure causes unnecessary expense. Utilities wanting to leave fuel bundles in core for longer than the conventional three-year fuel cycle are interested in extending spring lifetime.

Alloy 718 came into increased use following a rash of failures of the high-strength nickel-base alloy X-750. Alloys X-750 and 718 were originally developed for jet engine service. The melting, composition and thermomechanical processing were optimized for resistance to creep and oxidation. During reactor design it was assumed that the buffered aqueous environment typical of the reactor core would not be aggressive enough to attack these corrosion-resistant alloys, and the processing and heat treatment conditions developed for jet engine service were adopted for nuclear service. Alloy X-750 was widely employed for in-core springs, bolts, and beams. Most of the components made of alloy X-750 maintained their integrity. For those that failed, some were replaced with alloy X-750 given an alternative heat treatment developed for corrosion resistance in reactor environments.(1-3)

Other failed components, especially those requiring high tensile strength, were replaced with alloy 718. For alloy 718, heat treatments developed for jet engine service were used because no others were available. While alloy 718 performance has been better than alloy X-750 given jet engine heat treatments, there have been some failures. Most have been fuel assembly hold-down springs, with stress corrosion cracking the dominant failure mode for the leaf spring design, and fretting and fatigue causing failure of the helical spring design.

Metallurgy of Alloy 718 and Other Nickel-Base Alloys

The physical metallurgy of alloy 718 is very complex. Several time-temperature-transformation (TTT) diagrams exist in the literature; however, they are so different that they do not even list the same metallurgical phases. The TTT diagram shown in Figure 1-1 is in closest agreement with previous analytical electron microscopy (AEM) and atom probe field-ion microscopy (APFIM) investigations of alloy 718.(4)

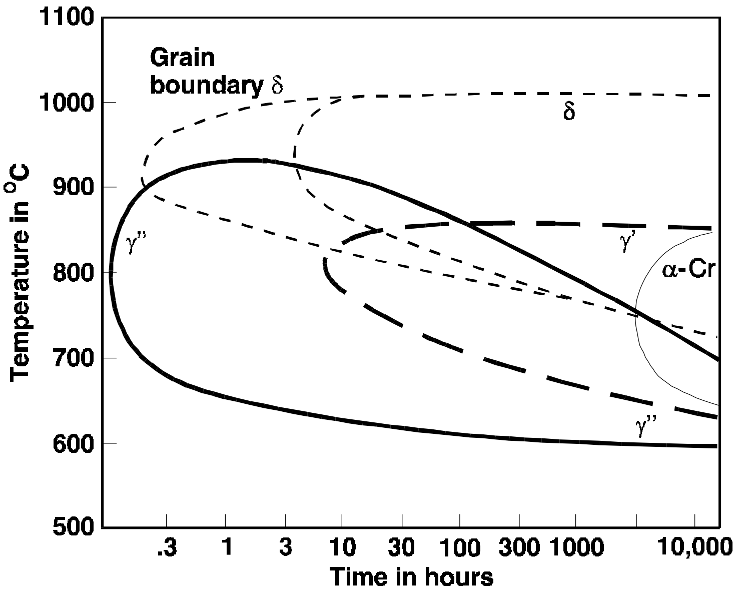

Figure 1-1 Time-temperature-transformation (TTT) diagram for alloy 718

Heat Treatment

Both alloy 718 and alloy X-750 are austenitic alloys hardened by precipitation of Ll_2-ordered γ′ [Ni_3(Ti,Al,Nb)], and in the case of alloy 718, also by DO_{22}-ordered γ″ [Ni_3(Nb,Ti,Al)]. Both alloys also form additional precipitates, some of which are detrimental to SCC performance. For example, aging alloy X-750 near 885 °C, which is done for aerospace applications, produces grain boundary η phase [Ni_3Ti]. Eta phase stabilizes grain boundaries for improved creep resistance but is detrimental to SCC performance. When given a heat treatment with a high annealing temperature (near 1100 °C) and a single aging treatment near 700 °C to precipitate γ′, the alloy has good resistance to SCC.

Similarly, alloy 718 is heat treated near 950 °C for aerospace applications. Near 950 °C δ phase, DO_a-ordered [Ni_3Nb] precipitates rapidly, stabilizing the grain boundaries for increased creep resistance. Delta phase in alloy 718 may act similarly to η in alloy X-750, causing degradation of corrosion resistance. Alloy 718 also forms Laves (A_2B), a nonequilibrium phase that forms if the local concentration of niobium is high, as well as MC-type carbides and carbonitrides. While the effect on corrosion resistance of the carbides is not known, Laves has been reported to adversely affect the SCC behavior of alloy 718.(5) Changes in the grain boundary precipitate structure may improve SCC performance in the PWR primary-side environment as for alloy X-750.

Melting and Processing

There may be an effect of melt practice on the SCC performance of alloy 718. Melt practice affects the degree of niobium segregation, which in turn affects the response of the material to heat treatment. Highly segregated alloy 718 will be susceptible to forming Laves phase in the niobium-rich regions. Melting and thermomechanical processing practices for alloy 718 have been reviewed by Loria.(6)

Alloy 718 components for the nuclear industry are usually fabricated from vacuum-induction-melted, electroslag-remelted (VIM-ESR) rolled barstock or plate. The ESR process produces better chemical homogeneity and cleanliness than the older vacuum-arc-remelting (VAR) process, and ESR ingots are more easily worked. Further improvements in cleanliness are provided by a triple-melt process (VIM-ESR-VAR). Additional newer melting practices include electron-beam, cold-hearth refining (EBCHR), plasma-melt refining (PMR) and vacuum-arc, double-electrode refining (VADER) processes but with higher cost and more limited availability.(6)

Three different thermomechanical processing options are available, including standard, high-strength (HS), and direct-age (DA) processes. All are two-step forging operations. The high-strength process employs lower forging temperatures than the standard process, and the direct-age process uses the lowest forging temperatures. Lower forging temperatures provide higher strength and smaller grain sizes. The direct-age process includes finish forging below the δ solvus, and is designed to allow age hardening after cooling from the finish forging temperature, with no intervening anneal. The direct-age process produces mechanical properties suitable for high-pressure turbine applications in advanced engines. The grain boundaries are pinned by precipitation of δ during final forging, and the effect of the resulting grain boundary precipitate structure on SCC resistance has not been investigated.

Composition

After lengthy exposure of alloy 718 to jet engine operating temperatures, an acicular variant of the grain-boundary δ-phase nucleates. Because of its crack-like shape, acicular δ is deleterious to fatigue and fracture toughness. Fifteen experimental alloys have been developed at the University of Texas, with the goal of reducing the tendency to form acicular δ (7). These alloys were developed by increasing the Al/Ti and (Al+Ti)/Nb ratios of alloy 718 (see Figure 1-2). Alloy 12, the most promising of the series, has been given the name "Ticolloy." Reducing the tendency to form δ holds promise not only for improved creep resistance but also for improved SCC resistance.

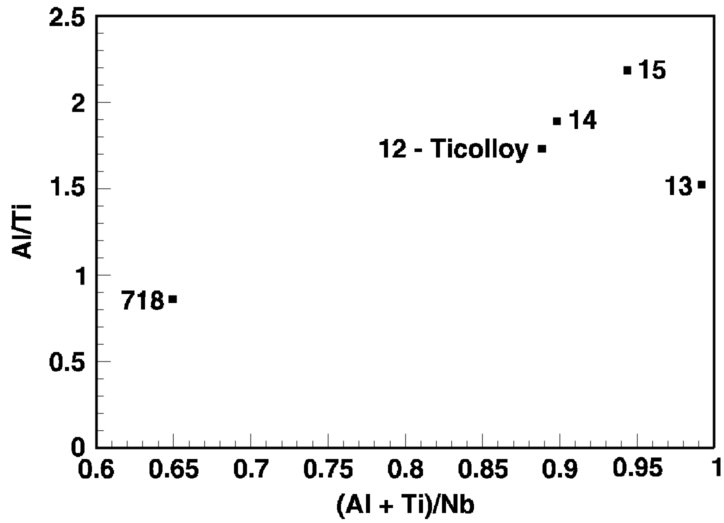

Figure 1-2 Composition of alternative alloys

For alloy X-750 it has been found that small additions of zirconium increase the resistance to stress corrosion cracking (8), although the mechanism is not known. It is possible that zirconium increases grain boundary nobility or that it accelerates the oxidation behavior of the alloy, improving its resistance to film rupture. Another refractory metal, yttrium, is postulated to improve the SCC resistance of alloy 718. Yttrium is thought to accelerate the formation of the protective chromia scale.

Hicoroy was developed by Hitachi Metals to be a more corrosion-resistant Ni-based alloy for nuclear service. It is similar to alloy 718 in Ni, Cr, and Fe levels, with a Ti/Nb ratio between alloy 718 and alloy X-750.

Present Program

The high cost of replacing failed in-core components has prompted the search for methods to improve the corrosion resistance of alloy 718. The program described below is designed to investigate variations in heat treatment and melt practice to produce optimal SCC resistance. Slight variations from nominal composition are also included. Past success in improving the SCC performance of alloy X-750 inspired the hope that similar improvements could be made with alloy 718.

The test program described here emphasizes the effects of heat treatment of alloy 718 on SCC resistance in the PWR primary-side environment. It also includes evaluating the influence of melt practice, thermomechanical processing, and alloy chemistry. Constant-displacement-rate K_{ISCC} tests are performed using alloy 718 fabricated using four different melt practices, three different forge processes, and a multitude of heat treatments. For comparison, alloy X-750 is tested in the HTH condition, and additional experimental alloys are also included.

2

EXPERIMENTAL PROCEDURES

Test Materials

Materials tested in this program include:

- Alloy 718 with conventional chemistry, melt practice, and thermomechanical processing.
- Alloy 718 with chemistry modifications.
- Alloy 718 with novel melt practice and/or themomechanical processing.
- Other age-hardenable, nickel-base alloys included are alloy X-750, the experimental alloys Hicoroy and Ticolloy, and three additional chemistries similar to Ticolloy.

Alloy Heats

The test materials are as follows:

- VIM-VAR Hot-Die (HD) Forged Alloy 718 — Teledyne Allvac heat No. E790, hot-die forged by the Wyman Gordon Company.
- VIM-ESR HS Forged Alloy 718—Guterl Special Steel heat No. 50006-1 melted in 1982 to meet AMS 5662C high-strength forged into 7.6-cm-diameter round bar.
- VIM-ESR DA Forged Alloy 718 — Teledyne Allvac heat No. 8211 melted in 1989 to meet AMS 5662F, chemistry only and direct-age forged into 7.6-cm-diameter round bar.
- VIM-ESR-VAR HS Forged Alloy 718 — Special Metals Company heat No. 89193 melted in 1989 to meet AMS5664B and forged into 8.9-cm-diameter round bar.
- VIM-EBCHR Alloy 718 — Melted by Nippon Mining Company and forged by Wyman Gordon.
- Alloy 718 + Yt — Melted by Teledyne Allvac and forged by Cameron Forge.
- VIM-VAR Alloy X-750 — Guterl Special Steel heat No. 26018-1 melted in 1982 to meet MIL-N-24114B and forged into 7.6-cm-diameter round bar.
- Hicoroy — Hitachi Metals heat No. Y7514 rolled into 1.3-cm-thick plate.(9)
- Ticolloy — Special Metals heat No. D53560 melted in 1988 and forged by Wyman Gordon into a 15-cm-diameter pancake.
- Alloys 13-15 — Special Metals heats No. D14418 through D14420 forged by Wyman Gordon.

The melting dates are reported because improvements in melt practice between 1982 and 1989 may prove to have some bearing on SCC resistance. Microstructural and mechanical property details about the high-strength 718 and the X-750 materials are provided by Miglin and Domian (1,2). Chemical compositions of the experimental heats are reported in Tables 2-1 and 2-2.

The experimental alloy Hicoroy, a chemistry variant of alloy X-750, was designed to resist stress corrosion cracking in nuclear reactor environments. Ticolloy, on the other hand, is a variant of alloy 718 designed to improve upon the performance of alloy 718 as a jet engine turbine disk material. It is optimized for resistance to fatigue at jet engine temperatures by increasing the stability of γ', which may convert into or nucleate the deleterious δ phase after long operating times. Ticolloy and the experimental alloys 13 through 15 have variations in Al, Ti, and Nb content that put them outside the alloy 718 chemistry specification. Controlling the Al/Ti and (Al + Ti)/Nb ratios can improve the stability of γ' and reduce the δ content.

Heat Treatments

The heat treatments used in this program are listed in Tables 2-3 and 2-4. Many of these heat treatments were taken from the literature, while others were developed for this program.

Most of the heat treatments include an annealing treatment at 1093 °C. This temperature was selected by annealing samples of the VIM-ESR DA heat at several temperatures and finding the lowest temperature that produced a microstructure free of ghost grain boundaries (determined via optical microscope). Annealing at 1093 °C causes considerable grain growth, as is apparent in Figure 2-1.

Table 2-3 lists the heat treatments used for the alloy 718 heats from Table 2-1. The heat treatment labeled “INEL,” developed at the Idaho National Engineering Laboratory for large components in a liquid metal fast breeder reactor, includes a furnace cool after annealing to avoid quench cracking. The conventional “CONV” heat treatment condition was developed for aerospace use and is now commonly found in light-water reactors. The AERO condition takes the aging sequence from the conventional heat treatment and combines it with a high-temperature anneal. An annealed (ANN) specimen is included to assess the baseline SCC susceptibility of non-heat-treated alloy 718.

Table 2-1
Chemical composition for Alloy 718 heats

Heat	Alloy 718 Spec.	VIM- VAR HDF	VIM- ESR HS	VIM- ESR DA	VIM - ESR- VAR HS	EBCHR	718+Yt
Ni	50-55	Bal.	50.3	51.5	54.1	53.1	53.1
Cr	17-21	18.3	19.4	17.6	17.9	17.9	17.9
Fe	Bal.	19.5	19.6	Bal.	Bal.	18.5	18.9
Ti	0.65-1.15	1.04	0.95	1.05	0.98	1.02	0.93
Al	0.2-0.8	0.46	0.43	0.55	0.46	0.50	0.54
Nb+Ta	4.75-5.5	5.28	5.31	5.21	5.40	5.32	5.38
Mo	2.8-3.3	3.11	3.00	2.92	2.94	3.01	2.90
Mn	0.35 max	0.16	0.16	0.08	0.05	0.01	0.02
Si	0.35 max	0.059	0.21	0.09	0.06	0.12	0.002
C	0.08 max	0.035	0.054	0.04	0.03	0.03	0.36
S	0.015	<0.001	0.001	0.0004	0.0007	0.0005	—
Co	1.00 max	0.24	0.26	0.32	0.09	0.35	—
B	0.006	0.004	0.005	0.004	0.0026	0.004	0.004
Cu	0.30 max	0.049	0.05	0.05	0.06	0.08	—
P	0.015	0.015	0.010	0.005	0.010	0.001	0.005
Yt	——	——	——	——	——	——	0.1

Table 2-2
Chemical Composition for Alternative Alloys

Heat	Alloy 718 Spec.	Alloy X-750	Hicoroy	Ticolloy	Alloy 13	Alloy 14	Alloy 15
Ni	50-55	72.1	Bal.	53.93	53.24	52.85	52.6
Cr	17-21	15.5	20.42	17.5	17.9	17.9	17.9
Fe	Bal.	7.97	15.1	17.8	18.3	18.2	18.3
Ti	0.65-1.15	2.35	1.54	.96	1.08	.94	.93
Al	0.2-0.8	0.47	0.48	0.94	0.89	0.96	1.08
Nb+Ta	4.75-5.5	1.03	3.84	5.74	5.46	5.89	6.07
Mo	2.8-3.3	0.06	3.10	3.05	3.03	3.01	3.03
Mn	0.35 max	0.25	0.032	0.02	0.01	0.02	0.01
Si	0.35 max	0.15	<0.002	0.11	—	0.02	—
C	0.08 max	0.047	0.016	0.03	0.03	0.03	0.03
S	0.015 max	0.002	<.002	0.002	0.002	0.002	0.002
Co	1.00 max	0.11	0.011	—	—	—	—
B	0.006 max	<.001	0.005	0.003	0.002	0.002	0.002
Cu	0.30 max	0.018	<.001	0.01	—	—	—
P	0.015 max	0.004	0.006	0.006	—	—	—-

Table 2-3
Heat Treatment for Alloy 718

Heat	Specimen ID	Hardness, R_c	Heat Treatment*
VIM-VAR			
HDF-718	INEL-1 INEL-2 INEL-3 INEL-4	37	1093°C/1h + 718°C/4h + 621°C/16h/AC
VIM-ESR			
HS-718	HS-CONV1	42	982 °C/1h/AC + 718 °C/8h +621 °C/8h/AC
	HS-CONV2		1093 °C/1h/WQ + 718 °C/8h +621 °C/8h/AC
	HS-AERO	37	
VIM-ESR			
DA-718	DA	44	As-hot-finished + 718 °C/8h + 621 °C/8h/AC
	DA-ANN	—	1093 °C/1h/WQ
	DA-CONV	44	982 °C/1h/AC + 718 °C/8h + 621 °C/8h/AC
	DA-AERO1	41	Same as HS-AERO.
	DA-AERO2		
	DA-OA-A	39	1098 °C/1h/WQ + 718 °C/50h/AC
	DA-OA-B	40	1093 °C/1h/WQ+788 °C/16h+718 °C/50h/AC
	DA-OA-C	42	1093 °C/1h/WQ+718 °C/50h+663 °C/50/AC
	DA-OA-D	40	1098 °C/1h/WQ+788 °C/16h+718 °C/50h+ 663 °C/50h/AC
	DA-1Age	37	1093 °C/1h/WQ+718 °C/8h/AC
	DA-2Age	37	1093 °C/1h/WQ+663 °C/100h/AC
	DA-HEA	39	1093 °C/1h/WQ+718 °C/8h+663 °C/8h/AC
	DA-HEB	43	1093 °C/1h/WQ+760 °C/11h+649 °C/9h/AC
	DA-OW	37	1093 °C/1h/WQ+788 °C/6h/AC
VIM-ESR-VAR			
HS-718	TM-CONV	44	954 °C/1h/AC+718 °C/8h+621 °C/8h/AC
	TM-AERO	31	Same as HS-AERO
VIM-EBCHR			
718	EBCHR	40	1093 °C/1h/WQ+718 °C/8h+621 °C/8h/AC
718+Yt	Yt718	42	1093 °C/1h/WQ+718 °C/8h+621 °C/8h/AC

* Unless otherwise indicated, the cooling rate between heat treatment steps is 55 °C/h.

Table 2-3 also includes a series of overaging (OA) heat treatment conditions. Experience with alloy X-750 shows that overaging the γ' improves SCC resistance.(1,2) when γ' is overaged, it becomes incoherent relative to the gamma matrix. As an incoherent precipitate, it cannot be cut by dislocations but must be bypassed, increasing the difficulty of slip-step formation. This may retard SCC by slowing the slip-step formation and dissolution process. The OA-A condition is designed to overage γ'', OA-B to overage δ and γ'', OA-C to overage δ and γ', and OA-D to overage all three. Specimens DA-1Age and DA-2Age are designed to test the effect of predominant γ'' and γ' hardening, respectively. Figure 2-2 illustrates the DA-2Age, OA-C, and AERO heat treatment conditions on a TTT diagram.

Finally, the HEA, HEB and OW heat treatments were borrowed from other industries. The HEA and HEB treatments are designed for use in the space shuttle main engine and are optimized for resistance to hydrogen embrittlement.(10) The PWR environment has a hydrogen overpressure, and hydrogen embrittlement is suspected to have played a role in some failures of alloy X-750 and alloy 718 in PWRs. The OW treatment is designed for resistance to cracking in the hydrogen-sulfide environments found in deep sour-gas wells.(11)

Table 2-4
Heat Treatments for Alternative Alloys

Heat	Specimen ID	Hardness, R_c	Heat Treatment*
X-750	HTH	28	1107 °C/1h/rapid AC+704 °C/20h/AC
HICOROY STAG		29	1000 °C/1h/OQ+720 °C/8h+620 °C /8h/AC
Ticolloy	TY-HS	36	954 °C/1h/WQ+760 °C/8h+649 °C/8h/AC
	TY-CONV	35	954 °C/1h/WQ+718 °C/8h+621 °C/8h/AC
	TY-AERO	34	Same as DA-AERO
Alloy 13	13-AERO	35	Same as DA-AERO
Alloy 14	14-AERO	38	Same as DA-AERO
	14HS	43	1093 °C/1h/WQ+760 °C/8h+649 °C /8h/AC
Alloy 15	15-AERO	39	Same as DA-AERO

* Unless otherwise indicated, the cooling rate between heat treatment steps is 55°C/h.

Table 2-4 lists heat treatments for alloy X-750, Hicoroy, and the experimental alloys tested. Alloy X-750 is in the HTH condition, which is a SCC-resistant heat treatment developed for nuclear service. Ticolloy and alloy 14 are given a high-strength (HS) treatment developed to maximize tensile properties.

Test Methods

Mechanical Tests.

Rockwell hardness tests are performed on all material conditions according to ASTM E-18, S*tandard Test Methods for Rockwell Hardness and Rockwell Superficial Hardness of Metallic Material*s. Tensile tests are performed on selected material conditions according to ASTM E-8, *Standard Test Methods for Tension Testing of Metallic Materials*.

Constant-displacement-rate K_{ISCC}.

The constant-displacement-rate K_{ISCC} test used for this work (12) is similar to that described by Mayville, *et al*. (13) and Dietzel, *et al*.(14). There are numerous methods of conducting K_{ISCC} tests (13-16), none of which has been standardized. The constant-displacement-rate (sometimes called rising-load) K_{ISCC} test method is selected because it generates results quickly. This method produces a curve of SCC growth rate versus applied stress intensity factor in as few as two or three weeks using a single specimen, rather than in many months using several specimens with self-loaded or dead-weight-loaded test methods. Recognizing that the severity of SCC depends upon applied strain rate, tests are conducted at progressively lower strain rates until the measured K_{ISCC} reaches a minimum. Crack length is monitored remotely during testing, in this case using a reversing direct current (d.c.) electrical potential drop technique.(17) Data are obtained in the form of crack growth rate as a function of applied stress intensity factor, K.

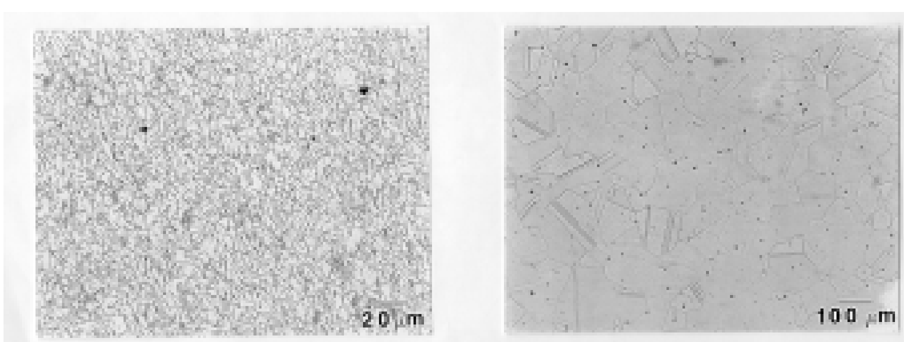

(a) As received (b) 1093ºC/1h/WQ

Figure 2-1 Effect of annealing on grain size of direct-aged forged alloy 718

Except for the first four specimens, which were tested at various strain rates to determine the effect of applied strain rate on SCC crack growth rate, all of the specimens were tested in groups of five in the specially designed autoclave facility shown in Figure 2-3. The first four specimens were tested individually in the same facility using conventional autoclave internals. The five-specimen loading fixture shown in Figure 2-3 is affixed to an autoclave mounted to a load frame with a screw-driven actuator. The autoclave is continuously refreshed with 360 °C PWR primary-side water, as specified in Table 2-5.

The test specimen is a standard 0.5-T compact fracture specimen, according to ASTM E399-90, "*Standard Test Method for Plane-Strain Fracture Toughness of Metallic Materials*." Before placing the specimen in the environment, it is precycled to grow a sharp fatigue crack at the notch tip, according to the procedure described in ASTM E399-90, with final cycling performed at very low loads. After fatigue precracking, the specimen is side-grooved to 10% of total thickness on each side, as described in E813-89, to maintain a straight SCC crack at right angles to the load line. This is important to maintain the validity of the stress intensity factor expressions.

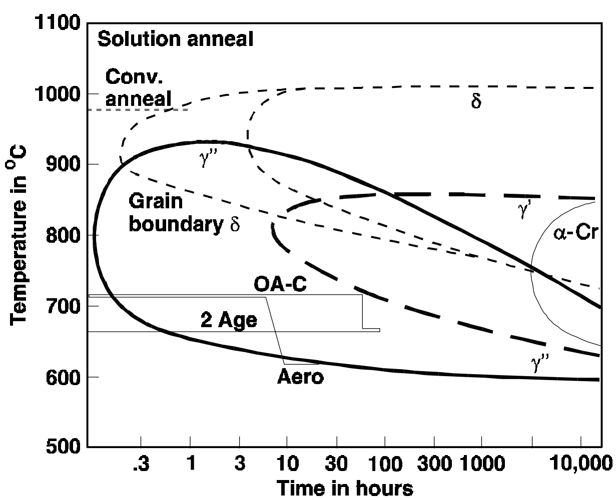

Figure 2-2 TTT diagram for alloy 718 showing the AERO, 2Age and OA-C heat treatments

A constant actuator displacement rate of 1.3×10^{-9} m/sec is used for all specimens in the test matrix, except for three of the specimens tested at the beginning of the program. Based on the results of these initial tests at displacement rates of 2.5×10^{-8} m/sec, 2.5×10^{-9} m/sec, 1.3×10^{-9} m/sec, and 2.5×10^{-10} m/sec, the value of 1.3×10^{-9} m/sec is used for the remainder of the program.

Table 2-5
Primary Water Specifications

Dissolved Oxygen	≤0.01 ppm
Boric Acid	5700 ppm (±500 ppm)
Lithium	2 ppm
pH	6.5 (±0.5)
Conductivity	< 20μmhos/cm
Dissolved Hydrogen	15-50 Std cc/kg H_2O
Chloride	< 0.1 ppm
Fluoride	< 0.1 ppm

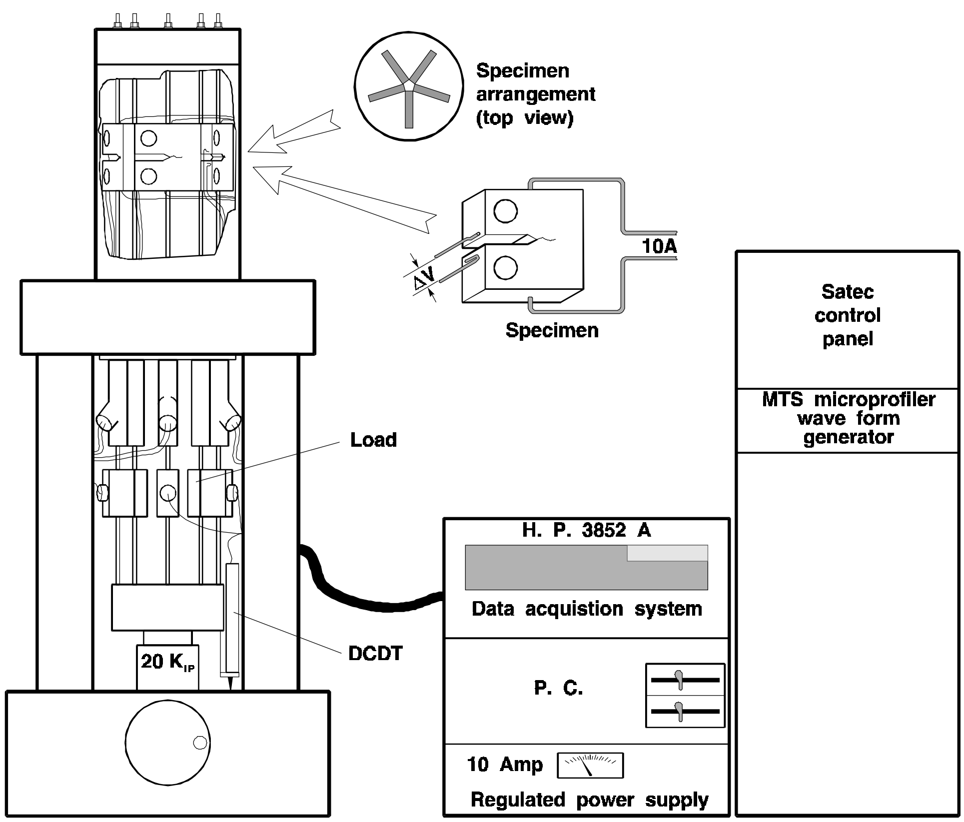

Figure 2-3 Test set-up for conducting constant displacement rate K_{ISCC} tests

A constant actuator displacement rate of 1.3×10^{-9} m/sec is used for all specimens in the test matrix, except for three of the specimens tested at the beginning of the program. Based on the results of these initial tests at displacement rates of 2.5×10^{-8} m/sec, 2.5×10^{-9} m/sec, 1.3×10^{-9} m/sec, and 2.5×10^{-10} m/sec, the value of 1.3×10^{-9} m/sec is used for the remainder of the program.

3

RESULTS

Mechanical Tests

The results of hardness testing are reported in Tables 2-3 and 2-4, and the tensile test results are reported in Table 3-1.

Constant-Displacement-Rate K_{ISCC} Tests

The results of the constant-displacement-rate K_{ISCC} tests are presented in their entirety in Appendix A. Selected results are presented below.

Data Analysis

The first step in data analysis is to produce a plot of potential drop crack length versus time. A polynomial, usually of second or third order, is fitted to the data. Figure 3-1 shows two examples of fitted crack length versus time data. Crack growth rates are calculated at specific crack length values using the coefficients of these curves rather than the actual data points. Using the actual data to calculate crack growth rates magnifies the noise that is inherent in DCPD (direct-current potential drop) crack length measurements, and is inescapable regardless of the crack length measurement procedure used. Crack tip stress intensity factors are also calculated using the calculated rather than the measured crack length values. The measured load values are used to calculate stress intensity factor, and a log-lin plot of crack growth rate versus applied stress intensity factor is generated. Figure 3-2 shows the K_{ISCC} curves generated using the data from Figure 3-1. The specimens in Figures 3-1 and 3-2 were taken from the same heat of material, and the results demonstrate the good reproducibility achievable with this test procedure.

Occasionally there will be apparent high crack growth rates in the early portion of the curve, as for specimen HS-CONV2 in Figure 3-2. This occurs when the fatigue precrack is not straight, but has a thumbnail shape (see Figure 3-3). SCC initiates first near the specimen surfaces, where the crack length is shorter and the local stress intensity factor higher than the global value indicated on the X axis. The higher local stress intensity factor produces faster crack growth rates than predicted by the global stress intensity factor value. Also, for a thumbnail crack shape, the DCPD-measured crack length will be influenced disproportionately by the near-surface ligaments. Therefore, DCPD is highly sensitive to early crack growth near the specimen surfaces. The end result is an upward curve in the data at low K levels, as shown in Figure 3-2 for specimen HS-CONV2, for specimens with a thumbnail-shaped precrack. Any other odd-shaped fatigue precrack will also produce anomalies in the low-K end of the curve.

Table 3-1
Tensile Properties

Heat Treatment	Yield Strength, MPa	Ultimate Strength, MPa	Elongation, %	Reduction of Area, %
HS-CONV	1144	1366	20.1	28.9
DA	1453	1587	15.5	31.5
DA-AERO	1145	1314	25.9	35.4
DA-OA-B	1025	1310	21.7	22.3
DA-HEA	1078	1252	31.7	49.9
DA-HEB	1145	1406	22.6	27.1
DA-OW	789	1181	31.2	40.0
X-750 HTH	741	1166	29.1	33.6
HICOROY STAG	854	1219	36.1	53.6

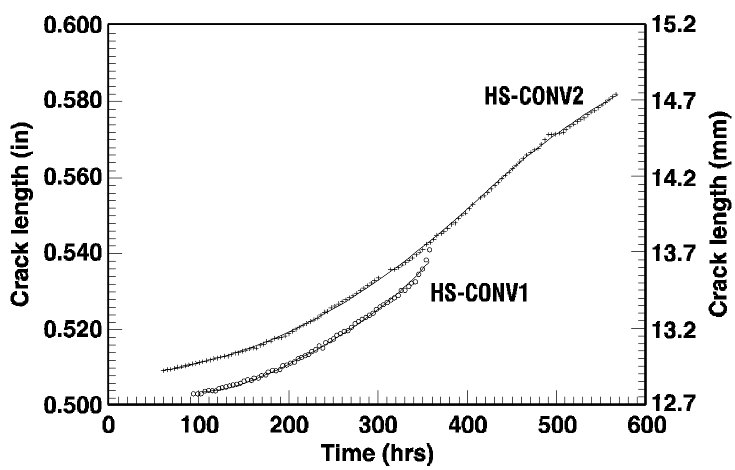

Figure 3-1 Crack length versus time for duplicate specimens HS-CONV1 and HS-CONV2 showing polynomial fits to the data

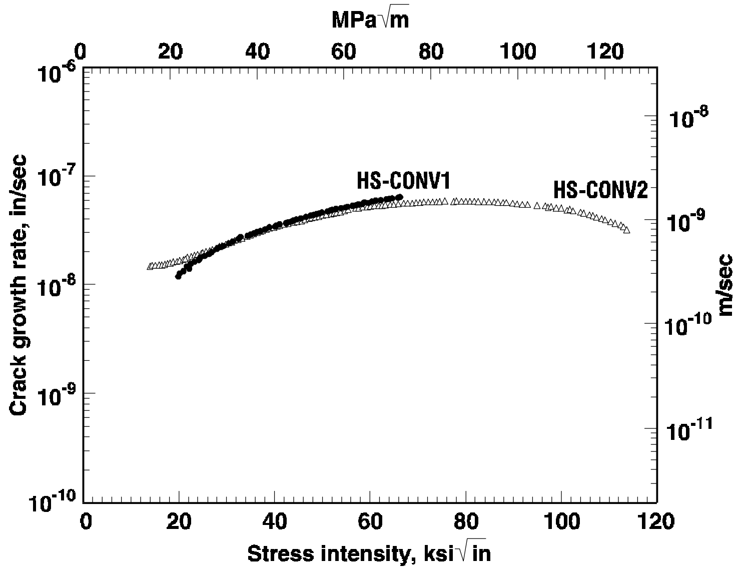

Figure 3-2 Crack growth rate results for duplicate specimens HS-CONV1 and HS-CONV2

Strain Rate Matrix

Results of the strain rate matrix are presented graphically in Figures 3-4 and 3-5. Specimen INEL-1, tested at 2.5 x 10^{-8} m/sec, did not show any evidence of SCC. Specimen INEL-2, tested at 2.5 x 10^{-9} m/sec, underwent SCC followed by ductile tearing. Specimens INEL-3, tested at 1.3 x 10^{-9} m/sec and INEL-4 (not plotted) experienced SCC. Fractographs of the four specimens are shown in Figure 3-6. Specimen INEL-4 was tested at the lowest strain rate, 2.5 x 10^{-10} m/sec, with a test duration of 2700 hours. At this slow displacement rate, the DCPD system did not function in the usual manner. Figure 3-5 shows the crack lengths versus time results for specimen INEL-4. It appears as if the crack tip was short-circuited by a process of repeated oxide formation and rupture. During oxidation, the measured crack length gradually decreases, until the oxide ruptures, abruptly increasing the crack length. The cyclic process of oxide formation and rupture may have masked steady-state crack propagation by SCC.

These results show that decreasing applied displacement rate increases susceptibility to SCC; this agrees with Parkins.(18) According to Parkins, for each alloy/environment combination in which the alloy is susceptible to SCC, there exists a critical displacement rate at which SCC susceptibility is maximized. It is clear that the SCC crack growth rate increases when displacement rate is reduced from 2.5 x 10^{-9} to 1.3 x 10^{-9} m/sec. Further reduction in strain rate to 2.5 x 10^{-10} m/sec produced more extensive SCC on the fracture surface of specimen INEL-4; however, the effect on crack growth rate is not certain without DCPD data.

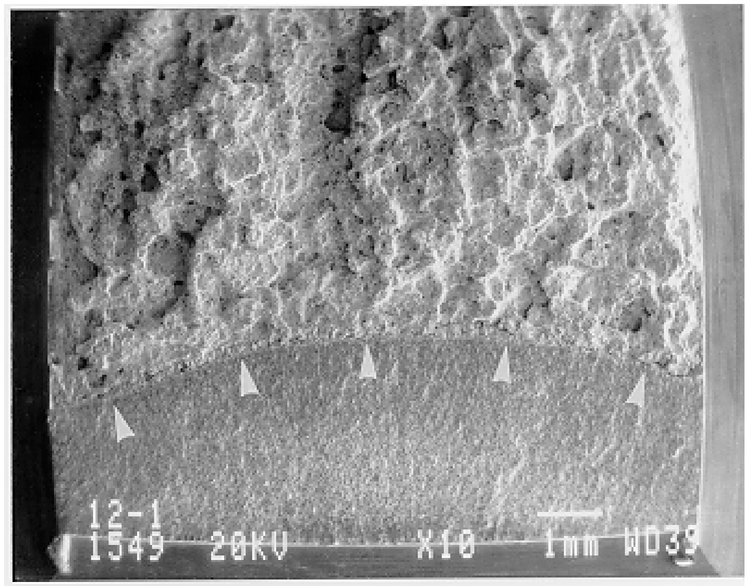

Figure 3-3 SEM fractograph of a failed constant displacement rate K_{ISCC} specimen. White arrows indicate thumbnail shape of fatigue precrack

Measuring the SCC crack length on the specimen surface and assuming that the entire 2700 hours were consumed by SCC crack growth (which is incorrect, because SCC converted to ductile tearing in the autoclave) yields a crack growth rate of approximately 3 x 10^{-10} m/sec, close to the plateau value of specimen INEL-3. Assuming that SCC converted to ductile tearing at 1600 hours, where there is a discontinuity in the crack length data, provides a crack growth rate of 5.7 x 10^{-10} m/sec. This is approximately the rate attained by specimen INEL-3 near the end of SCC crack growth. It appears that the critical displacement rate is closer to the slowest rate in this matrix. However, because of difficulties with the DCPD at this low rate, and because of the need to screen numerous material conditions within a reasonable time period, a rate of 1.3 x 10^{-9} m/sec is selected.

Alloy 718 Conditions

The test results for all of the alloy 718 heat treatments are presented in Appendix A. The best way to compare the various conditions is to compare the crack growth rates at a selected stress intensity, for example 60 MPa√m. For some of the heat treatment conditions, an estimate of K_{ISCC} can be made. For others, because of anomalous data near the beginning of the test resulting from irregular precrack fronts, estimating K_{ISCC} is not possible. For those specimens for which K_{ISCC} estimation is possible, an estimate is given in Table 3-2. For all specimens, the crack growth rate at 60 MPa√m is given.

Figure 3-7 presents results for selected material conditions. The results for the remaining alloy 718 conditions fall between the outermost (best and worst) curves on the graph in Figure 3-7, except for those conditions that did not undergo SCC. Comparing the curves for specimens TM-CONV and DA-CONV in Figure 3-7 shows that for the CONV heat treatment, triple-melting does not improve material performance when compared with the VIM-ESR material used for direct-age processing. However, the DA-AERO condition underwent SCC while the triple-melt TM-AERO condition did not.

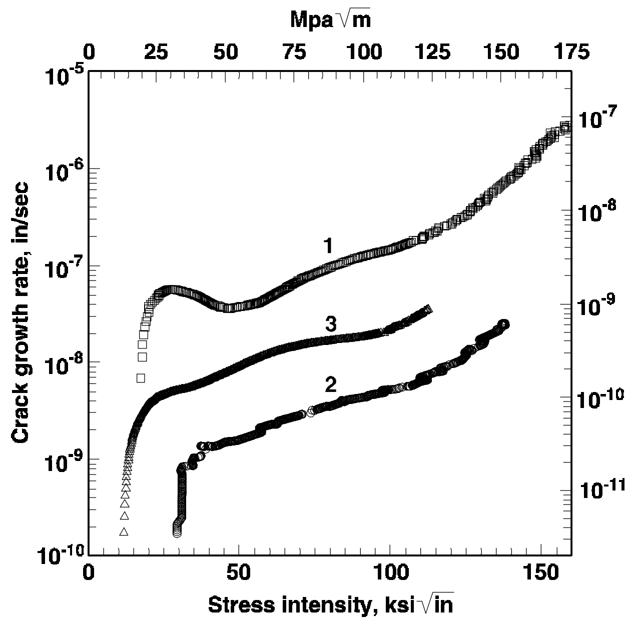

Figure 3-4 Crack growth rate versus applied stress intensity for alloy 718 (INEL-1 to 3) tested at: (1) 2.5 x 10^{-8} m/sec; (2) 2.5 x 10^{-9} m/sec; and (3) 1.3 x 10^{-9} m/sec

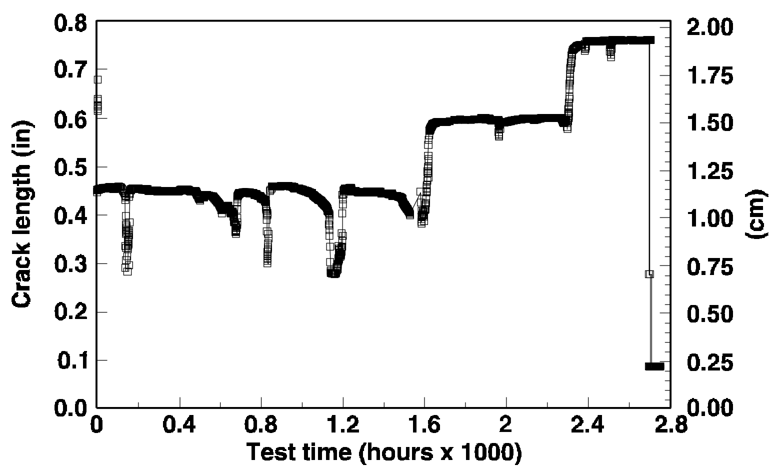

Figure 3-5 Crack length versus time for displacement rate 2.5 x10^{-10} m/sec

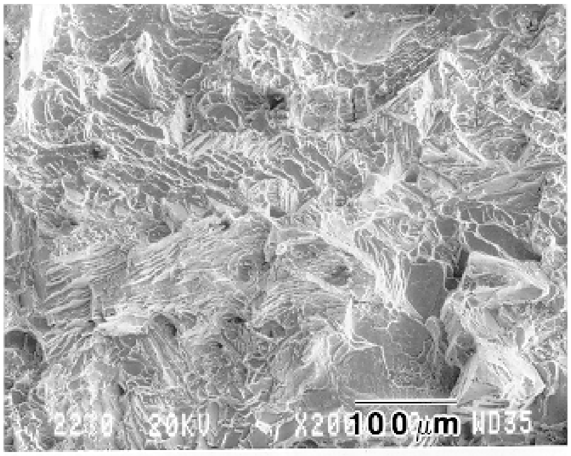

(a) Specimen INEL-1 tested at 2.5×10^{-8} m/sec

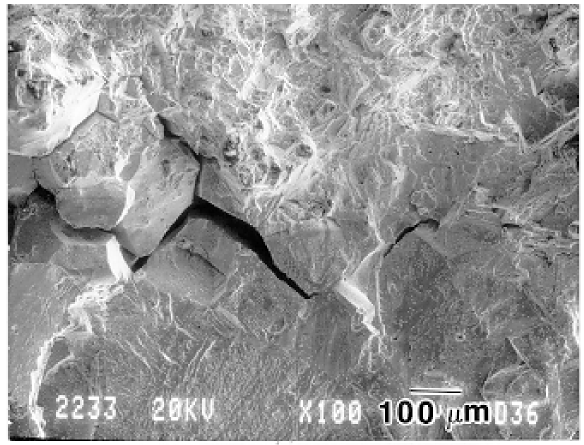

(b) Sepcimen INEL-2 tested at 2.5×10^{-9} m/sec

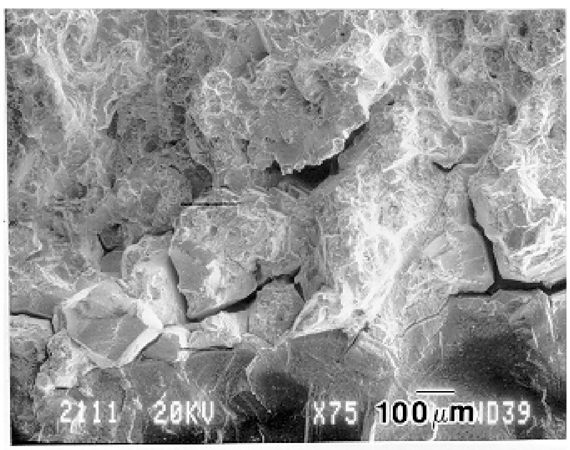

(a) Specimen INEL-3 tested at 1.3×10^{-9} m/sec

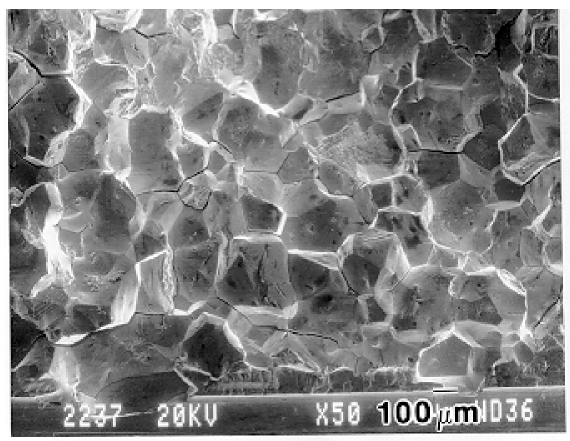

(b) Sepcimen INEL-4 tested at 2.5×10^{-10} m/sec

Figure 3-6 SEM fractographs of specimens tested at various displacement rates

Heat treatment affects SCC resistance significantly. Figure 3-8 compares the results for the heat treatment conditions, which were given a 1093 °C annealing treatment, using the VIM-ESR direct-age alloy 718. Comparison of the curves in Figure 3-8 shows that heat treatments including an aging step at or near 788 °C have higher crack growth rates than those aged at lower temperatures. The two heat treatments utilizing long-term, low-temperature aging treatments (DA-OA-C and DA-2Age) are immune to SCC under these test conditions.

Alternative Alloys.

The test results for the alternative alloys are presented in Appendix B. Table 3-3 lists crack growth rates at 60 MPa√m for the alternative alloys, as well as estimates of K_{ISCC}. Figures 3-9 through 3-11 present some of the results for the alternative alloys. Comparing the curves for TY-AERO and DA-AERO in Figure 3-9 demonstrates that some improvement in SCC resistance may be realized by switching from alloy 718 to Ticolloy. Figure 3-10 shows that the other experimental alloys in the Ticolloy series have significantly poorer performance in the rising-load K_{ISCC} test than Ticolloy or alloy 718.

Figure 3-11 compares Hicoroy with alloy X-750 and with the spread in performance for the alloy 718 conditions. Alloy X-750 has crack growth rates that are almost as low as the best alloy 718 conditions, while Hicoroy, which was designed for SCC resistance, performs on par with the average alloy 718 materials.

Table 3-2 K_{ISCC} and Crack Growth Rate Results for Alloy 718 Heat Treatments

Heat	Specimen ID	Crack Growth Rate at 60 MPa√m (m/sec x 10^{-10})	Estimated K_{ISCC}, MPa√m
VIM-VAR HDF-718	INEL-1	NO SCC	—
	INEL-2	SLIGHT SCC	—
	INEL-3	2.5	13
	INEL-4	SCC, NO DATA	—
VIM-ESR HS-718	HS-CONV1	12.6	<15
	HS-CONV2	12.6	<25
	HS-AERO	2.1	
VIM-ESR DA-718	DA	5.1	<25
	DA-ANN	NO SCC	—
	DA-CONV	9.2	<25
	DA-AERO1	2.2	18
	DA-AERO2	2.0	18
	DA-OA-A	2.9	25
	DA-OA-B	16.5	21
	DA-OA-C	NO SCC	—
	DA-OA-D	40.0	16
	DA-1Age	2.8	12
	DA-2Age	NO SCC	—
	DA-HEA	3.1	<25
	DA-HEB	10.5	<35
	DA-OW	21.2	<25
VIM-ESR-VAR HS-718	TM-CONV	11.0	10
	TM-AERO	NO SCC	—
VIM-EBCHR	EBCHR	SCC, NO DATA	—
Yt718	Yt718	NO SCC	—

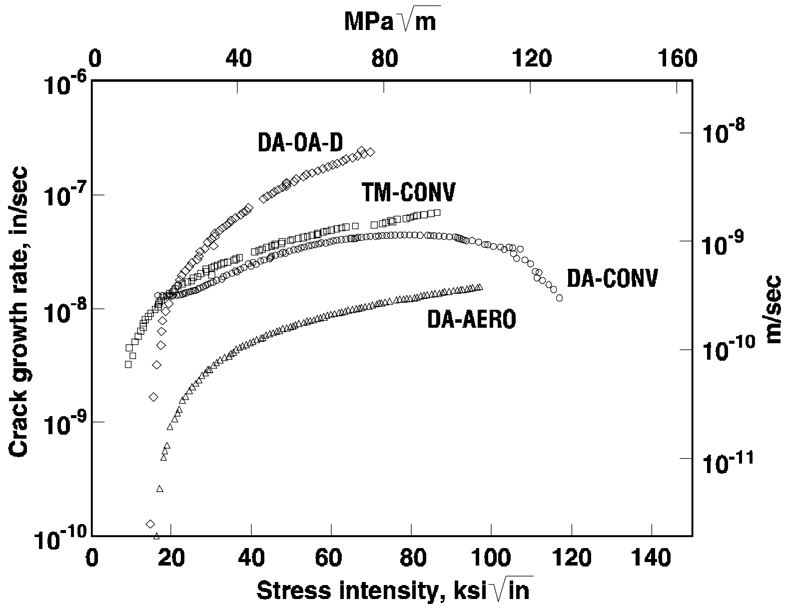

Figure 3-7 Melt practice effect on crack growth rates for the CONV condition. The DA-AERO condition underwent SCC while the triple-melt TM-AERO condition did not.

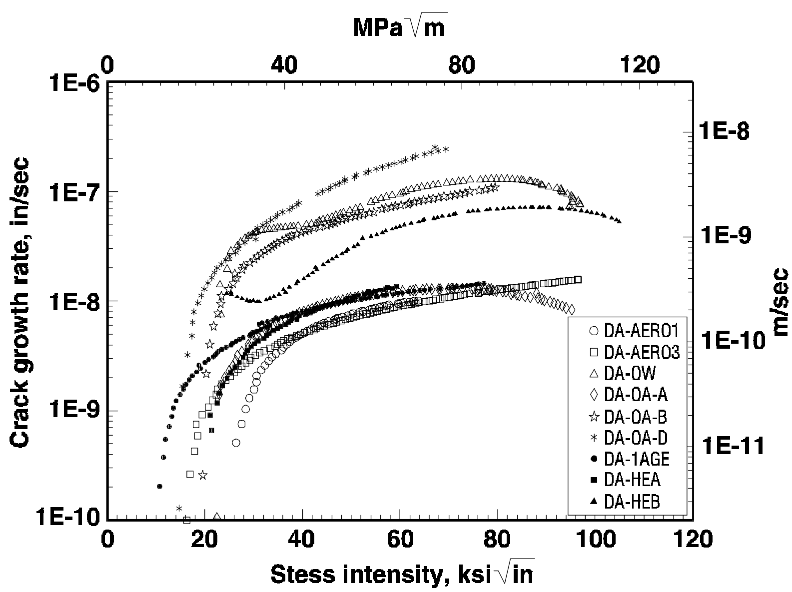

Figure 3-8 Crack growth rate versus applied stress intensity for VIM-ESR direct aged alloy 718 conditions annealed at 1093 °C. The four specimens with the highest crack growth rates were aged near 788 °C.

Table 3-3
K_{ISCC} and Crack Growth Rate Results for Alternative Alloys

Heat	Specimen ID	Crack Growth Rate at 60 MPa√m (m/sec x 10^{-10})	Estimated K_{ISCC}, MPa√m
X-750	HTH	3.6	22
HICOROY	STAG	8.3	26
Ticolloy	TY-HS	4.6	<24
	TY-CONV	14.0	20
	TY-AERO	1.3	<30
Alloy 13	13-AERO	16.0	20
Alloy 14	14-AERO	14.0	20
	14HS	84.0	12
Alloy 15	15-AERO	12.0	18

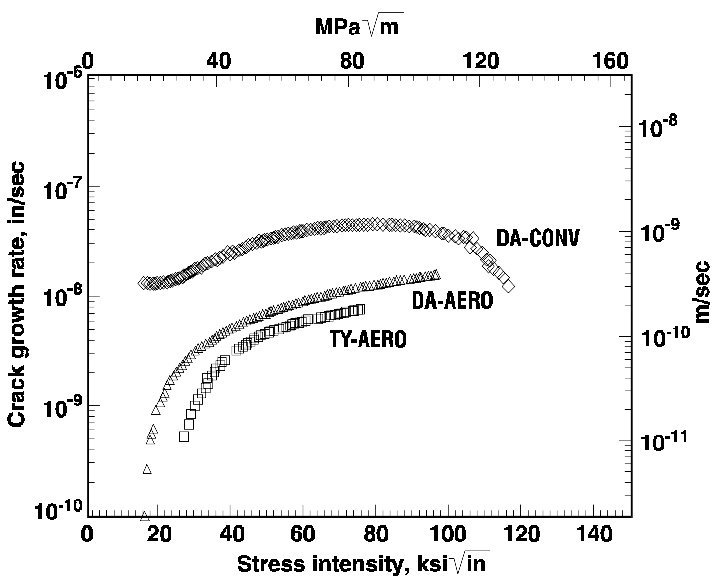

Figure 3-9 Improved SCC resistance of Ticolloy chemistry

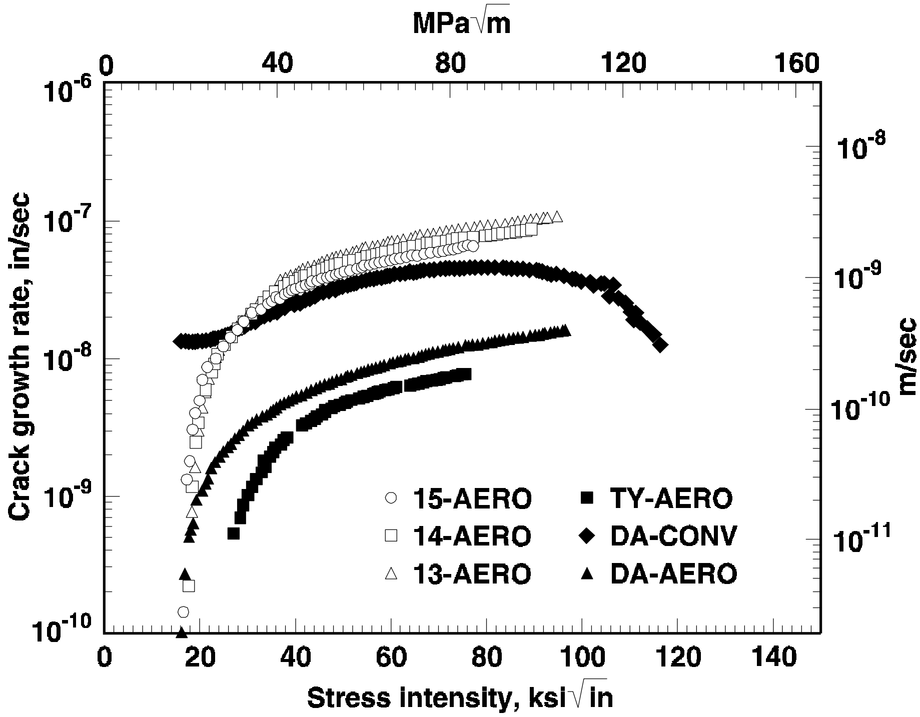

Figure 3-10 SCC resistance of alternative alloys

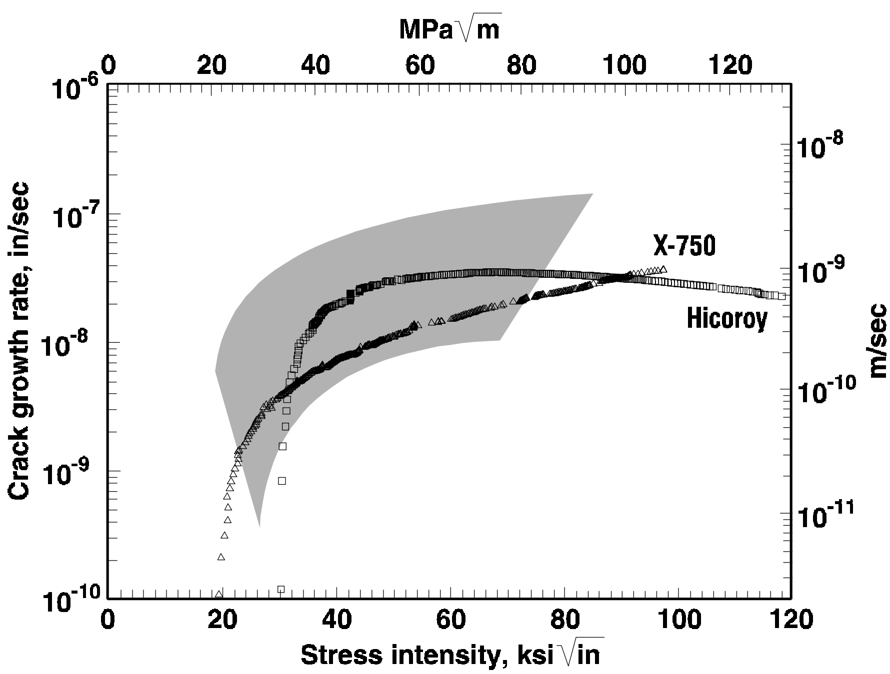

Figure 3-11 SCC resistance of alloy X-750 and Hicoroy compared to alloy 718

4

DISCUSSION

Constant-Displacement-Rate K_{ISCC} Test Method

The results presented above demonstrate that the constant-displacement-rate K_{ISCC} test method is a rapid means of providing the crack growth rate versus stress intensity factor curve for high-strength, nickel-base alloys. Older methods, such as constant displacement tests and constant load tests, can take 10 times longer to produce the same information, and multiple specimens are required. Long test durations with multiple specimens increase the potential for difficulties with remote crack length sensing techniques such as potential drop. Either a separate power supply is required for each specimen, or they must be wired in series, which allows the possibility of significant drops in potential between specimens. Increasing the current to overcome power losses along the chain can lead to polarization of the string away from the open circuit potential, interfering with the corrosion processes that are being measured.

The constant-displacement-rate method can provide the da/dt versus K curve using a single specimen in two or three weeks, depending upon the material/environment combination. Careful attention must be paid to fatigue precracking, because even slight irregularities in the precrack can shift the K_{ISCC} dramatically. Also, the final ΔK used for precracking should be as low as possible, because SCC data recorded at lower K levels than the final K_{max} used in precracking are influenced by residual stresses remaining from precracking. When comparing results for different material conditions, it is best to compare crack growth rates rather than K_{ISCC} values. Where design quality K_{ISCC} information is required, a constant K method is recommended. This method allows real-time correction of the load based on DCPD crack length measurements to maintain a constant crack tip stress intensity factor. The K level is reduced incrementally until the crack growth rate drops below a given minimum value, such as 10^{-11} m/sec.

Alloy 718 Conditions

Melt Practice

The alloy 718 results show that SCC resistance in the PWR primary-side environment is affected by melt practice and heat treatment. For the materials studied, heat treatment appears to have a more dramatic effect than melt practice.(19) Comparing the triple-melt (VIM-ESR-VAR) and VIM-ESR direct-age heats in the CONV condition (see Fig. 3-7) indicates no significant effect of melt practice on SCC resistance in this highly susceptible heat treatment condition. The CONV condition has copious grain boundary δ resulting from the one hour exposure at 954 °C, which may overwhelm the effect of improved cleanliness in the triple-melt heat. However, note that both of these heats are clean relative to other commercially available material. Cleanliness has been shown to affect SCC resistance among heats with high inclusion content even in conventionally heat treated material.(16)

Comparison of the triple-melt, VIM-ESR direct-age, and EBCHR heats in the AERO condition shows that melt practice does make a difference. The triple-melt heat did not undergo SCC in the AERO condition, while the other two heats did. While the superior performance of the triple-melt heat may be a result of the extra melting step, it may also result from lower strength. The R_C hardness of the TM-AERO specimen is 10 points lower than the hardness of the DA-AERO or EBCHR-AERO specimens. The lower hardness is likely a result of fewer inclusions available for retarding grain growth during annealing.

Heat Treatment

A significant influence of heat treatment on SCC performance is readily apparent. Careful comparison of the test results points to the involvement of grain boundary precipitates in the SCC of alloy 718.(20,21) The annealed (DA-ANN) specimen did not undergo SCC, indicating that susceptibility to SCC is caused by a phenomenon occurring during precipitation hardening. Comparing the curves in Figure 13 shows that heat treatments including an aging step at or near 788 °C, where δ precipitates, have higher crack growth rates than those aged at lower temperatures.

It is believed that grain boundary δ phase exacerbates SCC by forming a galvanic couple between itself and the neighboring grains, providing a driving force for corrosion at the grain boundaries.(22) Hydrogen may also play a role in the SCC of alloy 718, with the δ precipitates acting as hydrogen traps. Even at 360 °C, hydrogen embrittlement is possible in alloy 718 in the PWR primary-side environment.(16) Curiously, specimen DA, which had no anneal to dissolve the delta formed during direct-age processing, also showed good SCC resistance. One might expect the morphology and possibly stoichiometry of the δ formed during thermomechanical processing to differ from that of δ formed during isothermal age hardening.

The DA-1Age specimen (718 °C/8h) was aged in the γ″ region without crossing the δ curve as it is drawn in Figure 2-2. (However, without a detailed metallographic exam, it cannot be concluded that the material is free from δ phase). The DA-1Age specimen underwent SCC, but at a slower rate than conditions aged near 788 °C, as shown in Figure 3-8. Lengthening the exposure at 718 °C to 50h creates the DA-OA-A (718 °C/50h) condition, which has similar crack growth rates but a higher K_{ISCC} value.

Adding to OA-A an additional 50h treatment at 663 °C creates OA-C (718 °C/50h + 663 °C/50h), which showed no SCC. Apparently long-term aging in the γ″ region improves SCC resistance, but the mechanism is not known. Examination in the TEM shows fine rather than overaged γ′ and γ″. The OA-C condition shows promise for service application because of its combination of high hardness and good SCC resistance.

These results are important for application of alloy 718 in corrosive environments. The CONV condition is most commonly used, but produces poor SCC resistance. Improvement can be obtained by switching to the OA-A or the AERO condition with only slight reduction in material hardness. Examining the DA-CONV, DA-AERO, and DA-2Age conditions in a transmission electron microscope (TEM) determined that the DA-CONV material has intergranular delta phase. The more resistant DA-AERO and DA-2Age conditions have precipitate-free grain boundaries. All three conditions have uniform distributions of fine γ′ and γ″.(23,24)

Besides the annealed (DA-ANN) condition, three material conditions did not undergo SCC under the test conditions. The DA-OA-C and DA-2Age conditions, which were each aged for 100 h, and the Yt718 condition, which was given the same aging treatment as the AERO conditions, are immune to SCC under these test conditions. The reason for the immunity is not clear, although it goes beyond clean grain boundaries. Alloy 718 in the AERO condition has clean grain boundaries, but it does exhibit SCC under these test conditions. The DA-OA-C and DA-2Age treatments were intended to produce overaged γ′ to impede slip-step formation, but TEM examination shows fine, coherent precipitates.

The Yt718 material has an addition of 0.1% yttrium. Yttrium is expected to segregate to the grain boundaries, making the grain boundaries more electrochemically noble than the surrounding matrix, and thereby inhibiting intergranular SCC. Yttrium may also accelerate formation of the protective chromia scale. Additions of zirconium, another refractory metal, are routinely made to alloy X-750 with similar results.

Alternative Alloys

The alloy chemistry series from the University of Texas has mixed effects on SCC resistance. The Ticolloy chemistry has better SCC resistance than standard alloy 718 chemistry, as anticipated. TEM examination reveals δ-free grain boundaries for the TY-AERO specimen. Standard alloy 718 in the AERO condition also has δ-free grain boundaries, and the improvement realized by the Ticolloy chemistry may result from differences in grain boundary chemistry or in chemistry of the γ′ and/or γ″ precipitates. Since γ′ and γ″ are also present intergranularly, changes in the composition could affect resistance to intergranular SCC.

Comparing the results from specimens 13-AERO, 14-AERO, and 15-AERO shows very similar behavior for all three alloy chemistries. The three chemistries have K_{ISCC} values similar to alloy 718 and Ticolloy in the same heat treatment condition, but the crack growth rates are almost an order of magnitude faster for these three special chemistries.

Examination in a scanning-electron microscope shows grain boundary δ for alloys 13, 14, and 15, and δ-free grain boundaries for Ticolloy and alloy 718 in the same heat treatment condition.(23,25) The grain boundary δ is not predicted based on the compositions and heat treatment. In particular, it is surprising to see grain boundary δ in alloy 13, which has a lower concentration of Nb + Ta than Ticolloy. Regrettably, alloys 13, 14, and 15 were melted, forged, and heat treated by different suppliers than those that prepared the Ticolloy. It is possible that a difference in preparation caused the poor performance for alloys 13, 14, and 15.

The HTH heat treatment for alloy X-750 was developed to be resistant to SCC in the PWR environment. The alloy Hicoroy was developed with the same objective. Neither performs as well as the more SCC-resistant alloy 718 conditions. The alloy 718 conditions are also stronger. The DA-AERO condition has a yield strength of 1145 MPa compared with 741 MPa for alloy X-750 HTH and 854 MPa for Hicoroy. For PWR applications where SCC is a concern, alloy 718 is the best choice.

5

CONCLUSIONS

From the work presented here, the following conclusions can be drawn regarding SCC of alloy 718 and related alloys in constant-displacement-rate (1.3 x 10^{-9} m/sec) K_{ISCC} tests in 360 °C PWR primary water:

Excellent specimen-to-specimen reproducibility in crack growth rate measurements is obtainable using the constant-displacement-rate K_{ISCC} test method. Occasional anomalies near crack initiation can introduce uncertainty into the K_{ISCC} estimate, and it is preferable to compare materials on the basis of crack growth rates.

Annealing temperature affects the K_{ISCC} value and SCC growth rate for alloy 718. Material given a high-temperature anneal (1093 °C) performs better than material annealed at a lower temperature (954 °C) when both are given the same commonly used two-step aging treatment (718 °C/8h + 621 °C/8h/AC).

Aging treatment affects the SCC resistance of alloy 718. Aging material at the nose of the precipitation curve for d degrades SCC performance, while long-term aging at lower temperatures improves SCC performance.

Long-term aging at low temperatures is beneficial to SCC resistance. Material given a high-temperature anneal (1093 °C) followed by two-step aging for long times (718 °C/50h + 663 °C/50h) produces no SCC under the test conditions, despite a Rockwell C hardness of 42. Material given the same anneal and a single lengthy age (663 °C/100h) has a somewhat lower hardness (37 R_C) and produces no SCC under the test conditions.

Triple-melted (VIM-ESR-VAR) alloy 718 has better resistance to SCC than material remelted by the ESR or EBCHR processes when all are given an SCC-resistant heat treatment (1093 °C/1h/WQ + 718 °C/8h + 621 °C/8h/AC), although the triple-melted material has much lower hardness (by 10 R_C). When in a more susceptible heat treatment condition (954 °C/1h/AC + 718 °C/8h + 621 °C/8h/AC), no effect of melt practice is observed for the melt practices tested.

Alloy 718 with an addition of 0.1% yttrium has improved SCC resistance compared with the standard composition.

Ticolloy, an alloy 718 chemistry variant with higher Nb + Ta and Al, has improved SCC resistance compared with the standard composition.

Alloy 718 given a high-temperature anneal (1093 °C) followed by two-step aging (718 °C/8h + 621 °C/8h/AC) has a yield strength of 1145 MPa, compared with 741 MPa for alloy X-750 (HTH condition) and 854 MPa for Hicoroy. For PWR applications where SCC is a concern, alloy 718 provides the best combination of strength and corrosion resistance.

6

REFERENCES

1. Miglin, M.T., *Microstructure and Stress Corrosion Resistance of Alloy X-750, 718, and A-286 in Light-Water-Reactor Environments*, Report No. NP-6363 and NP-6392-M, Electric Power Research Institute, Palo Alto, CA, 1989.

2. Miglin, M.T., and Domian, H.A., "Microstructure and Stress Corrosion Resistance of Alloys X-750, 718, and A-286 in Light-Water-Reactor Environments", *Journal of Materials Engineering*, Vol. 9, No. 2, June 1987, pp. 113-132.

3. Miglin, M.T., and Domian, H.A., "Metallurgical Characterization of Ni-Cr-Fe Alloys as Related to Stress Corrosion Cracking in Light Water Reactors", *Proceedings of the International conference on Corrosion of Nickel-Base Alloys*, 1985, ASM, Metals Park, OH, pp. 147-164.

4. Burke, M.G., and Miller, M.K., "Precipitation in Alloy 718: A Combined AEM and APFIM Investigation," *Superalloys 718, 625 and Various Derivatives*, E.A. Loria, Ed., TMS-AIME, 1991, pp. 337-350.

5. Wilson I.L.W., and Burke, M.G., "The Effect of Microstructure on the SCC Behavior of Alloy 718", *Superalloys 718, 625 and Various Derivatives*, E.A. Loria, Ed., TMS-AIME, 1991, pp. 681-693.

6. Loria, E.A., "The Status and Prospects of Alloy 718," *Journal of Metals*, July, 1988, pp. 36-41.

7. Collier, J.P., Wong, S.H., Phillips, J.C., and Tien, J.K., "The Effect of Varying Al, Ti, and Nb Content on the Phase Stability of Inconel 718," *Metallurgical Transactions A*, Vol. 19A, July 1988, pp. 1657-1666.

8. Floreen, S., and Nelson, J.L., "The Effects of Heat Treatment and Composition on the Stress Corrosion Cracking Resistance of Inconel X-750," *Met. Trans. A.*, Vol. 14A, January 1983, pp. 133-139.

9. Hattori, S., Yamauchi, K., Urayama, Y., Kuniya, J., and Itow, H., *Proceedings of the Fourth International Symposium on Environmental Degradation of Materials in Nuclear Power Systems—Water Reactors*, NACE, Houston, 1990, pp. 11-1 - 11-11.

10. Fritzemeier, L.G., and Chandler, W.T., *Superalloys, Supercomposites, and Superceramics*, J.K. Tien and T. Caulfield, Eds., Academic Press, 1989, pp. 491-524.

11. Onyewenyi, O.A., *Superalloy 718: Metallurgy and Applications*, E.A. Loria, Ed., TMS-AIME, 1989, pp. 345-362.

12. Miglin, M.T., and Nelson, J.L., "Strain Rate Sensitivity of Alloy 718 to Stress Corrosion Cracking", *Superalloys 718, 625 and Various Derivatives*, E.A. Loria, Ed., TMS-AIME, Warrendale, PA, 1991, pp. 695-704.

13. Mayville, R.A., Warren, T.W., and Hilton, P.D., *Journal of Testing and Evaluation*, Vol. 17, No. 4, July 1989, pp. 203-211.

14. Dietzel, W., and Schwalbe, K.H., *Materialprufung*, Vol. 28, No. 11, Nov. 1986, pp. 368-372.

15. Judy, Jr., R.W., King, Jr., W.E., Hauser II, J.A., and Crooker, T.W., Naval Research Laboratory Memorandum Report No. 5896, Dec. 30, 1986.

16. Miglin, B.P., Miglin, M.T., Monter, J.V., Sato, T., and Aoki, K., "Stress Corrosion Cracking of Commercial Grade Alloy 718 in Pressurized-Water-Reactor Primary Water," *Proceedings of the Fourth International Symposium on Environmental Degradation of Materials in Nuclear Power Systems—Water Reactors,* National Association of Corrosion Engineers, Houston, 1990, pp. 11-32—11-44.

17. Schwalbe, K.H., and Hellmann, D., *Journal of Testing and Evaluation*, Vol. 9, No. 3, 1981, pp. 218-220.

18. Parkins, R.N., *British Corrosion Journal*, Vol. 14, No. 1, 1979.

19. Miglin, M.T., Monter, J.V., Wade, C.S., and Nelson, J.L., "Improved Stress Corrosion Performance for Alloy 718 via Melt Practice and Heat Treatment Variation," *Proceedings of the 12th International Corrosion Congress*, National Association of Corrosion Engineers, Houston, TX, September, 1993.

20. Miglin, M.T., Monter, J.V., Wade, C.S., Tien, J.K., and Nelson, J.L., "Stress Corrosion Cracking of Chemistry and Heat Treat Variants of Alloy 718, Part 1: Stress Corrosion Test Results", *Proceedings of the Sixth International Symposium on Environmental Degradation of Materials in Nuclear Power Systems—Water Reactors*, R.E. Gold and E.P. Simonen, Eds., The Minerals, Metals, and Materials Society, Warrendale, PA, 1993, pp. 815-820.

21. Miglin, M.T., Monter, J.V., Wade, C.S., and Nelson, J.L., "Effect of Heat Treatment on Stress Corrosion of Alloy 718 in Pressurized-Water-Reactor Primary Water," *Proceedings of the Fifth International Symposium on Environmental Degradation of Materials in Nuclear Power Systems—Water Reactors*, E.P. Simonen and R.E. Gold, Eds., American Nuclear Society, LaGrange Park, IL, 1991, pp. 279-286.

22. Hwang, I.S., Ballinger, R.G., and Prybylowski, J.W., *Journal of the Electrochemical Society*, Vol. 136, No. 7, July 1989.

23. Burke, M.G., Mager, T.R., Miglin, M.T., and Nelson, J.L., "The Effect of Thermal Treatment on SCC of Alloy 718: A Structure-Properties Study", *Superalloys 718, 625, 706 and Derivatives*, The Minerals, Metals and Materials Society, Warrendale, PA, 1994.

24. Burke, M.G., Mager, T.R., and Nelson, J.L., "Stress Corrosion Cracking of Chemistry Variants of Alloy 718, Part 2: Microstructural Characterization," *Proceedings of the Sixth International Symposium on Environmental Degradation of Materials in Nucelar Power Systems—Water Reactors*, The Minerals, Metals and Materials Society, Warrendale, PA, 1993, pp. 821-827.

25. Sheth, N.K., Manriquez, J.A., Freitas, C.A., Sanchez, J.M., Miglin, M.T., and Nelson, J.L., "Delta (Ni_3Nb) and IGSCC Degradation in Alloy 718 and Derivatives," *Proceedings of the Sixth International Symposium on Environmental Degradation of Materials in Nuclear Power Systems—Water Reactors*, R.E. Gold and E.P. Simonen, Eds., The Minerals, Metals, and Materials Society, 1993, pp. 815-820.

A

RESULTS OF CONSTANT DISPLACEMENT RATE K_{ISCC} TESTS FOR ALLOY 718 CONDITIONS

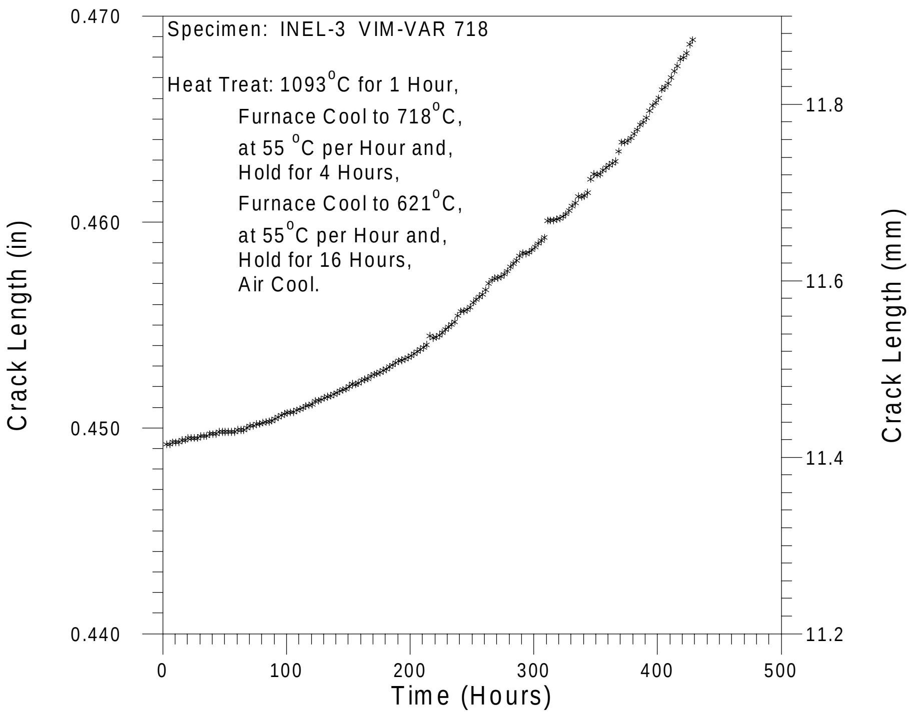
Specimen: INEL-3 VIM-VAR 718
Heat Treat: 1093°C for 1 Hour,
Furnace Cool to 718°C,
at 55 °C per Hour and,
Hold for 4 Hours,
Furnace Cool to 621°C,
at 55°C per Hour and,
Hold for 16 Hours,
Air Cool.
Crack Length (in)
0.470
0.460
0.450
0.440
Crack Length (mm)
11.8
11.6
11.4
11.2
Time (Hours)
0
100
200
300
400
500

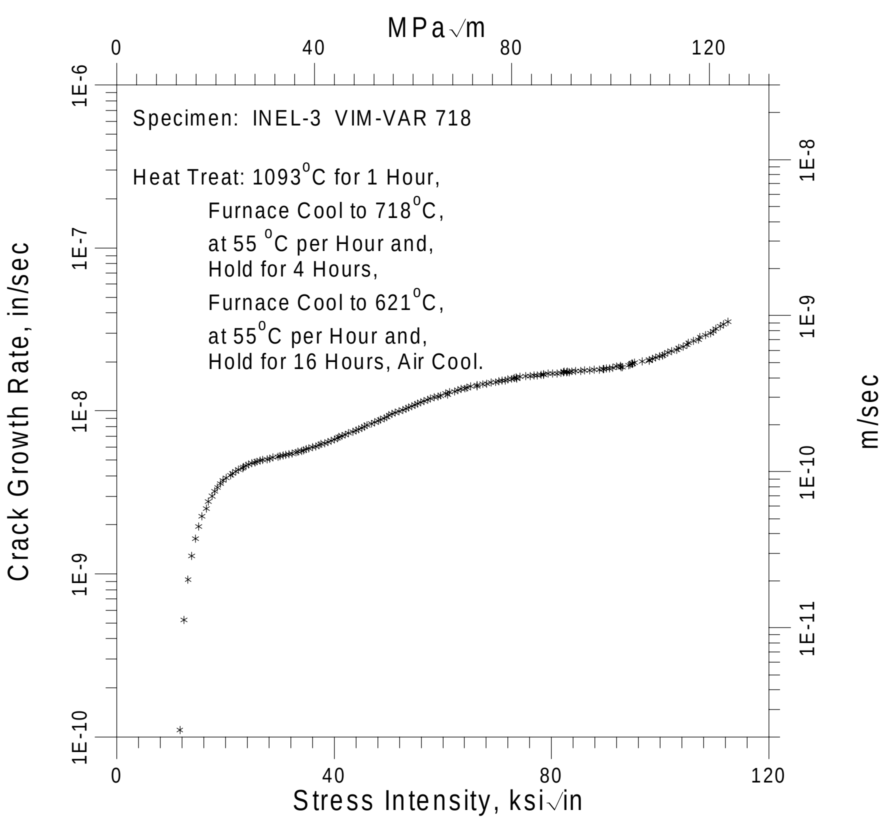
MPa√m
0
40
80
120
Specimen: INEL-3 VIM-VAR 718
Heat Treat: 1093°C for 1 Hour,
Furnace Cool to 718°C,
at 55 °C per Hour and,
Hold for 4 Hours,
Furnace Cool to 621°C,
at 55°C per Hour and,
Hold for 16 Hours, Air Cool.
Crack Growth Rate, in/sec
1E-6
1E-7
1E-8
1E-9
1E-10
m/sec
1E-8
1E-9
1E-10
1E-11
Stress Intensity, ksi√in
0
40
80
120

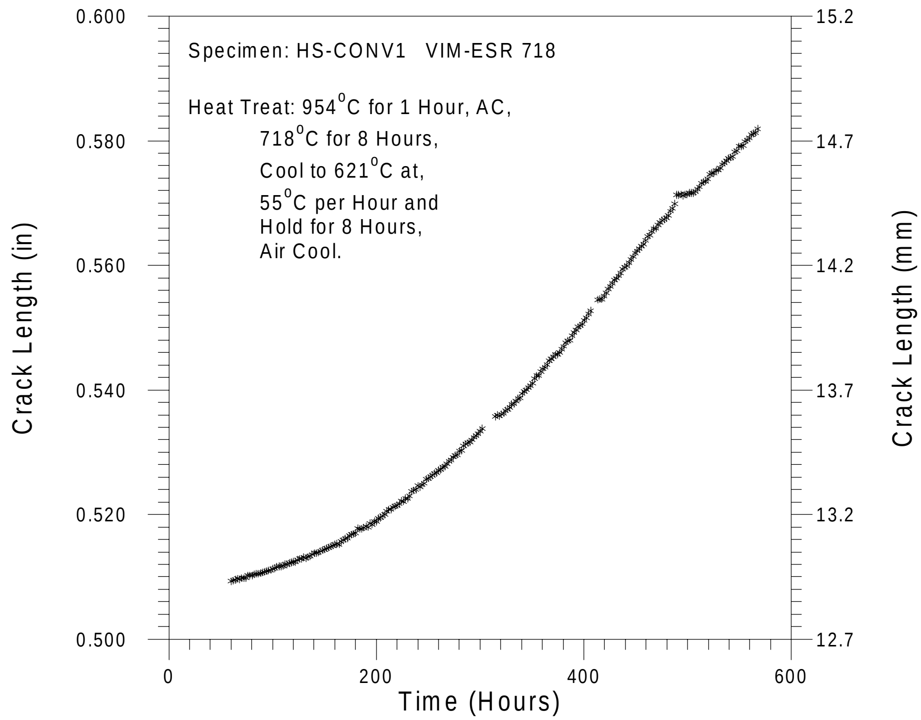
Specimen: HS-CONV1 VIM-ESR 718
Heat Treat: 954°C for 1 Hour, AC,
718°C for 8 Hours,
Cool to 621°C at,
55°C per Hour and
Hold for 8 Hours,
Air Cool.
Crack Length (in)
Crack Length (mm)
Time (Hours)
0.600
0.580
0.560
0.540
0.520
0.500
15.2
14.7
14.2
13.7
13.2
12.7
0
200
400
600

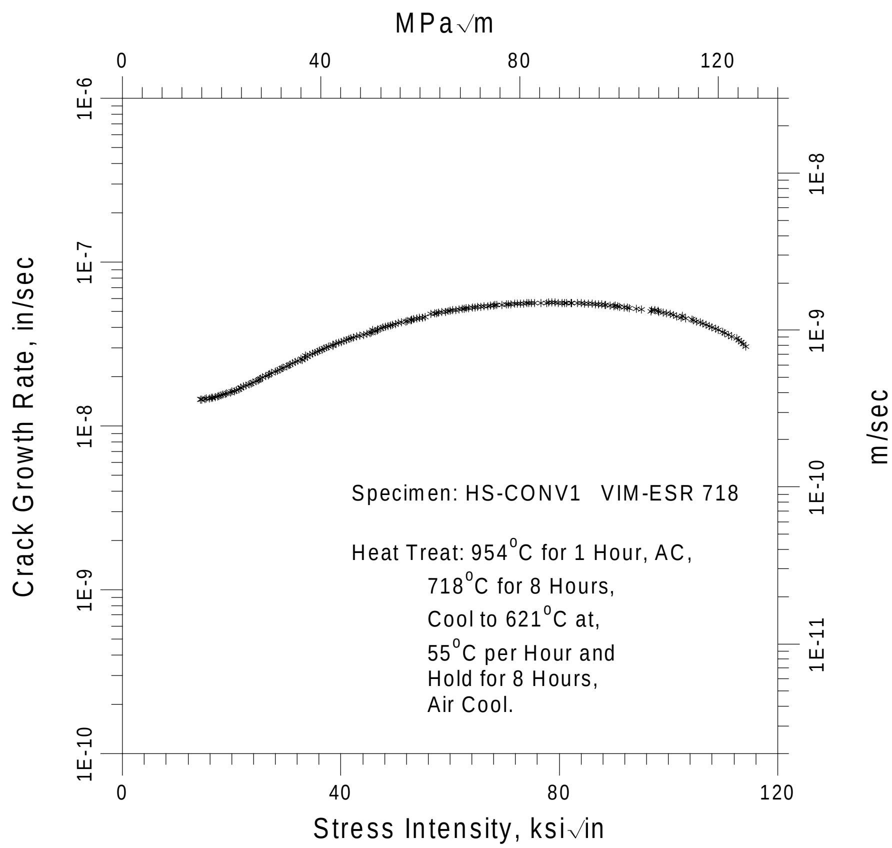
MPa√m
0
40
80
120
Crack Growth Rate, in/sec
m/sec
1E-6
1E-7
1E-8
1E-9
1E-10
1E-8
1E-9
1E-10
1E-11
Specimen: HS-CONV1 VIM-ESR 718
Heat Treat: 954°C for 1 Hour, AC,
718°C for 8 Hours,
Cool to 621°C at,
55°C per Hour and
Hold for 8 Hours,
Air Cool.
0
40
80
120
Stress Intensity, ksi√in

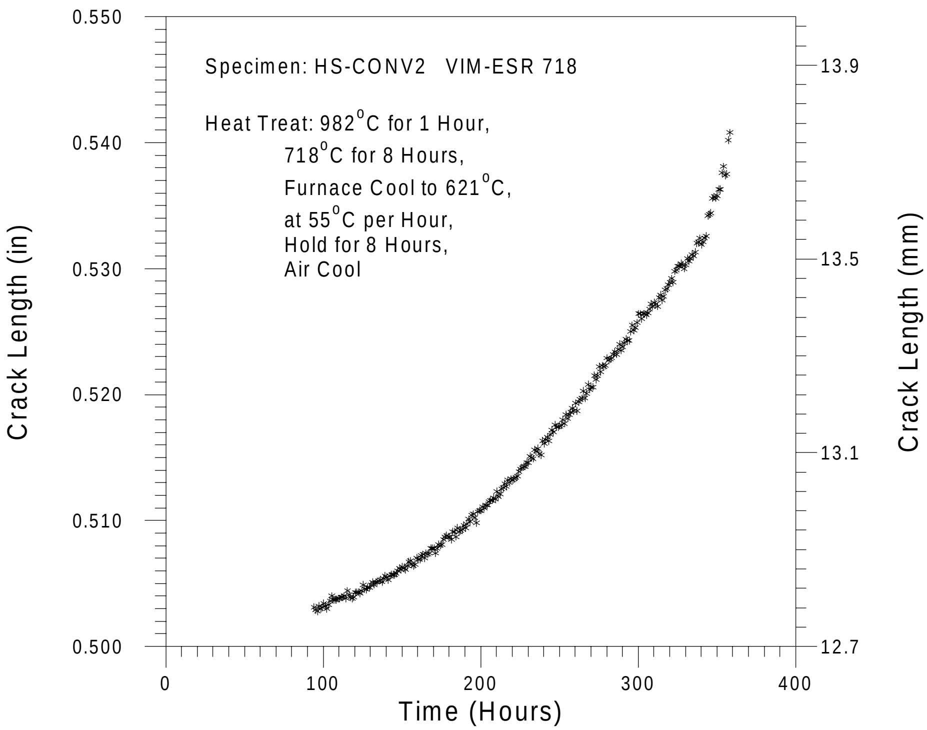
Specimen: HS-CONV2 VIM-ESR 718
Heat Treat: 982°C for 1 Hour,
718°C for 8 Hours,
Furnace Cool to 621°C,
at 55°C per Hour,
Hold for 8 Hours,
Air Cool
Crack Length (in)
Crack Length (mm)
Time (Hours)
0.500
0.510
0.520
0.530
0.540
0.550
12.7
13.1
13.5
13.9
0
100
200
300
400

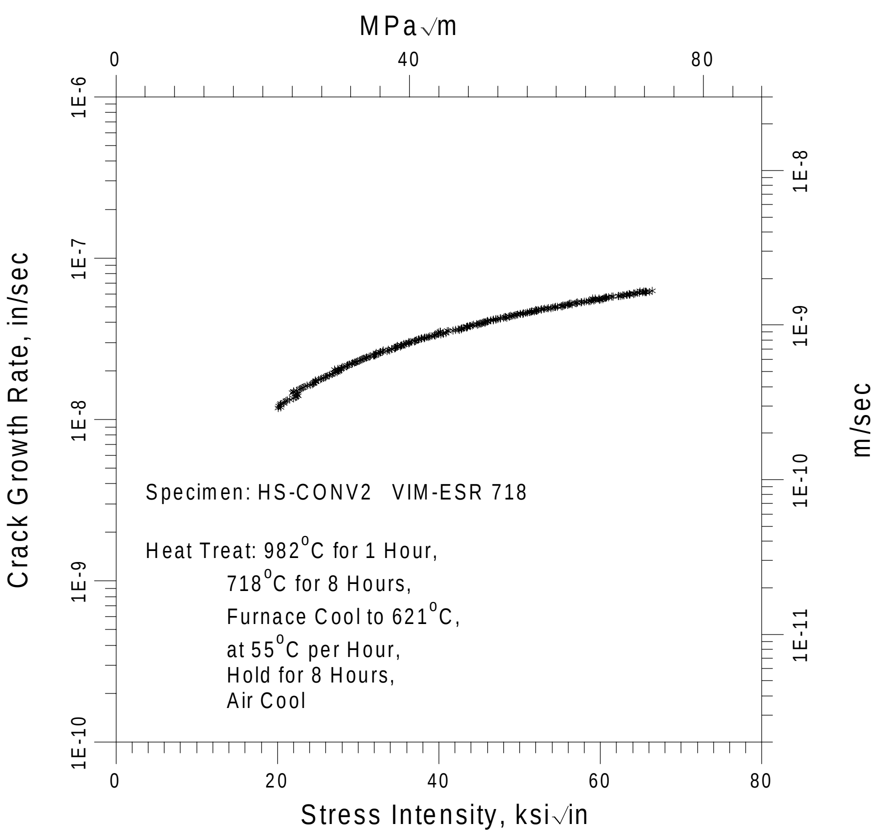
MPa√m
0
40
80
Specimen: HS-CONV2 VIM-ESR 718
Heat Treat: 982°C for 1 Hour,
718°C for 8 Hours,
Furnace Cool to 621°C,
at 55°C per Hour,
Hold for 8 Hours,
Air Cool
Crack Growth Rate, in/sec
m/sec
Stress Intensity, ksi√in
1E-6
1E-7
1E-8
1E-9
1E-10
1E-8
1E-9
1E-10
1E-11
0
20
40
60
80

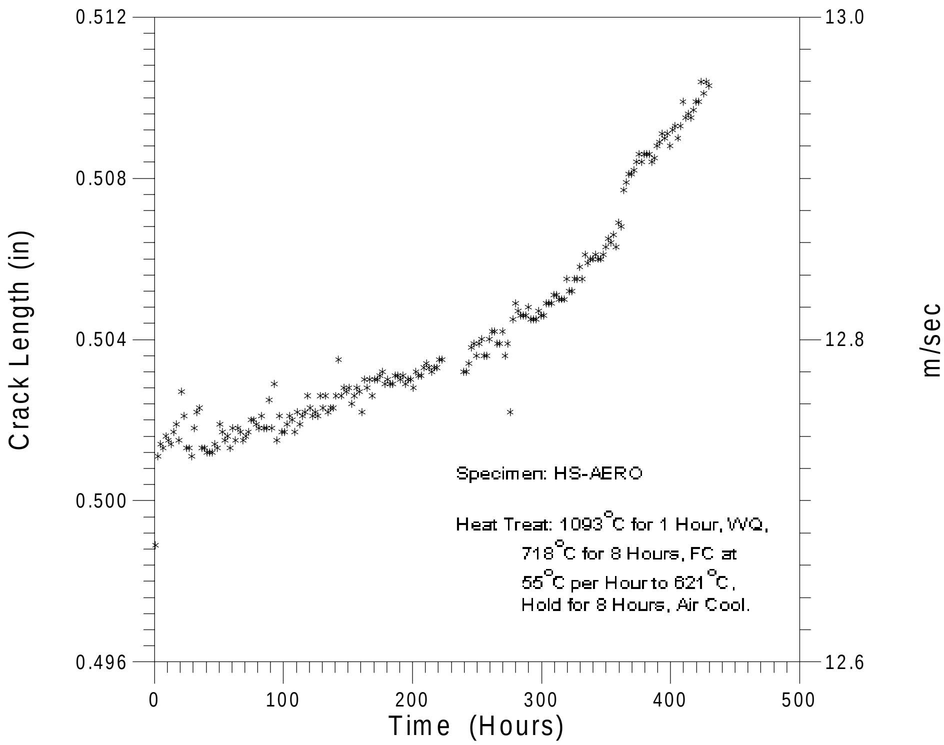
Crack Length (in)
0.512
0.508
0.504
0.500
0.496
13.0
12.8
12.6
m/sec
0
100
200
300
400
500
Time (Hours)
Specimen: HS-AERO
Heat Treat: 1093°C for 1 Hour, WQ,
718°C for 8 Hours, FC at
55°C per Hour to 621°C,
Hold for 8 Hours, Air Cool.

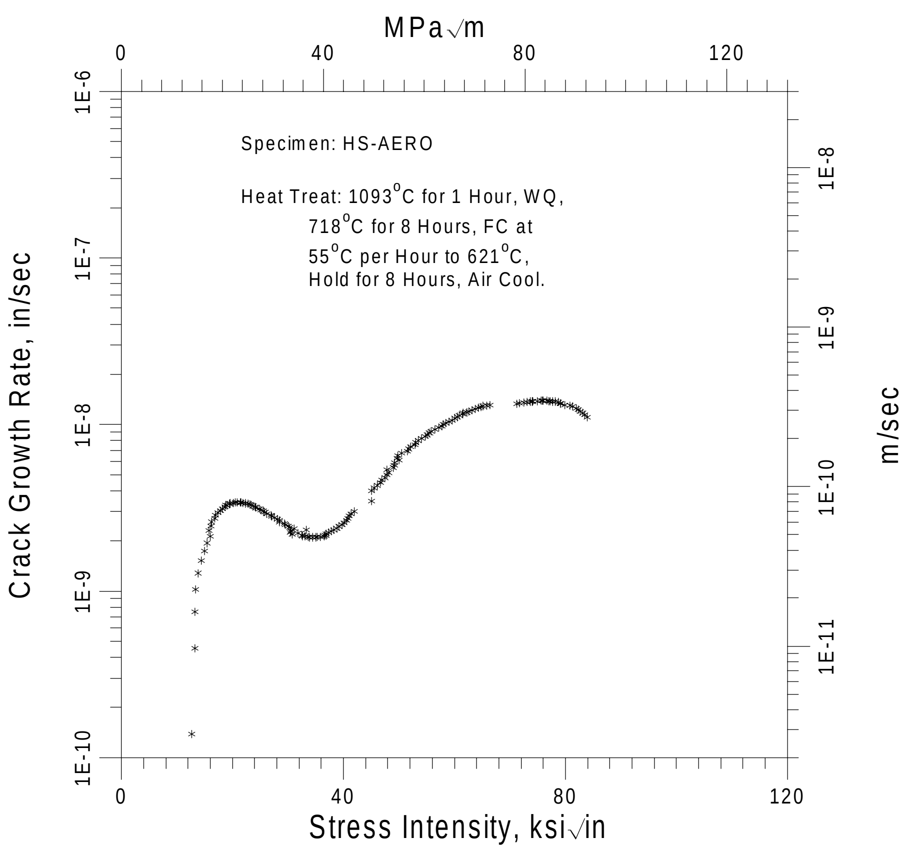
MPa√m
0
40
80
120
1E-6
1E-7
1E-8
1E-9
1E-10
Crack Growth Rate, in/sec
1E-8
1E-9
1E-10
1E-11
m/sec
Specimen: HS-AERO
Heat Treat: 1093°C for 1 Hour, WQ,
718°C for 8 Hours, FC at
55°C per Hour to 621°C,
Hold for 8 Hours, Air Cool.
0
40
80
120
Stress Intensity, ksi√in

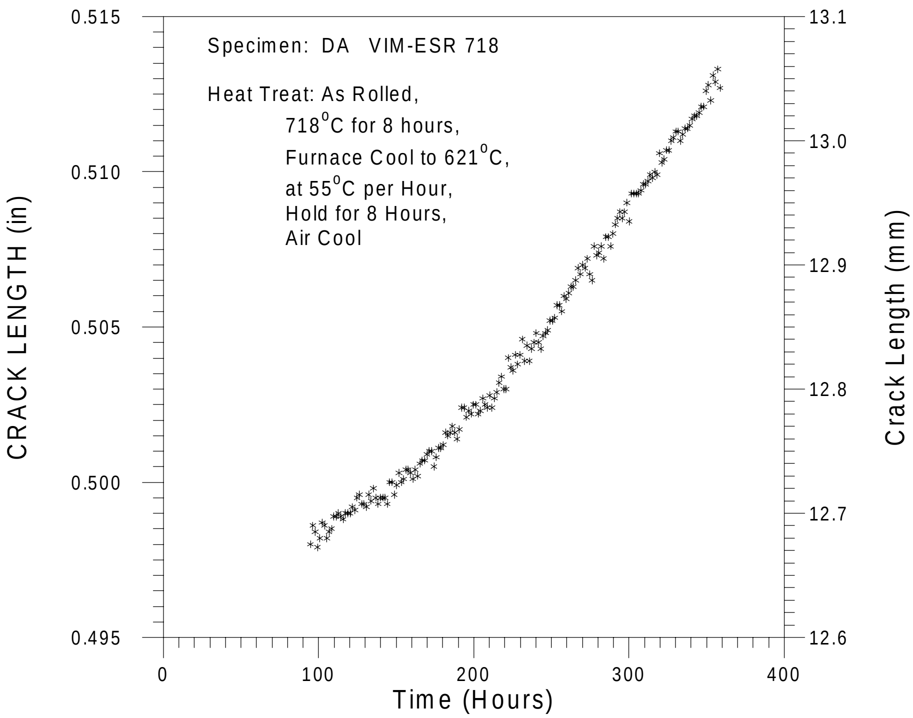
Specimen: DA VIM-ESR 718
Heat Treat: As Rolled,
718°C for 8 hours,
Furnace Cool to 621°C,
at 55°C per Hour,
Hold for 8 Hours,
Air Cool
CRACK LENGTH (in)
Crack Length (mm)
Time (Hours)
0.515
0.510
0.505
0.500
0.495
13.1
13.0
12.9
12.8
12.7
12.6
0
100
200
300
400

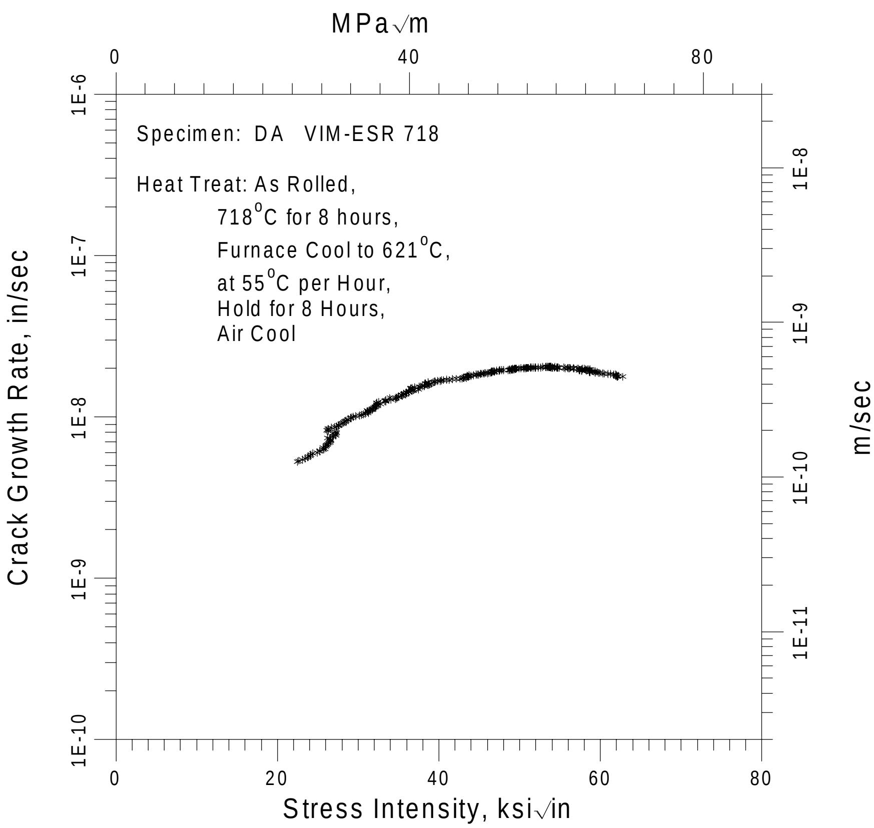
MPa√m
0
40
80
Specimen: DA VIM-ESR 718
Heat Treat: As Rolled,
718°C for 8 hours,
Furnace Cool to 621°C,
at 55°C per Hour,
Hold for 8 Hours,
Air Cool
Crack Growth Rate, in/sec
m/sec
1E-6
1E-7
1E-8
1E-9
1E-10
1E-8
1E-9
1E-10
1E-11
0
20
40
60
80
Stress Intensity, ksi√in

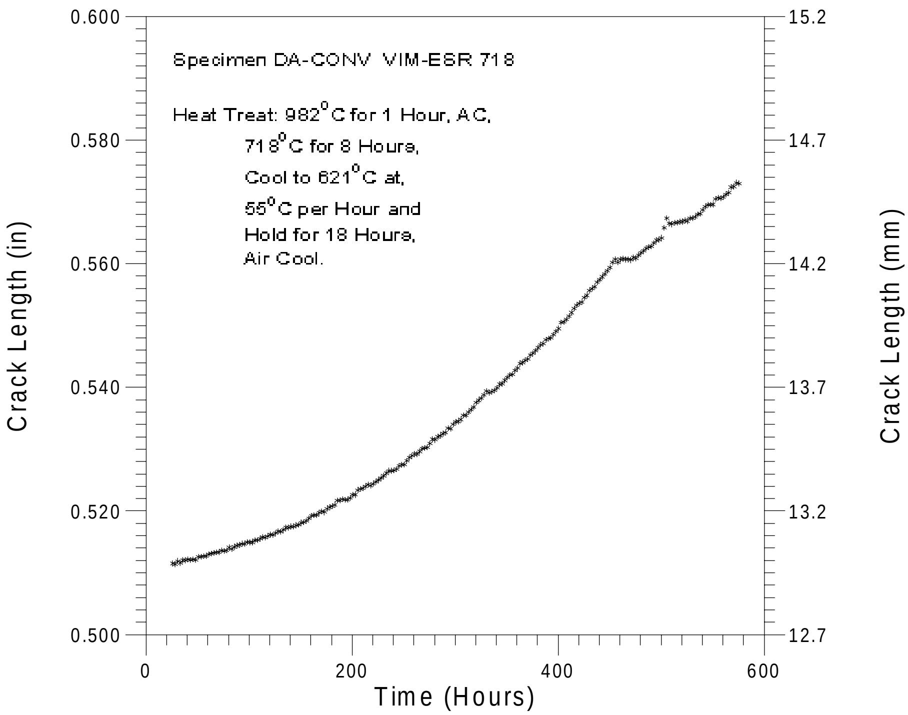
Specimen DA-CONV VIM-ESR 718
Heat Treat: 982°C for 1 Hour, AC,
718°C for 8 Hours,
Cool to 621°C at,
55°C per Hour and
Hold for 18 Hours,
Air Cool.
Crack Length (in)
Crack Length (mm)
Time (Hours)
0.600
0.580
0.560
0.540
0.520
0.500
15.2
14.7
14.2
13.7
13.2
12.7
0
200
400
600

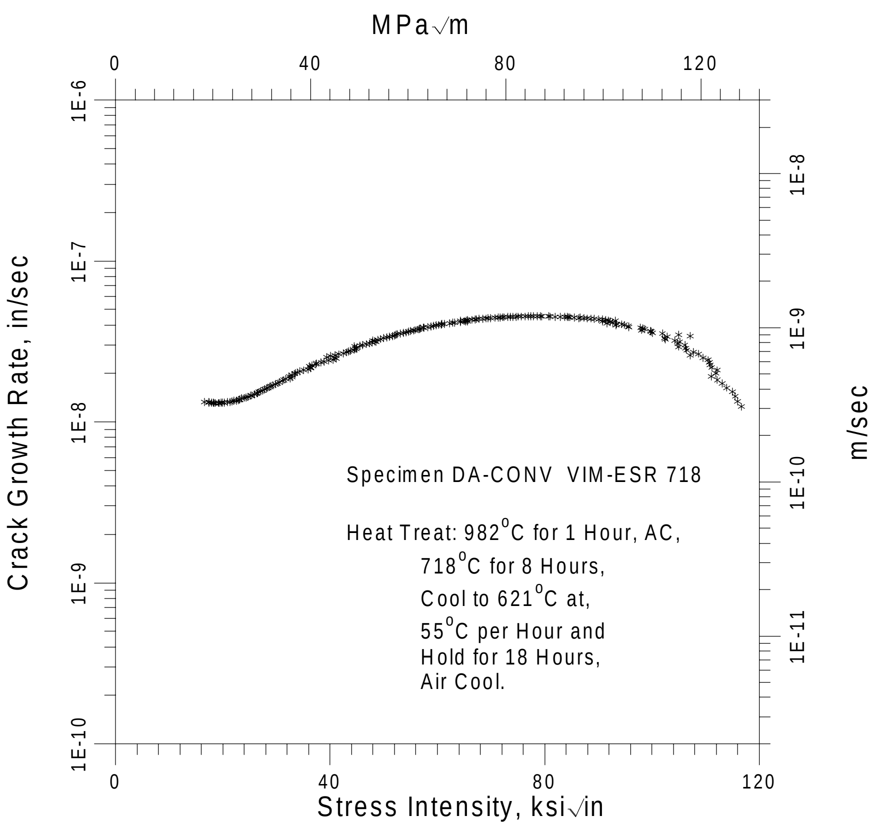
MPa√m
0
40
80
120
Crack Growth Rate, in/sec
m/sec
1E-6
1E-7
1E-8
1E-9
1E-10
1E-8
1E-9
1E-10
1E-11
Specimen DA-CONV VIM-ESR 718
Heat Treat: 982°C for 1 Hour, AC,
718°C for 8 Hours,
Cool to 621°C at,
55°C per Hour and
Hold for 18 Hours,
Air Cool.
0
40
80
120
Stress Intensity, ksi√in

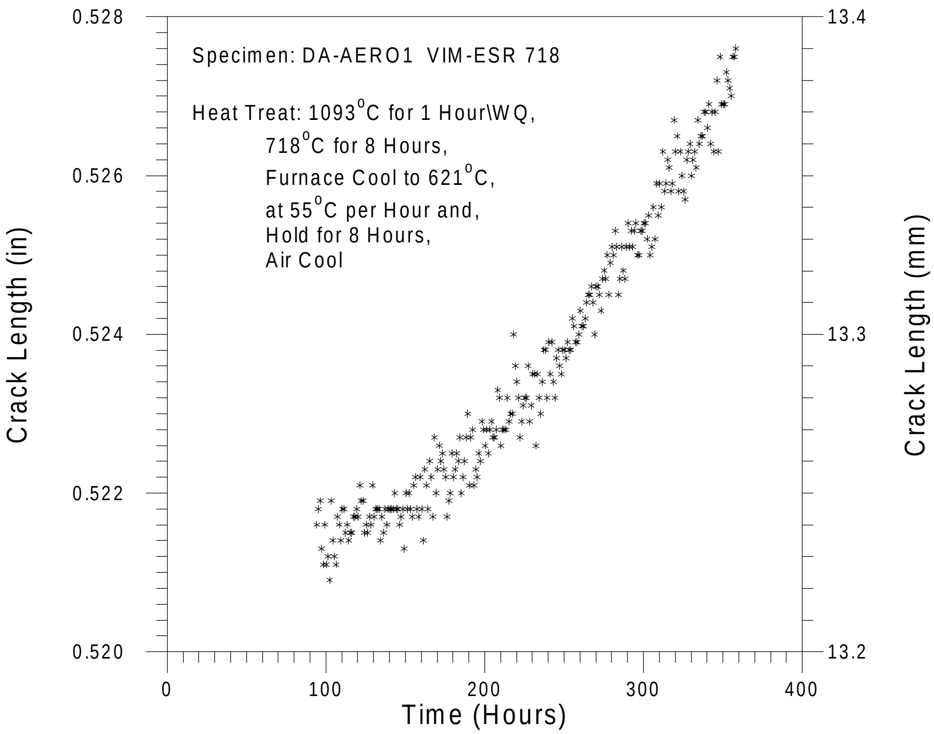
Specimen: DA-AERO1 VIM-ESR 718
Heat Treat: 1093°C for 1 Hour\WQ,
718°C for 8 Hours,
Furnace Cool to 621°C,
at 55°C per Hour and,
Hold for 8 Hours,
Air Cool
Crack Length (in)
Crack Length (mm)
Time (Hours)
0.528
0.526
0.524
0.522
0.520
13.4
13.3
13.2
0
100
200
300
400

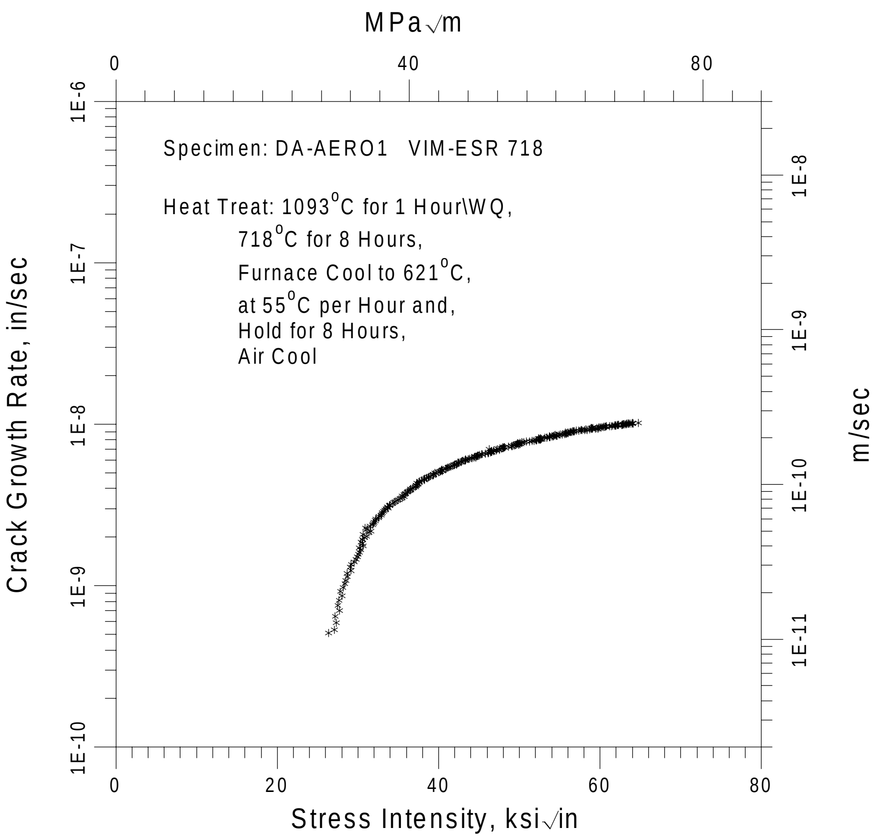
MPa√m
0
40
80
Specimen: DA-AERO1 VIM-ESR 718
Heat Treat: 1093°C for 1 Hour\WQ,
718°C for 8 Hours,
Furnace Cool to 621°C,
at 55°C per Hour and,
Hold for 8 Hours,
Air Cool
Crack Growth Rate, in/sec
m/sec
1E-6
1E-7
1E-8
1E-9
1E-10
1E-8
1E-9
1E-10
1E-11
0
20
40
60
80
Stress Intensity, ksi√in

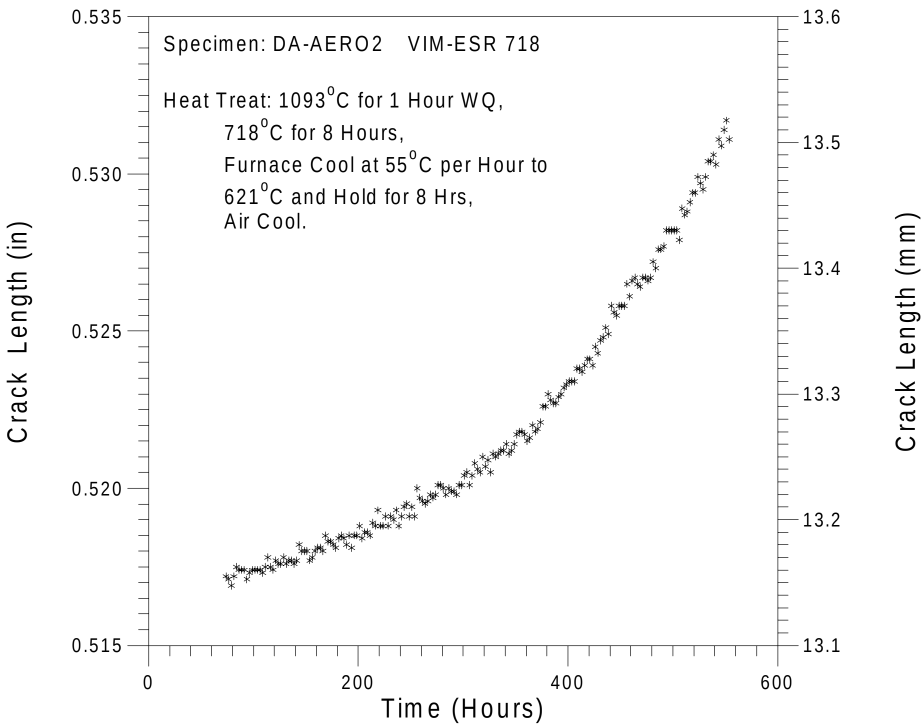
Specimen: DA-AERO2 VIM-ESR 718
Heat Treat: 1093°C for 1 Hour WQ,
718°C for 8 Hours,
Furnace Cool at 55°C per Hour to
621°C and Hold for 8 Hrs,
Air Cool.
Crack Length (in)
Crack Length (mm)
Time (Hours)
0.535
0.530
0.525
0.520
0.515
13.6
13.5
13.4
13.3
13.2
13.1
0
200
400
600

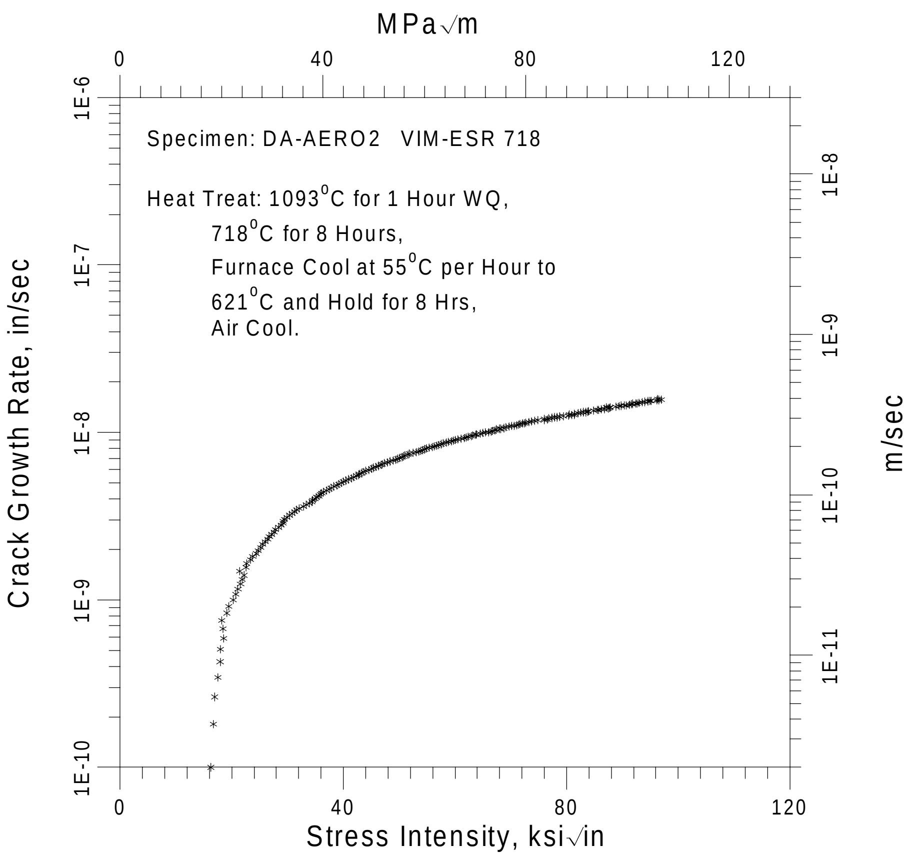
MPa√m
Specimen: DA-AERO2 VIM-ESR 718
Heat Treat: 1093°C for 1 Hour WQ,
718°C for 8 Hours,
Furnace Cool at 55°C per Hour to
621°C and Hold for 8 Hrs,
Air Cool.
Crack Growth Rate, in/sec
m/sec
Stress Intensity, ksi√in
1E-6
1E-7
1E-8
1E-9
1E-10
1E-8
1E-9
1E-10
1E-11
0
40
80
120

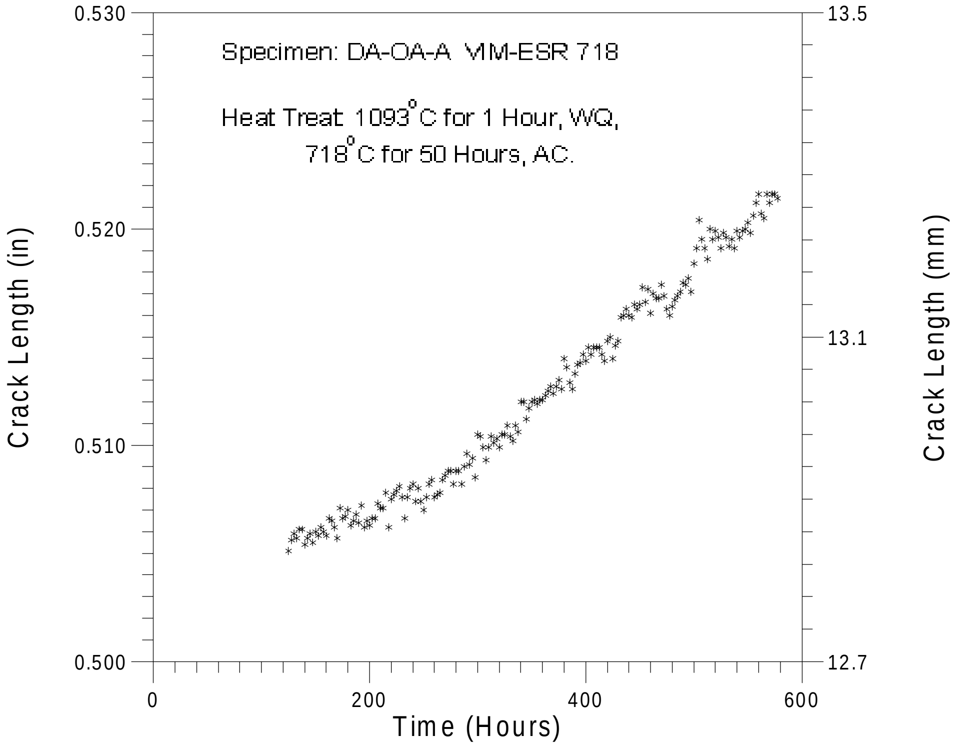
Specimen: DA-OA-A VIM-ESR 718
Heat Treat: 1093°C for 1 Hour, WQ,
718°C for 50 Hours, AC.
Crack Length (in)
Crack Length (mm)
Time (Hours)
0.530
0.520
0.510
0.500
13.5
13.1
12.7
0
200
400
600

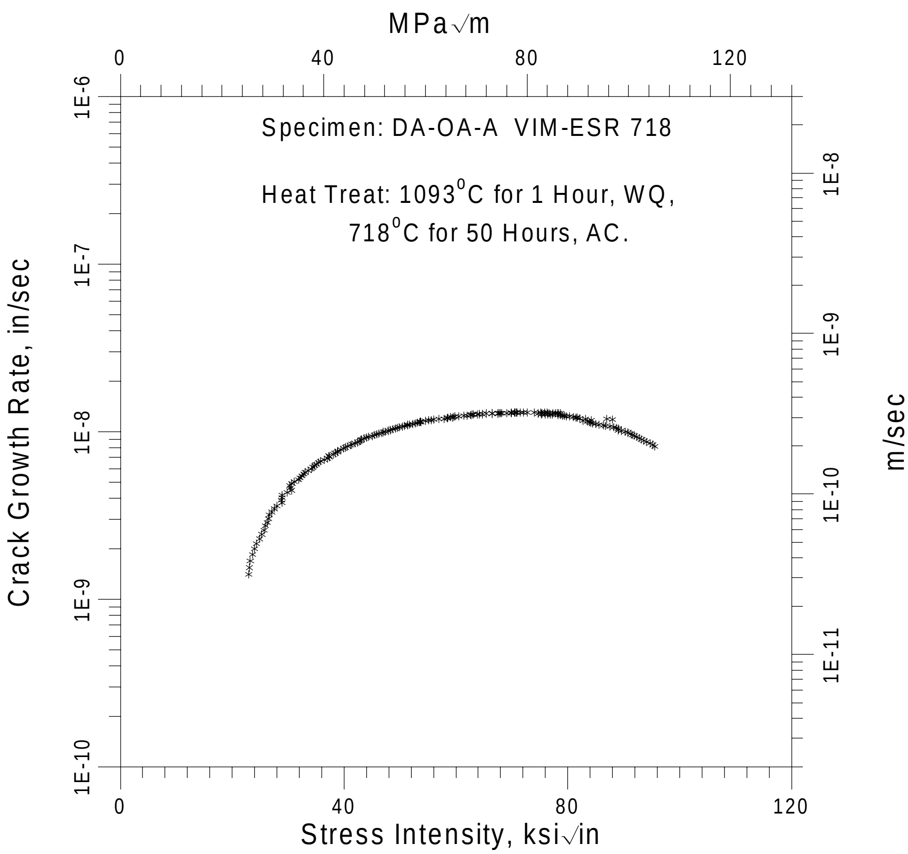
MPa√m
0
40
80
120
Specimen: DA-OA-A VIM-ESR 718
Heat Treat: 1093°C for 1 Hour, WQ,
718°C for 50 Hours, AC.
Crack Growth Rate, in/sec
m/sec
1E-6
1E-7
1E-8
1E-9
1E-10
1E-8
1E-9
1E-10
1E-11
Stress Intensity, ksi√in

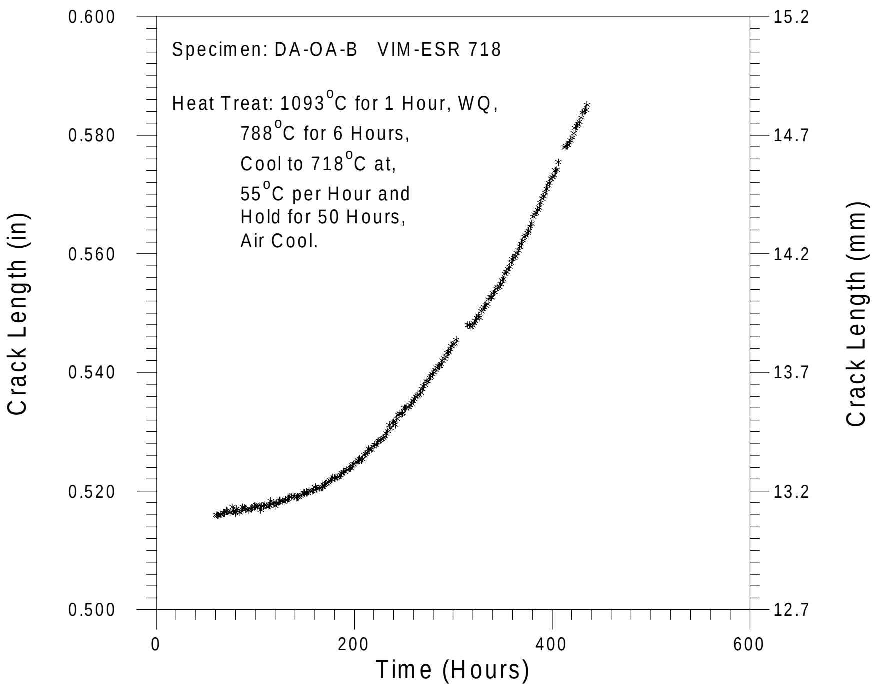
Specimen: DA-OA-B VIM-ESR 718
Heat Treat: 1093°C for 1 Hour, WQ,
788°C for 6 Hours,
Cool to 718°C at,
55°C per Hour and
Hold for 50 Hours,
Air Cool.
Crack Length (in)
Crack Length (mm)
Time (Hours)
0.600
0.580
0.560
0.540
0.520
0.500
15.2
14.7
14.2
13.7
13.2
12.7
0
200
400
600

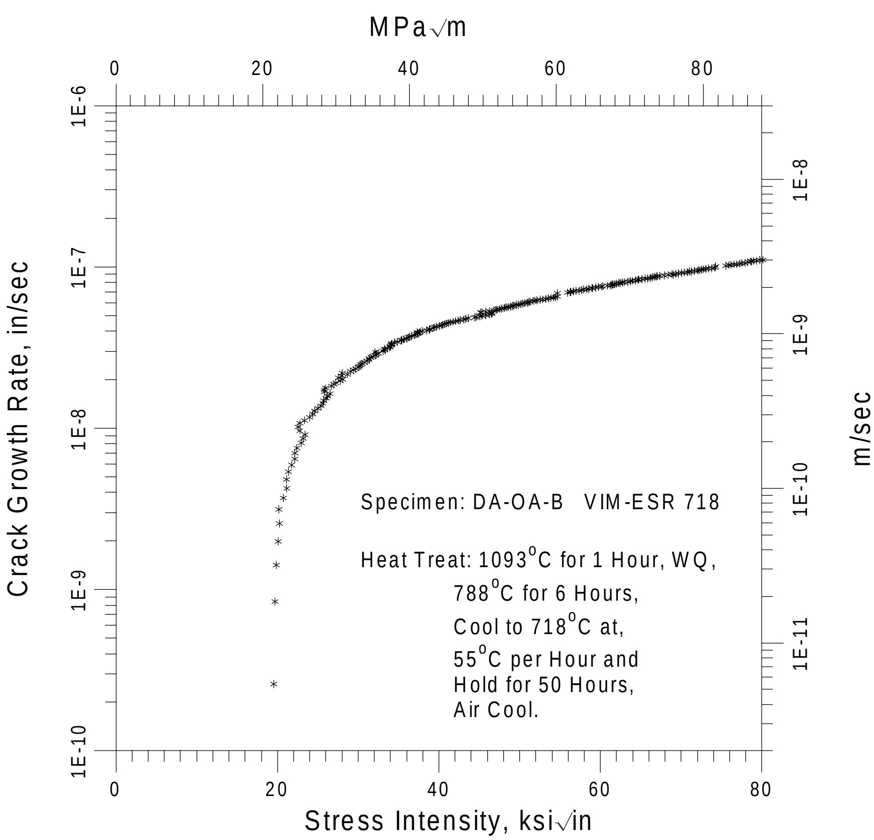
MPa√m
0
20
40
60
80
Specimen: DA-OA-B VIM-ESR 718
Heat Treat: 1093°C for 1 Hour, WQ,
788°C for 6 Hours,
Cool to 718°C at,
55°C per Hour and
Hold for 50 Hours,
Air Cool.
Crack Growth Rate, in/sec
m/sec
1E-6
1E-7
1E-8
1E-9
1E-10
1E-8
1E-9
1E-10
1E-11
Stress Intensity, ksi√in

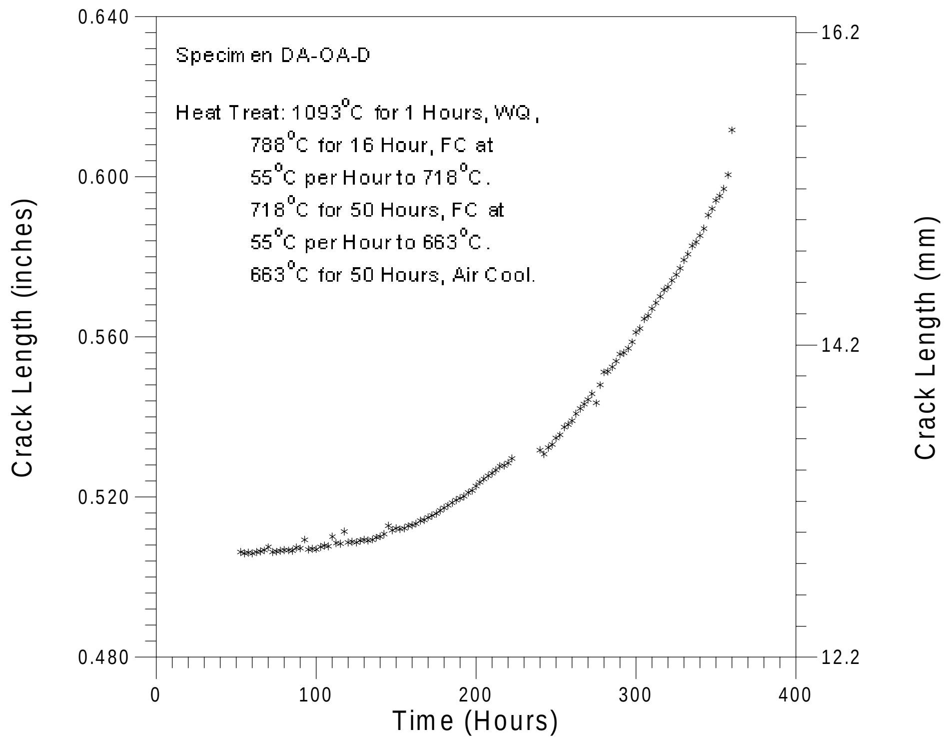
Specimen DA-OA-D
Heat Treat: 1093°C for 1 Hours, WQ,
788°C for 16 Hour, FC at
55°C per Hour to 718°C.
718°C for 50 Hours, FC at
55°C per Hour to 663°C.
663°C for 50 Hours, Air Cool.
Crack Length (inches)
Crack Length (mm)
Time (Hours)
0.640
0.600
0.560
0.520
0.480
16.2
14.2
12.2
0
100
200
300
400

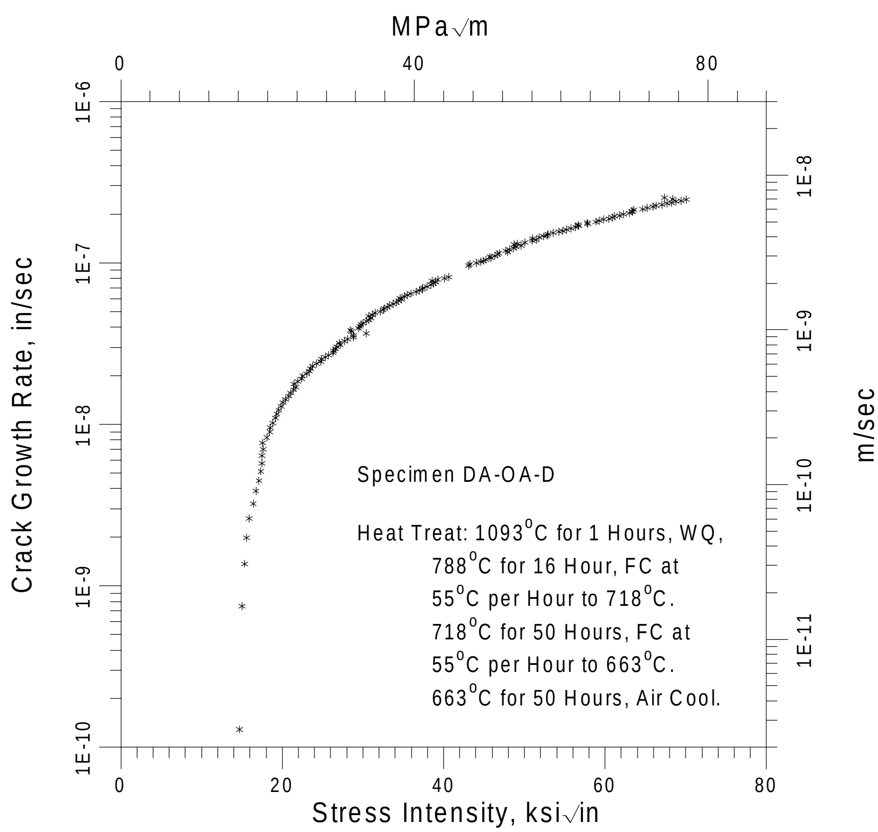
MPa√m
0
40
80
Specimen DA-OA-D
Heat Treat: 1093°C for 1 Hours, WQ,
788°C for 16 Hour, FC at
55°C per Hour to 718°C.
718°C for 50 Hours, FC at
55°C per Hour to 663°C.
663°C for 50 Hours, Air Cool.
Crack Growth Rate, in/sec
m/sec
Stress Intensity, ksi√in
1E-6
1E-7
1E-8
1E-9
1E-10
1E-8
1E-9
1E-10
1E-11
0
20
40
60
80

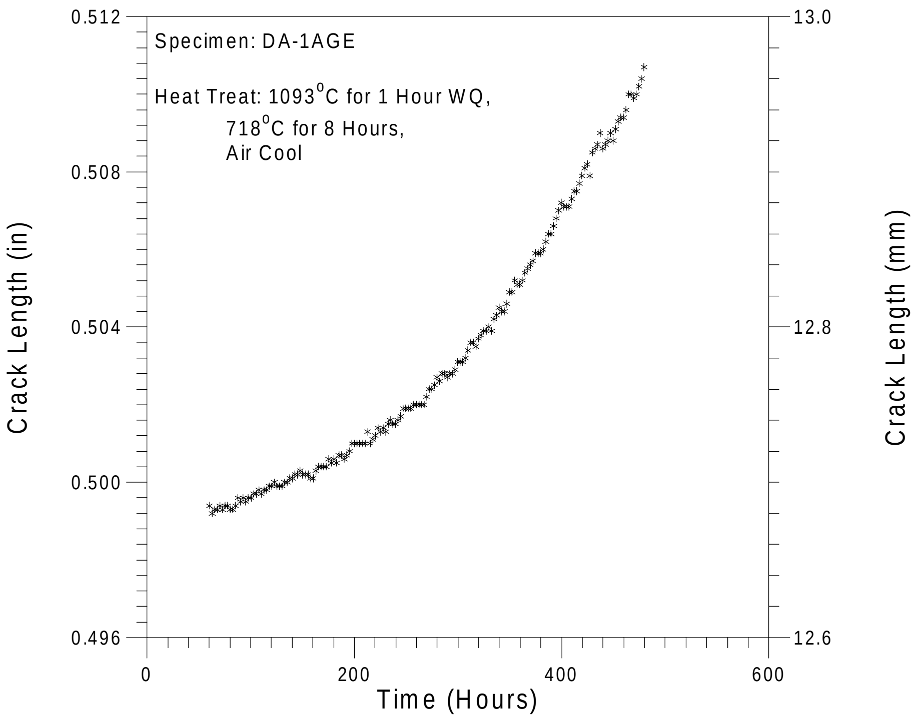
Specimen: DA-1AGE
Heat Treat: 1093°C for 1 Hour WQ,
718°C for 8 Hours,
Air Cool
Crack Length (in)
Crack Length (mm)
Time (Hours)
0.512
0.508
0.504
0.500
0.496
13.0
12.8
12.6
0
200
400
600

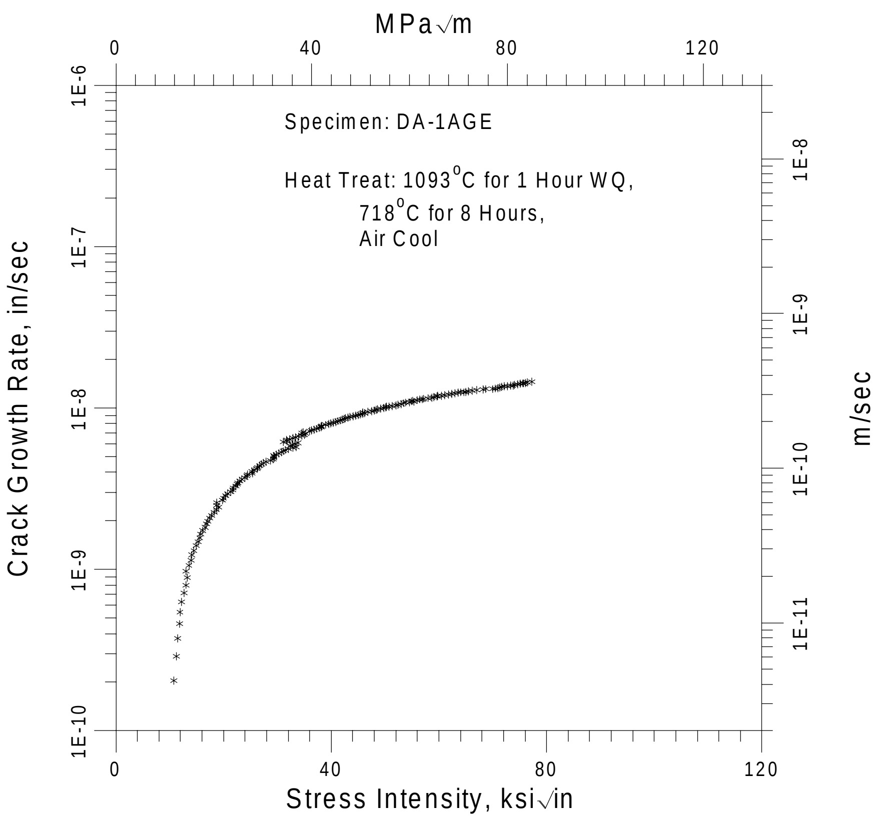
MPa√m
0
40
80
120
Specimen: DA-1AGE
Heat Treat: 1093°C for 1 Hour WQ,
718°C for 8 Hours,
Air Cool
Crack Growth Rate, in/sec
m/sec
1E-6
1E-7
1E-8
1E-9
1E-10
1E-8
1E-9
1E-10
1E-11
Stress Intensity, ksi√in

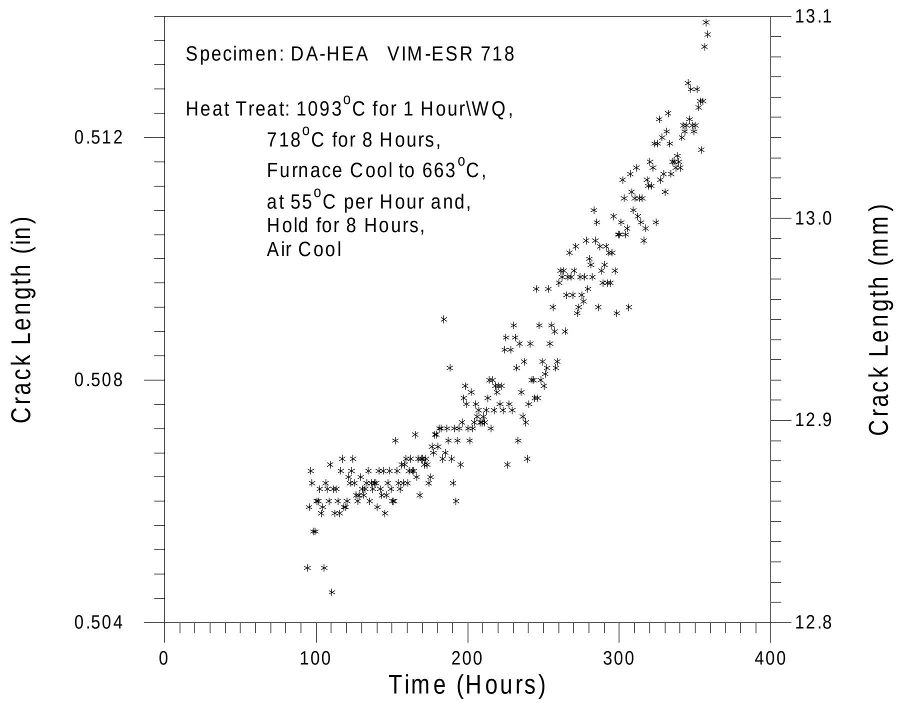
Specimen: DA-HEA VIM-ESR 718
Heat Treat: 1093°C for 1 Hour\WQ,
718°C for 8 Hours,
Furnace Cool to 663°C,
at 55°C per Hour and,
Hold for 8 Hours,
Air Cool
Crack Length (in)
Crack Length (mm)
Time (Hours)
0.504
0.508
0.512
12.8
12.9
13.0
13.1
0
100
200
300
400

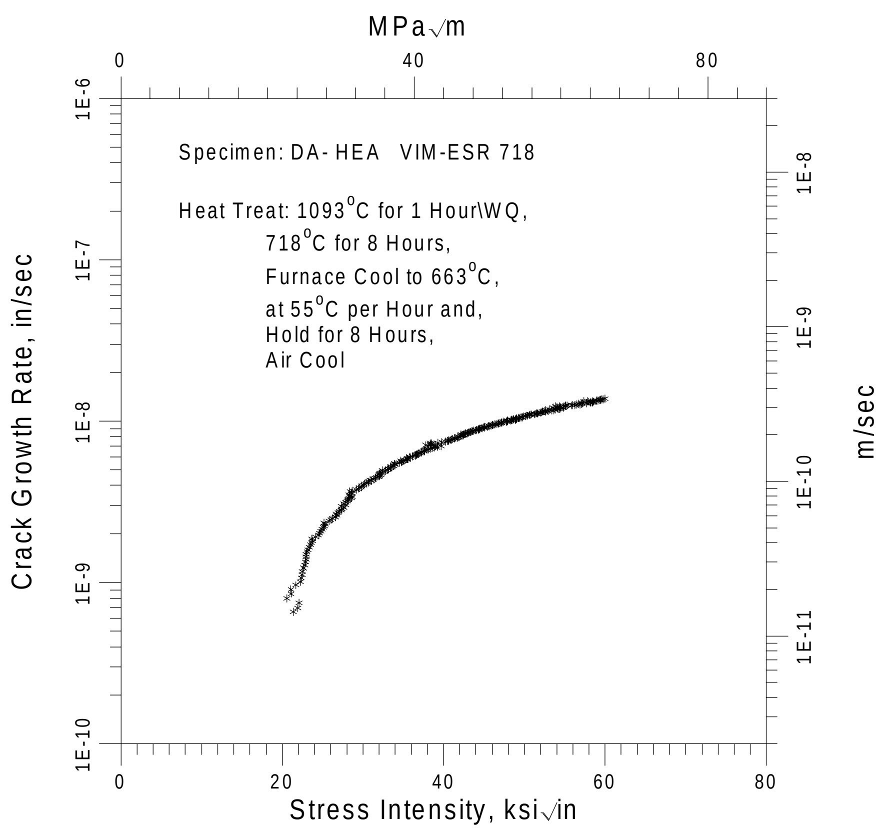
MPa√m
0
40
80
Specimen: DA- HEA VIM-ESR 718
Heat Treat: 1093°C for 1 Hour\WQ,
718°C for 8 Hours,
Furnace Cool to 663°C,
at 55°C per Hour and,
Hold for 8 Hours,
Air Cool
Crack Growth Rate, in/sec
m/sec
1E-6
1E-7
1E-8
1E-9
1E-10
1E-8
1E-9
1E-10
1E-11
0
20
40
60
80
Stress Intensity, ksi√in

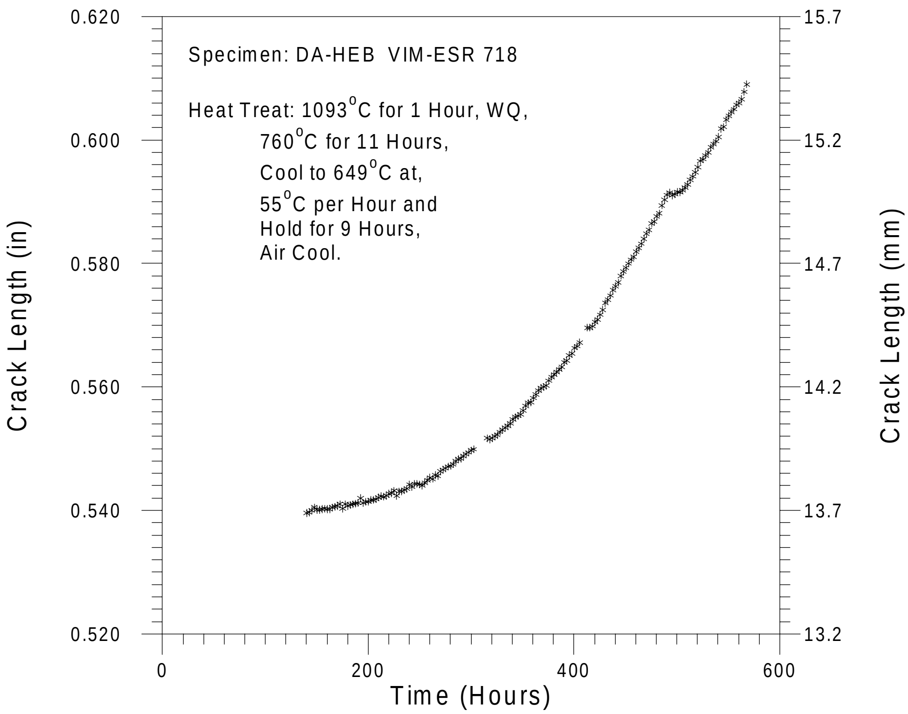
Specimen: DA-HEB VIM-ESR 718
Heat Treat: 1093°C for 1 Hour, WQ,
760°C for 11 Hours,
Cool to 649°C at,
55°C per Hour and
Hold for 9 Hours,
Air Cool.
Crack Length (in)
Crack Length (mm)
Time (Hours)
0.620
0.600
0.580
0.560
0.540
0.520
15.7
15.2
14.7
14.2
13.7
13.2
0
200
400
600

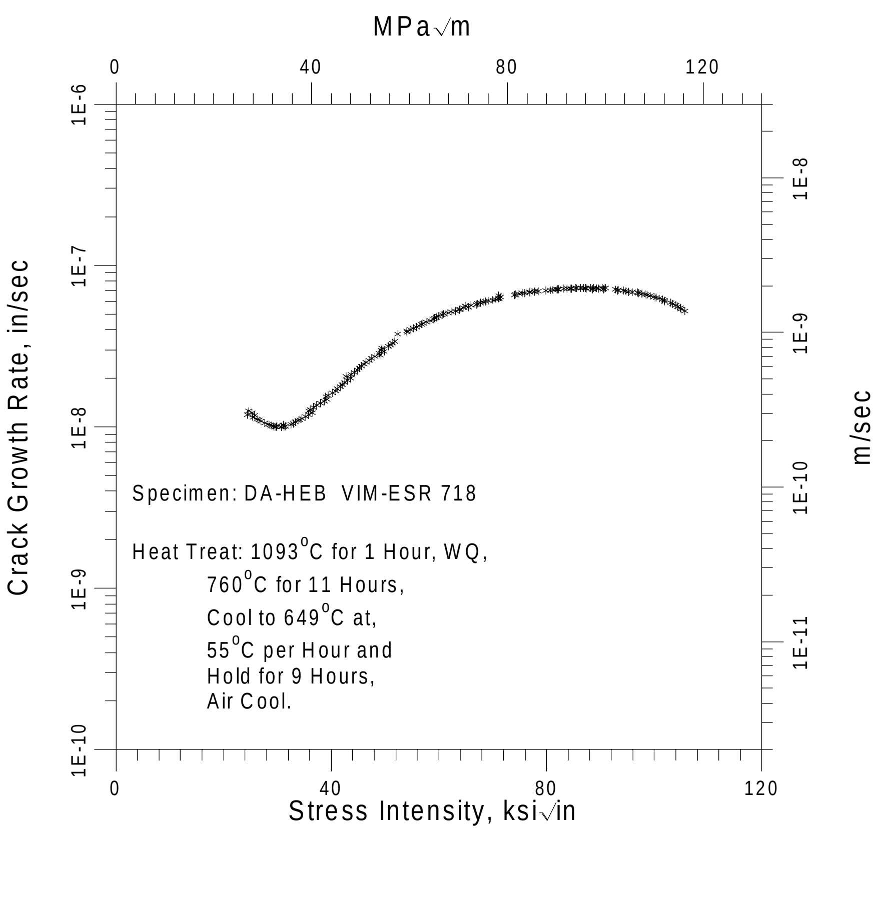
MPa√m
0
40
80
120
Specimen: DA-HEB VIM-ESR 718
Heat Treat: 1093°C for 1 Hour, WQ,
760°C for 11 Hours,
Cool to 649°C at,
55°C per Hour and
Hold for 9 Hours,
Air Cool.
Crack Growth Rate, in/sec
m/sec
1E-6
1E-7
1E-8
1E-9
1E-10
1E-8
1E-9
1E-10
1E-11
Stress Intensity, ksi√in
0
40
80
120

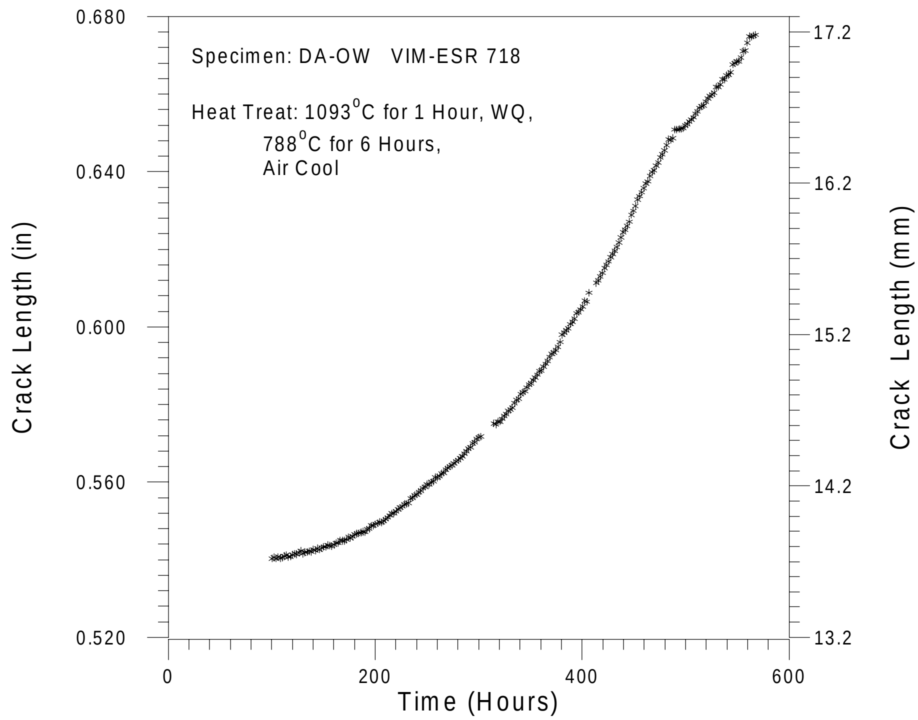
Specimen: DA-OW VIM-ESR 718
Heat Treat: 1093°C for 1 Hour, WQ,
788°C for 6 Hours,
Air Cool
Crack Length (in)
Crack Length (mm)
Time (Hours)
0.680
0.640
0.600
0.560
0.520
17.2
16.2
15.2
14.2
13.2
0
200
400
600

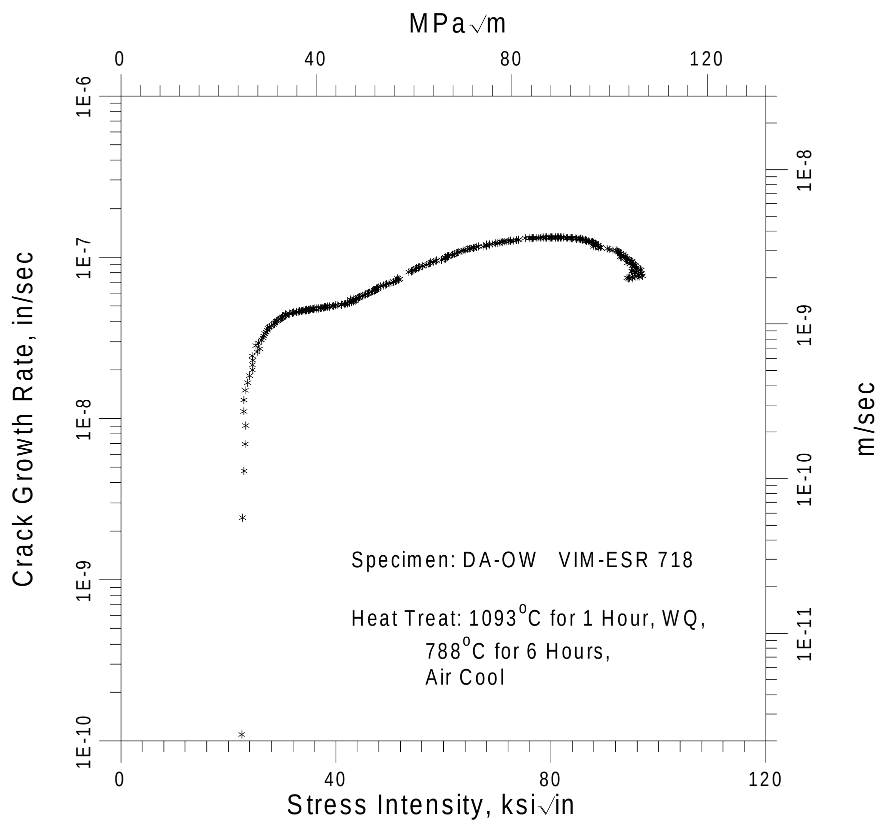
MPa√m
0
40
80
120
Crack Growth Rate, in/sec
1E-6
1E-7
1E-8
1E-9
1E-10
m/sec
1E-8
1E-9
1E-10
1E-11
Specimen: DA-OW VIM-ESR 718
Heat Treat: 1093°C for 1 Hour, WQ,
788°C for 6 Hours,
Air Cool
Stress Intensity, ksi√in

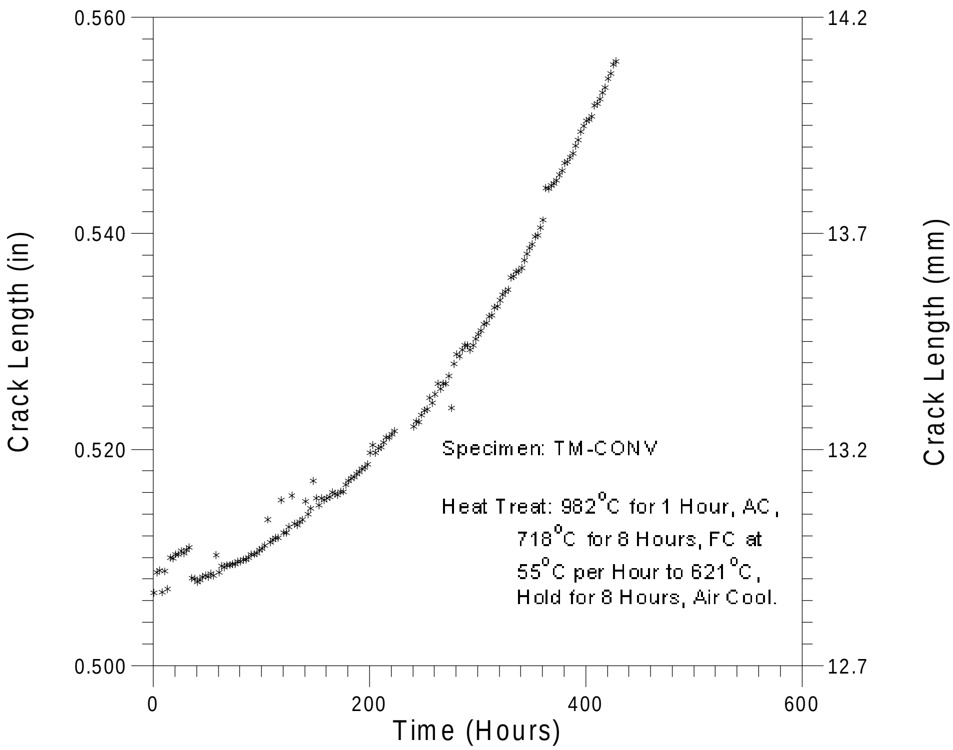
0.560
0.540
0.520
0.500
14.2
13.7
13.2
12.7
Crack Length (in)
Crack Length (mm)
0
200
400
600
Time (Hours)
Specimen: TM-CONV
Heat Treat: 982°C for 1 Hour, AC,
718°C for 8 Hours, FC at
55°C per Hour to 621°C,
Hold for 8 Hours, Air Cool.

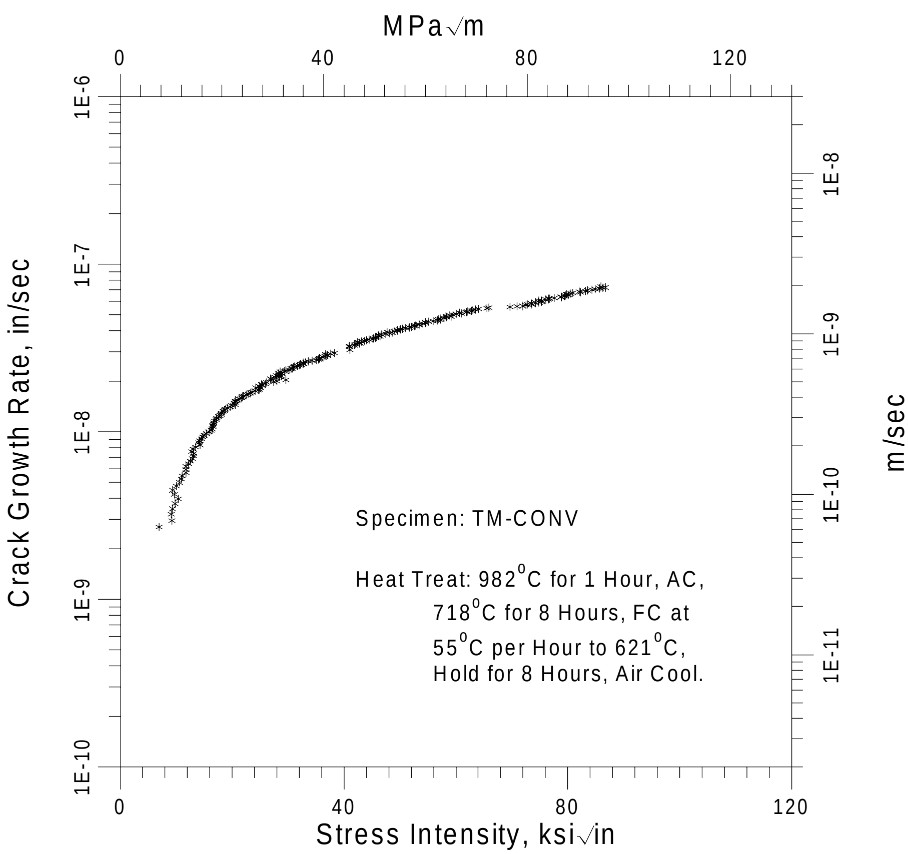
MPa√m
0
40
80
120
1E-6
1E-7
1E-8
1E-9
1E-10
1E-8
1E-9
1E-10
1E-11
Crack Growth Rate, in/sec
m/sec
Specimen: TM-CONV
Heat Treat: 982°C for 1 Hour, AC,
718°C for 8 Hours, FC at
55°C per Hour to 621°C,
Hold for 8 Hours, Air Cool.
0
40
80
120
Stress Intensity, ksi√in

B

RESULTS OF CONSTANT DISPLACEMENT RATE K_{ISCC} TESTS FOR ALTERNATIVE ALLOYS

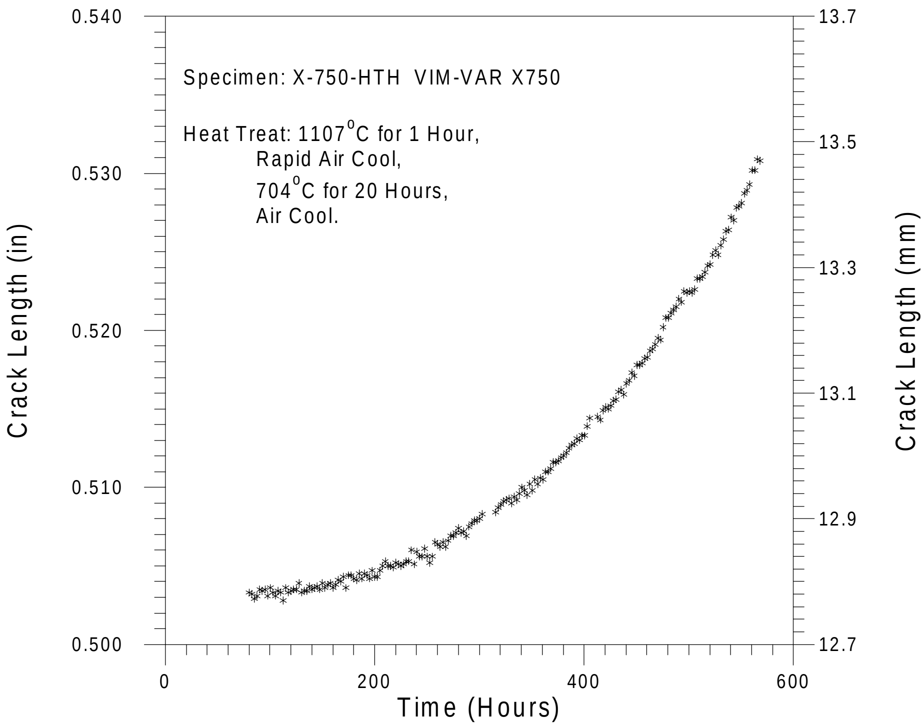
Specimen: X-750-HTH VIM-VAR X750
Heat Treat: 1107°C for 1 Hour,
Rapid Air Cool,
704°C for 20 Hours,
Air Cool.
Crack Length (in)
Crack Length (mm)
Time (Hours)
0.540
0.530
0.520
0.510
0.500
13.7
13.5
13.3
13.1
12.9
12.7
0
200
400
600

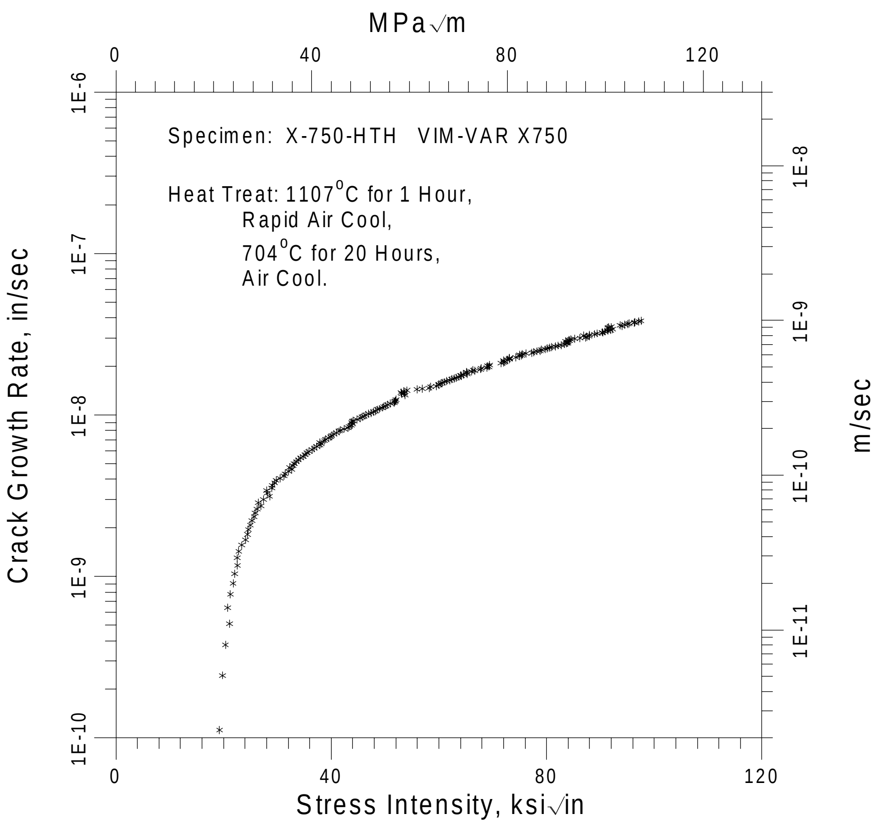
MPa√m
Specimen: X-750-HTH VIM-VAR X750
Heat Treat: 1107°C for 1 Hour,
Rapid Air Cool,
704°C for 20 Hours,
Air Cool.
Crack Growth Rate, in/sec
m/sec
Stress Intensity, ksi√in
1E-6
1E-7
1E-8
1E-9
1E-10
1E-8
1E-9
1E-10
1E-11
0
40
80
120

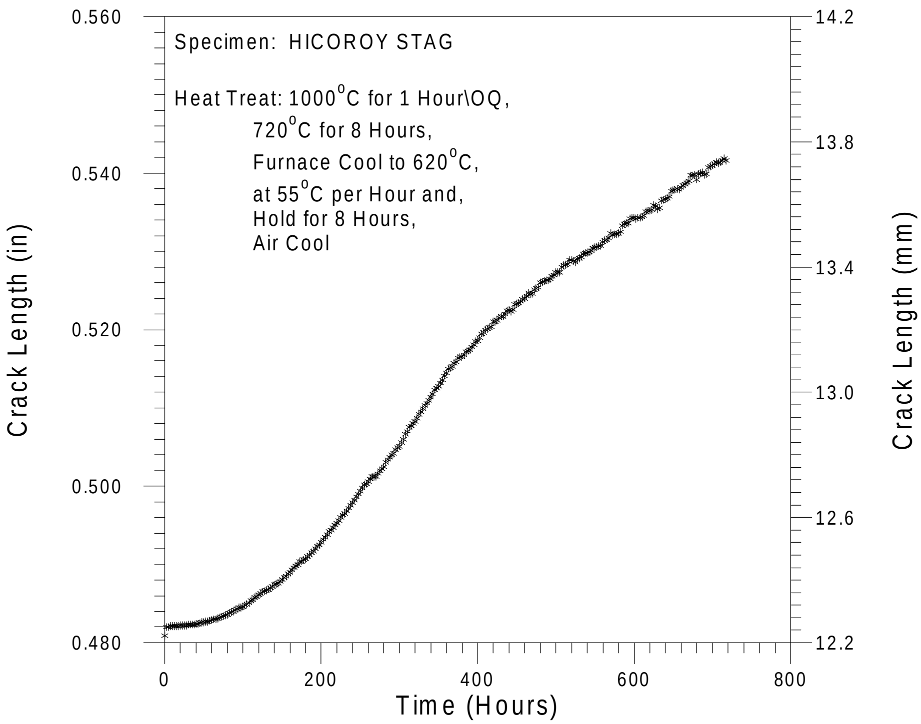
Specimen: HICOROY STAG
Heat Treat: 1000°C for 1 Hour\OQ,
720°C for 8 Hours,
Furnace Cool to 620°C,
at 55°C per Hour and,
Hold for 8 Hours,
Air Cool
Crack Length (in)
Crack Length (mm)
Time (Hours)
0.560
0.540
0.520
0.500
0.480
14.2
13.8
13.4
13.0
12.6
12.2
0
200
400
600
800

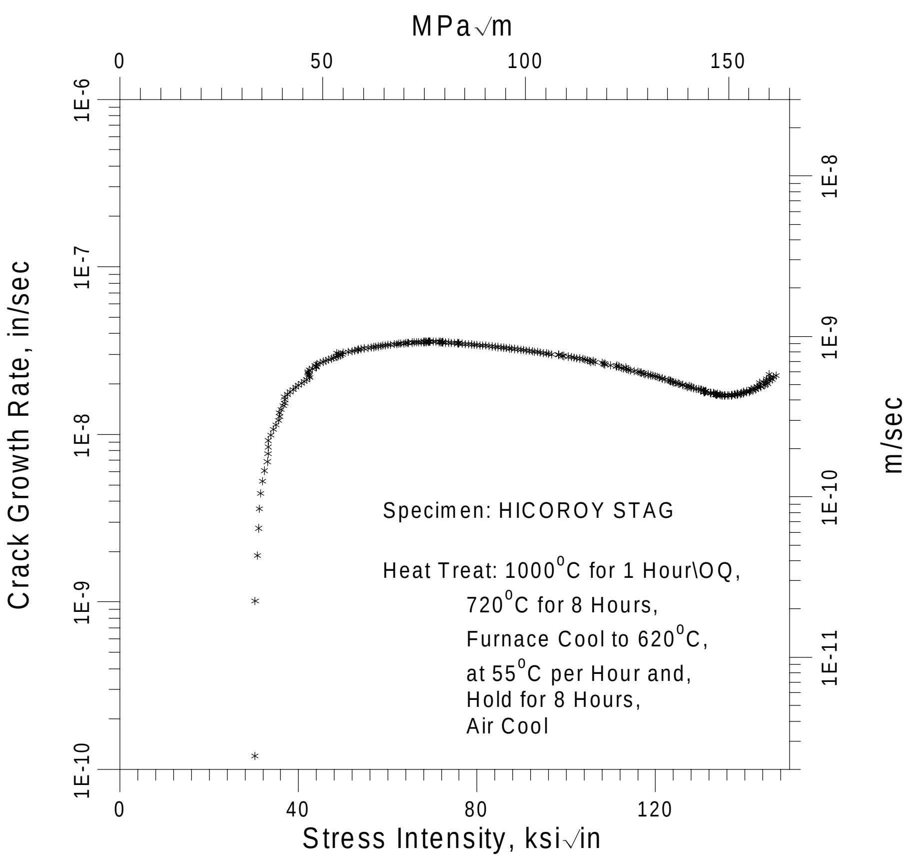
MPa√m
0
50
100
150
Specimen: HICOROY STAG
Heat Treat: 1000°C for 1 Hour\OQ,
720°C for 8 Hours,
Furnace Cool to 620°C,
at 55°C per Hour and,
Hold for 8 Hours,
Air Cool
Crack Growth Rate, in/sec
m/sec
1E-6
1E-7
1E-8
1E-9
1E-10
1E-8
1E-9
1E-10
1E-11
0
40
80
120
Stress Intensity, ksi√in

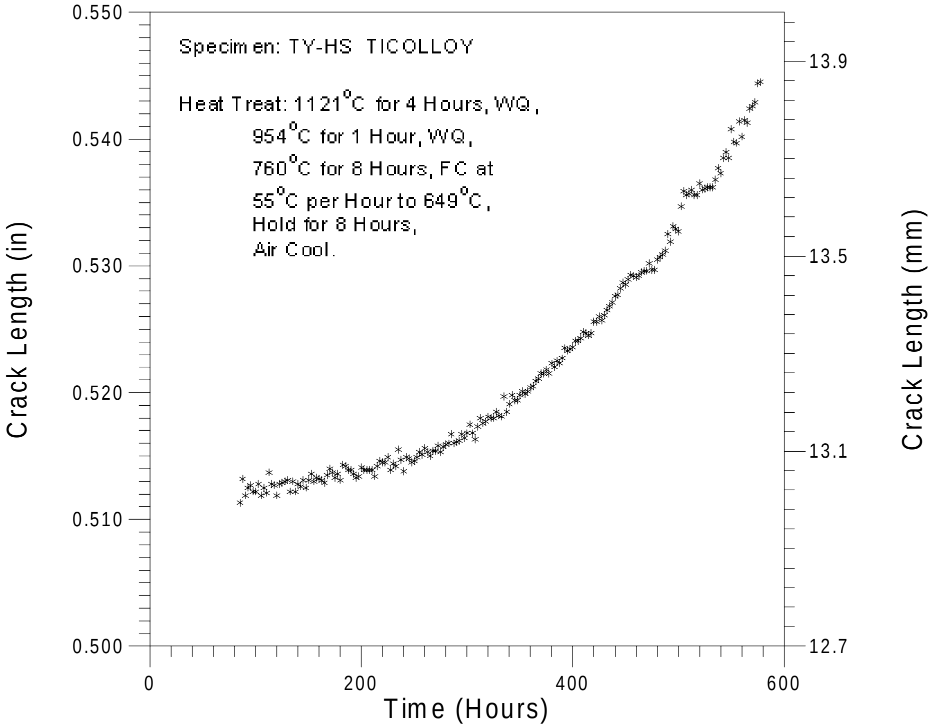
Specimen: TY-HS TICOLLOY
Heat Treat: 1121°C for 4 Hours, WQ,
954°C for 1 Hour, WQ,
760°C for 8 Hours, FC at
55°C per Hour to 649°C,
Hold for 8 Hours,
Air Cool.
Crack Length (in)
0.550
0.540
0.530
0.520
0.510
0.500
Crack Length (mm)
13.9
13.5
13.1
12.7
0
200
400
600
Time (Hours)

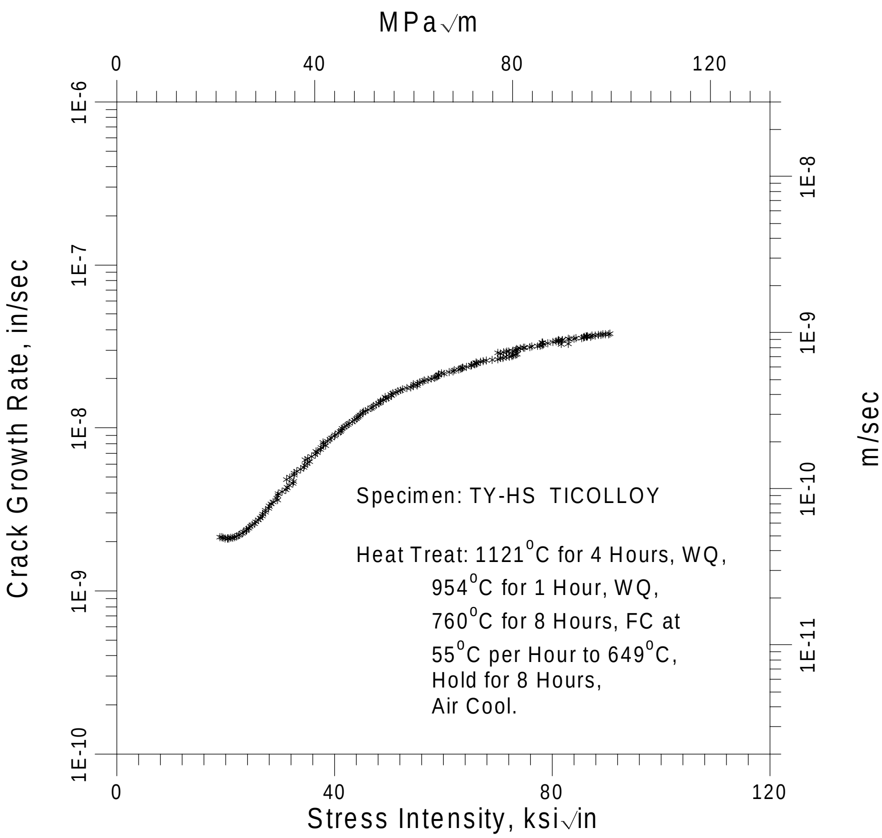
MPa√m
0
40
80
120
Crack Growth Rate, in/sec
1E-6
1E-7
1E-8
1E-9
1E-10
m/sec
1E-8
1E-9
1E-10
1E-11
Specimen: TY-HS TICOLLOY
Heat Treat: 1121°C for 4 Hours, WQ,
954°C for 1 Hour, WQ,
760°C for 8 Hours, FC at
55°C per Hour to 649°C,
Hold for 8 Hours,
Air Cool.
0
40
80
120
Stress Intensity, ksi√in

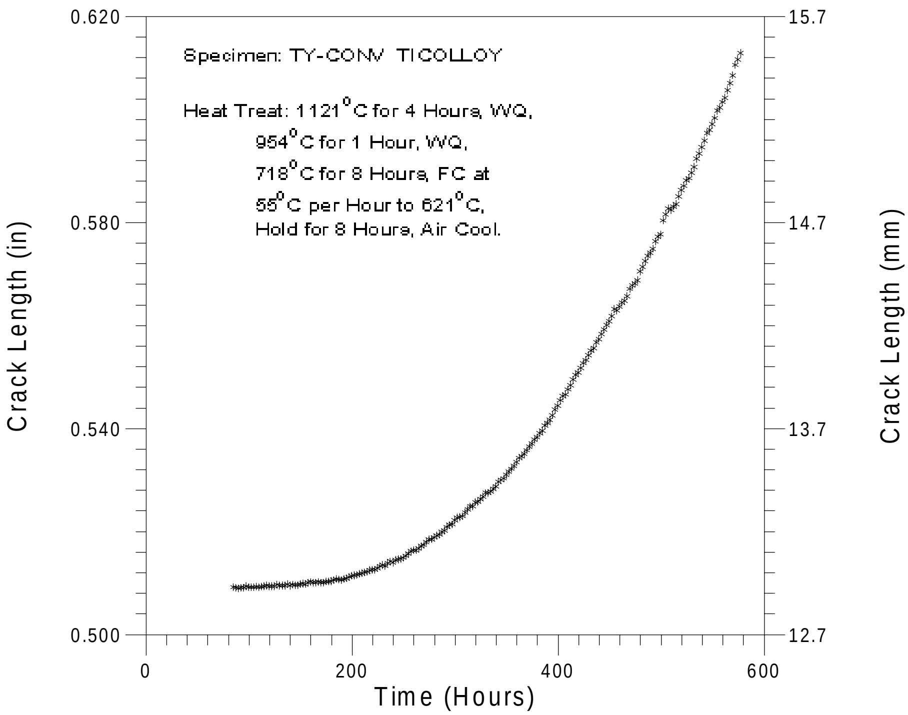
0.620
0.580
0.540
0.500
15.7
14.7
13.7
12.7
0
200
400
600
Time (Hours)
Crack Length (in)
Crack Length (mm)
Specimen: TY-CONV TICOLLOY
Heat Treat: 1121°C for 4 Hours, WQ,
954°C for 1 Hour, WQ,
718°C for 8 Hours, FC at
55°C per Hour to 621°C,
Hold for 8 Hours, Air Cool.

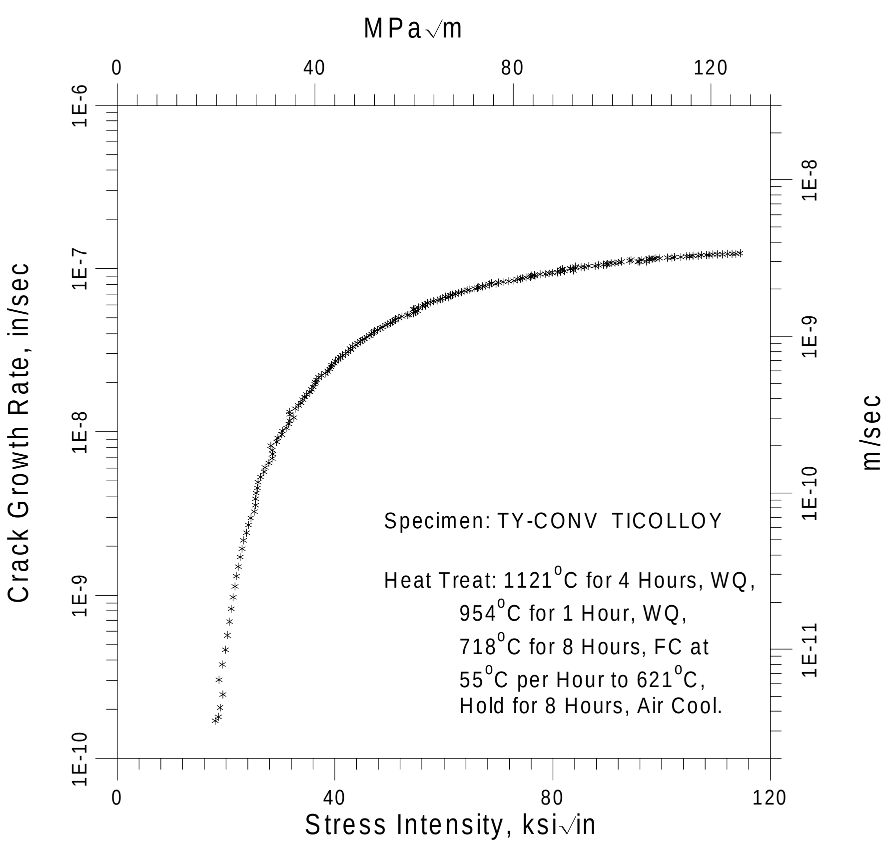
MPa√m
0
40
80
120
1E-6
1E-7
1E-8
1E-9
1E-10
1E-8
1E-9
1E-10
1E-11
Crack Growth Rate, in/sec
m/sec
Stress Intensity, ksi√in
Specimen: TY-CONV TICOLLOY
Heat Treat: 1121°C for 4 Hours, WQ,
954°C for 1 Hour, WQ,
718°C for 8 Hours, FC at
55°C per Hour to 621°C,
Hold for 8 Hours, Air Cool.

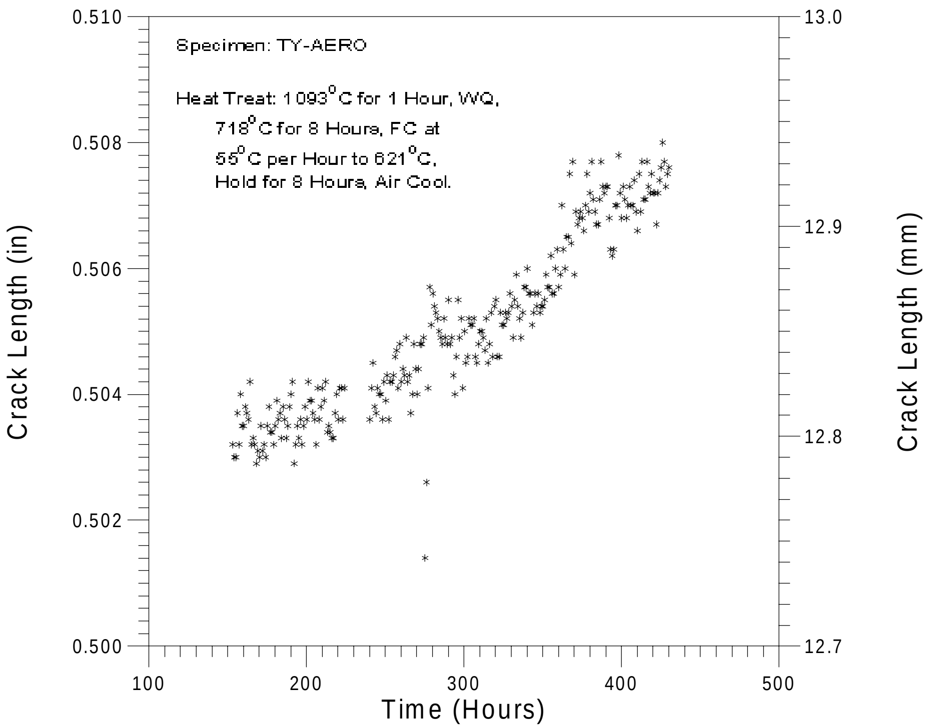
Specimen: TY-AERO
Heat Treat: 1093°C for 1 Hour, WQ,
718°C for 8 Hours, FC at
55°C per Hour to 621°C,
Hold for 8 Hours, Air Cool.
Crack Length (in)
Crack Length (mm)
Time (Hours)
0.510
0.508
0.506
0.504
0.502
0.500
13.0
12.9
12.8
12.7
100
200
300
400
500

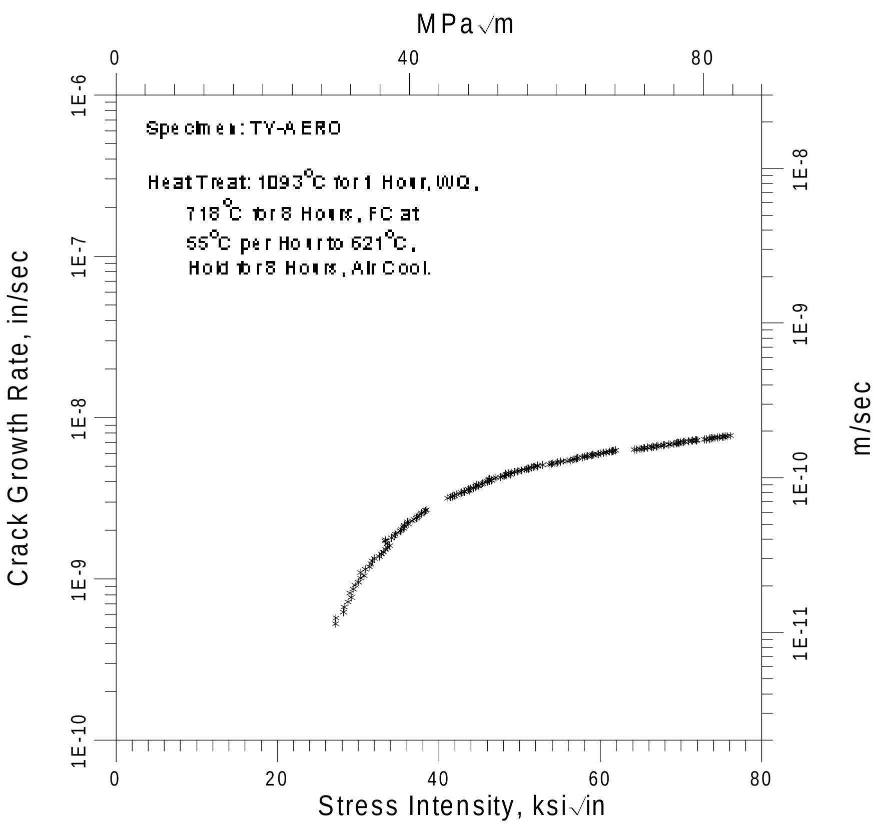
MPa√m
Specimen: TY-AERO
Heat Treat: 1093°C for 1 Hour, WQ,
718°C for 8 Hours, FC at
55°C per Hour to 621°C,
Hold for 8 Hours, Air Cool.
Crack Growth Rate, in/sec
m/sec
Stress Intensity, ksi√in
1E-6
1E-7
1E-8
1E-9
1E-10
1E-8
1E-9
1E-10
1E-11
0
40
80
0
20
40
60
80

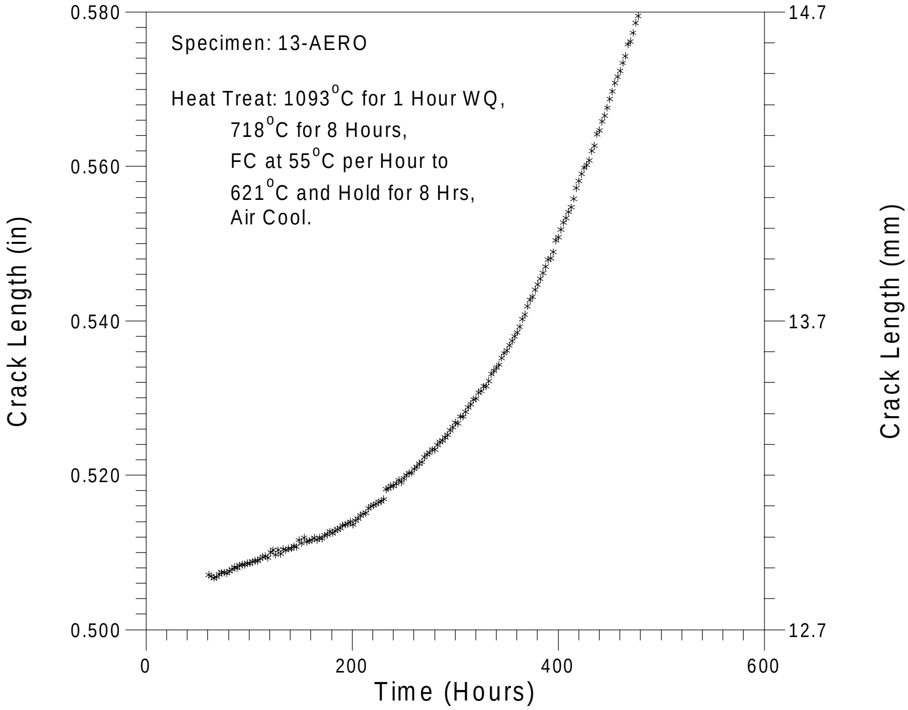
Specimen: 13-AERO
Heat Treat: 1093°C for 1 Hour WQ,
718°C for 8 Hours,
FC at 55°C per Hour to
621°C and Hold for 8 Hrs,
Air Cool.
Crack Length (in)
Crack Length (mm)
Time (Hours)
0.580
0.560
0.540
0.520
0.500
14.7
13.7
12.7
0
200
400
600

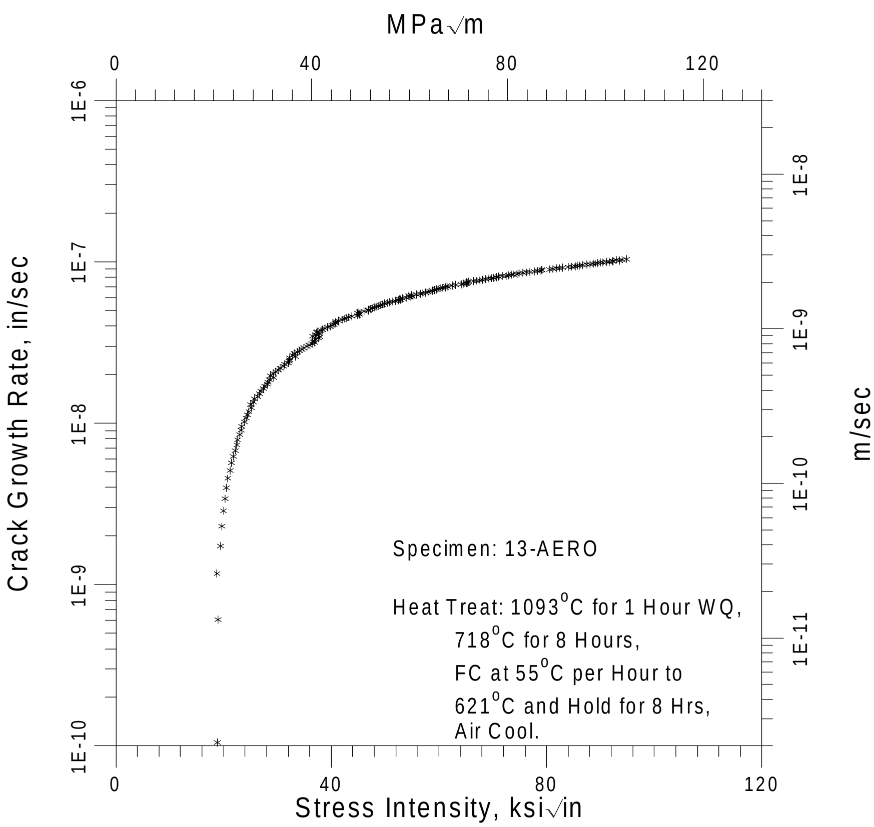
MPa√m
Crack Growth Rate, in/sec
m/sec
Stress Intensity, ksi√in
Specimen: 13-AERO
Heat Treat: 1093°C for 1 Hour WQ,
718°C for 8 Hours,
FC at 55°C per Hour to
621°C and Hold for 8 Hrs,
Air Cool.
1E-6
1E-7
1E-8
1E-9
1E-10
1E-8
1E-9
1E-10
1E-11
0
40
80
120

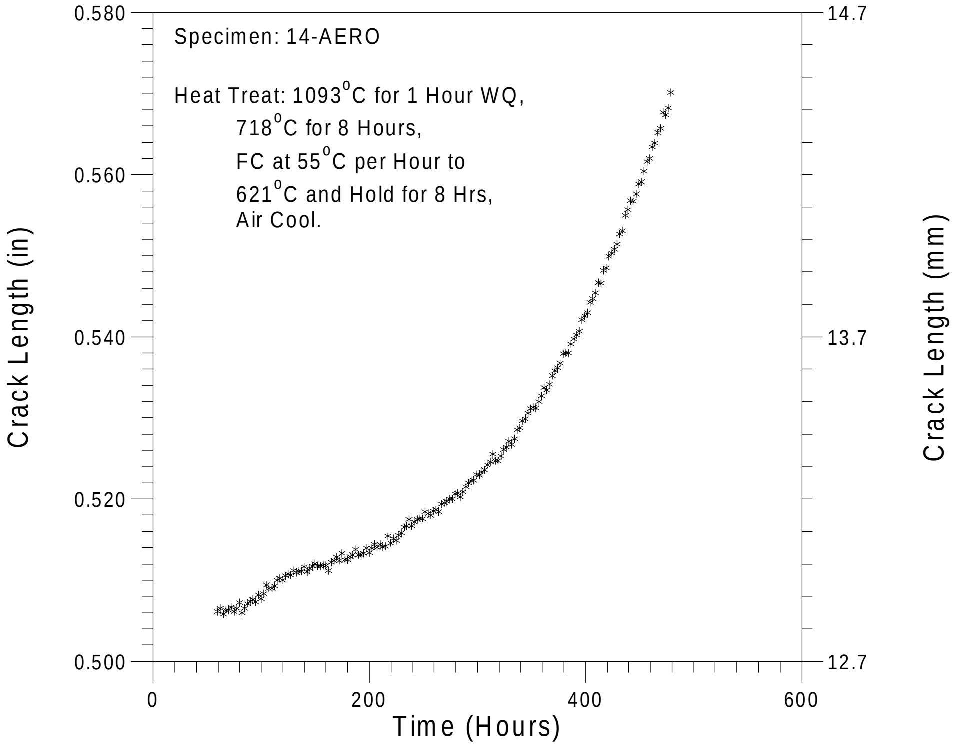
Specimen: 14-AERO
Heat Treat: 1093°C for 1 Hour WQ,
718°C for 8 Hours,
FC at 55°C per Hour to
621°C and Hold for 8 Hrs,
Air Cool.
Crack Length (in)
Crack Length (mm)
Time (Hours)
0.580
0.560
0.540
0.520
0.500
14.7
13.7
12.7
0
200
400
600

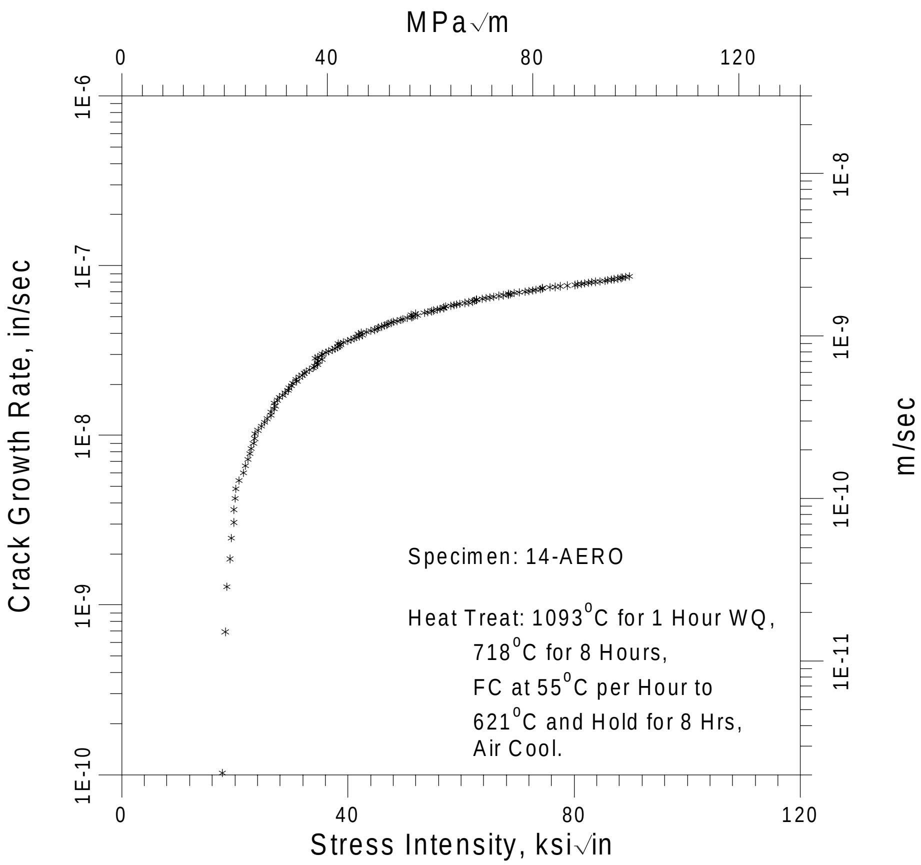
MPa√m
Specimen: 14-AERO
Heat Treat: 1093°C for 1 Hour WQ,
718°C for 8 Hours,
FC at 55°C per Hour to
621°C and Hold for 8 Hrs,
Air Cool.
Crack Growth Rate, in/sec
m/sec
Stress Intensity, ksi√in
1E-6
1E-7
1E-8
1E-9
1E-10
1E-8
1E-9
1E-10
1E-11
0
40
80
120

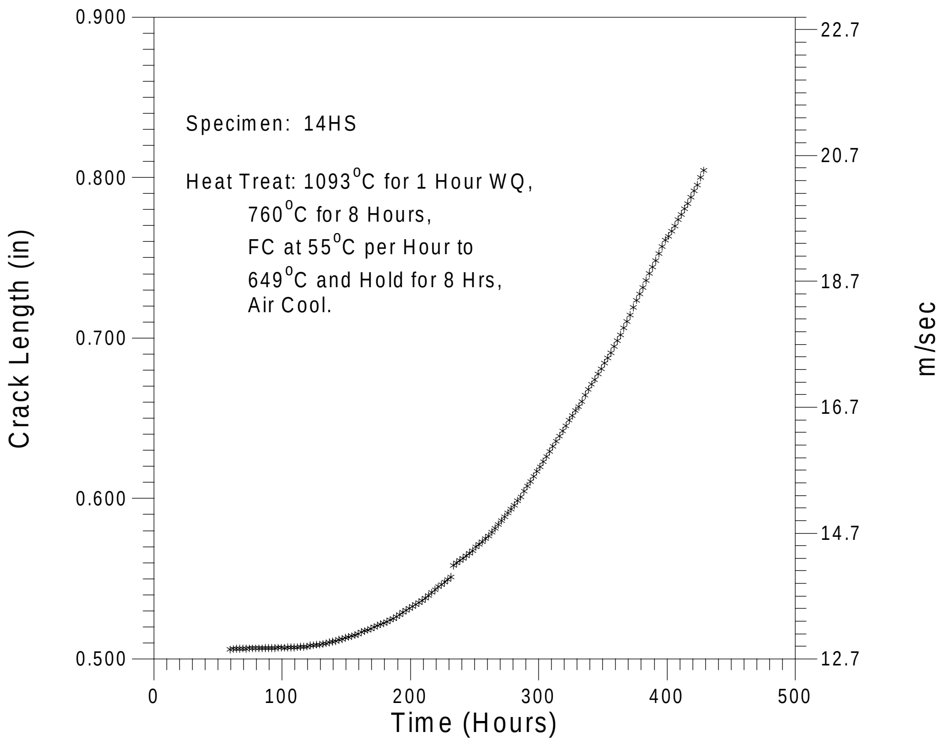
Specimen: 14HS
Heat Treat: 1093°C for 1 Hour WQ,
760°C for 8 Hours,
FC at 55°C per Hour to
649°C and Hold for 8 Hrs,
Air Cool.
Crack Length (in)
Time (Hours)
m/sec

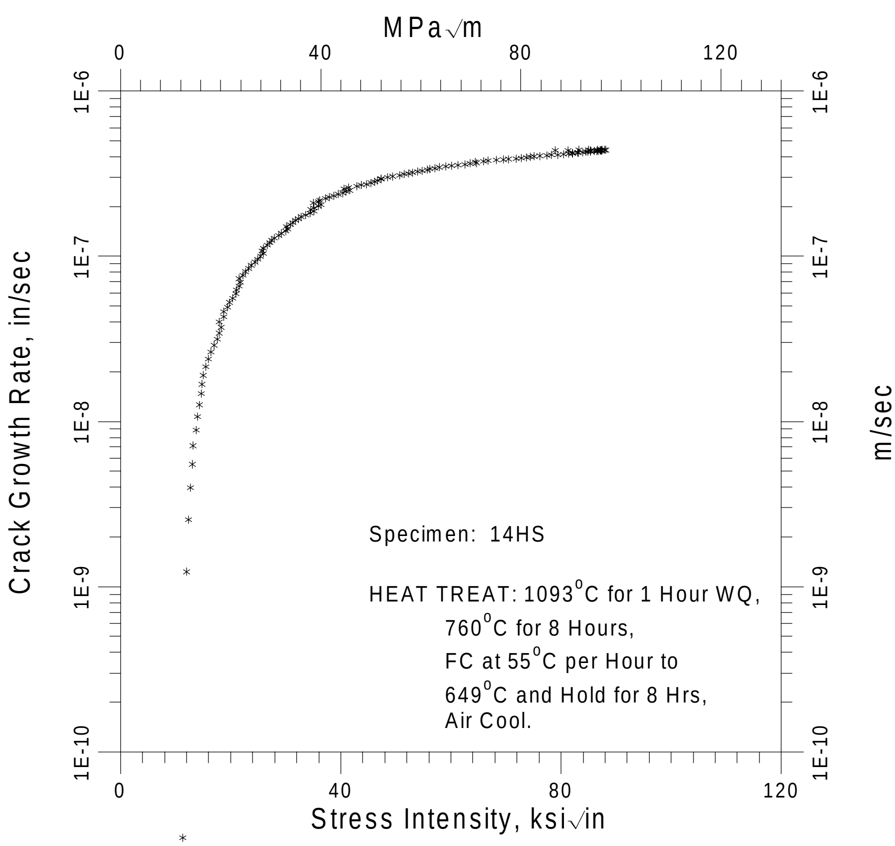
MPa√m
Specimen: 14HS
HEAT TREAT: 1093°C for 1 Hour WQ,
760°C for 8 Hours,
FC at 55°C per Hour to
649°C and Hold for 8 Hrs,
Air Cool.
Crack Growth Rate, in/sec
Stress Intensity, ksi√in
m/sec

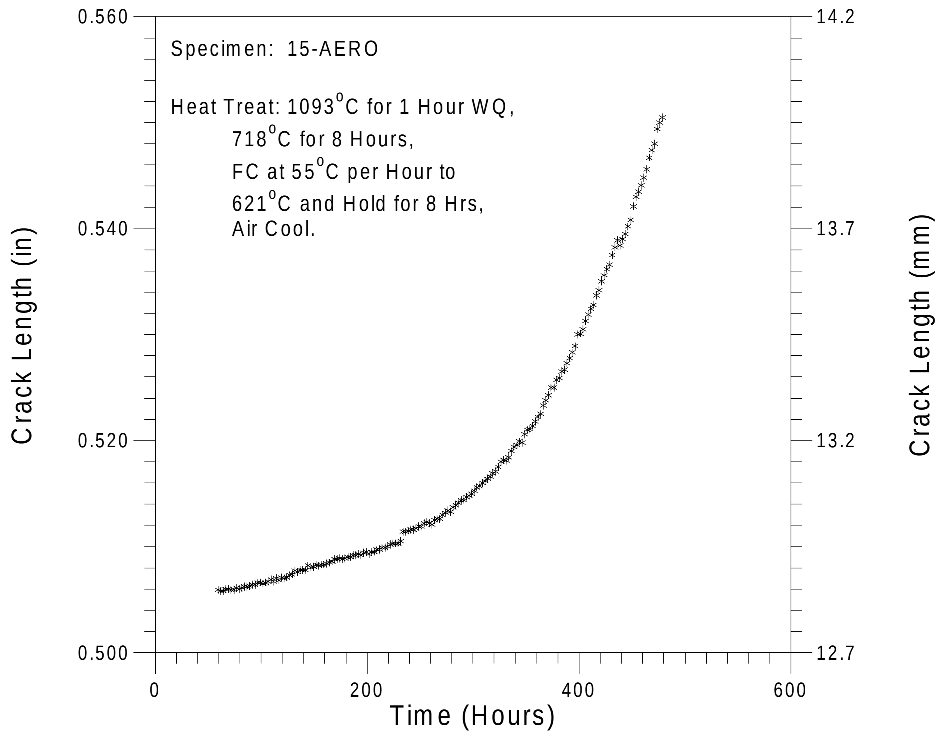
Specimen: 15-AERO
Heat Treat: 1093°C for 1 Hour WQ,
718°C for 8 Hours,
FC at 55°C per Hour to
621°C and Hold for 8 Hrs,
Air Cool.
Crack Length (in)
Crack Length (mm)
Time (Hours)
0.560
0.540
0.520
0.500
14.2
13.7
13.2
12.7
0
200
400
600

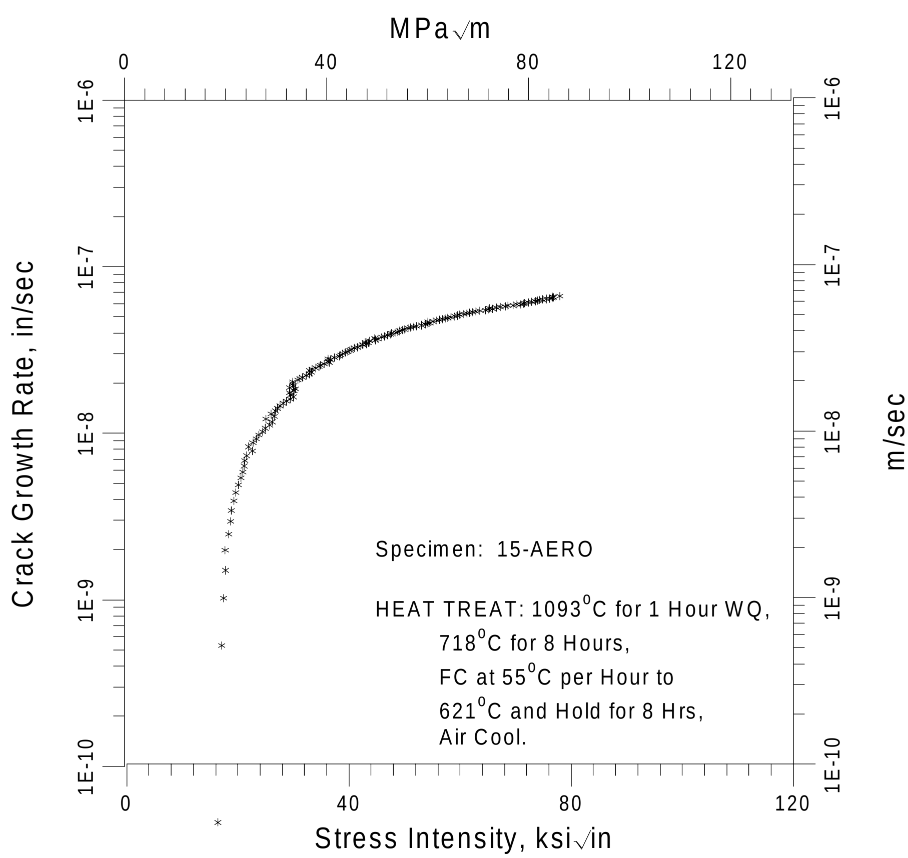
MPa√m
0
40
80
120
Crack Growth Rate, in/sec
m/sec
1E-6
1E-7
1E-8
1E-9
1E-10
Specimen: 15-AERO
HEAT TREAT: 1093°C for 1 Hour WQ,
718°C for 8 Hours,
FC at 55°C per Hour to
621°C and Hold for 8 Hrs,
Air Cool.
Stress Intensity, ksi√in

About EPRI

EPRI creates science and technology solutions for the global energy and energy services industry. U.S. electric utilities established the Electric Power Research Institute in 1973 as a nonprofit research consortium for the benefit of utility members, their customers, and society. Now known simply as EPRI, the company provides a wide range of innovative products and services to more than 1000 energy-related organizations in 40 countries. EPRI's multidisciplinary team of scientists and engineers draws on a worldwide network of technical and business expertise to help solve today's toughest energy and environmental problems.

EPRI. Electrify the World

Program: TR-105808

Nuclear Power

EPRI • 3412 Hillview Avenue, Palo Alto, California 94304 • PO Box 10412, Palo Alto, California 94303 • USA
800.313.3774 • 650.855.2121 • askepri@epri.com • www.epri.com